Solute Effects
on the Production and Decay of Primary Species
in the Flash Photolysis of Indole

by

Wm. Grant McGimpsey, B.Sc. (Hons.)

A Thesis

submitted to the Department of Chemistry

in partial fulfilment of the requirements

for the degree of

Master of Science

May 1981

Brock University

St. Catharines, Ontario

ABSTRACT

Maximum production rates of, and decay kinetics for the hydrated electron, the indolyl neutral radical and the indole triplet state have been obtained in the microsecond, broadband ($\lambda > 260$ nm) flash photolysis of helium-saturated, neutral aqueous solutions of indole, in the absence and in the presence of the solutes NaBr, $BaCl_2 \cdot 2H_2O$ and $CdSO_4$.

Fluorescence spectra and fluorescence lifetimes have also been obtained in the absence and in the presence of the above solutes.

The hydrated electron is produced monophotonically and biphotonically at an apparent maximum rate which is increased by $BaCl_2 \cdot 2H_2O$ and decreased by NaBr and $CdSO_4$. The neutral indolyl radical may be produced monophotonically and biphotonically or strictly monophotonically at an apparent maximum rate which is increased by NaBr and $CdSO_4$ and is unaffected by $BaCl_2 \cdot 2H_2O$. The indole triplet state is produced monophotonically at a maximum rate which is increased by all solutes.

The hydrated electron decays by pseudo first order processes, the neutral indolyl radical decays by second order recombination and the indole triplet state decays by combined first and second order processes.

Hydrated electrons are shown to react with H^+, H_2O, indole, Na^+ and Cd^{++}. No evidence has been found for the reaction of hydrated electrons with Ba^{++}. The specific rate of second order neutral

indolyl radical recombination is unaffected by NaBr and $BaCl_2 \cdot 2H_2O$, and is increased by $CdSO_4$. Specific rates for both first and second order triplet state decay processes are increased by all solutes.

While NaBr greatly reduced the fluorescence lifetime and emission band intensity, $BaCl_2 \cdot 2H_2O$ and $CdSO_4$ had no effect on these parameters.

It is suggested that in solute-free solutions and in those containing $BaCl_2 \cdot 2H_2O$ and $CdSO_4$, direct excitation occurs to CTTS states as well as to first excited singlet states. It is further suggested that in solutions containing NaBr, direct excitation to first excited singlet states predominates. This difference serves to explain increased indole triplet state production (by ISC from CTTS states) and unchanged fluorescence lifetimes and emission band intensities in the presence of $BaCl_2 \cdot 2H_2O$ and $CdSO_4$, and increased indole triplet state production (by ISC from S_1^0 states) and decreased fluorescence lifetime and emission band intensity in the presence of NaBr.

Evidence is presented for

(a) very rapid ($t_{\frac{1}{2}} \sim 1$ μs) processes involving reactions of the hydrated electron with Na^+ and Cd^{++} which compete with the reformation of indole by hydrated electron-indole radical cation recombination, and

(b) first and second order indole triplet decay processes involving the conversion of first excited triplet states to vibrationally excited ground singlet states.

ACKNOWLEDGEMENTS

I would like to express my greatest appreciation to Professor E. A. Cherniak for his counsel and guidance. They were invaluable to me.

I would also like to thank Professor E. R. Muller and Professor K. J. Srivastava of Mathematics for aid in analyses, Professor P. Nicholls and Professor P. Rand for loan of equipment, Dr. M. J. Ettinger, Department of Biochemistry, State University of New York at Buffalo, for the use of a spectrofluorometer, Dr. F. Janzen of Photochemical Research Associates, London, Ontario, for the use of a pulsed, single photon counting fluorometer, and my friends at Brock.

TABLE OF CONTENTS

LIST OF TABLES

LIST OF ILLUSTRATIONS

Page

INTRODUCTION

The ionization potential of indole (I), in the gas phase, is 780 kJ mol^{-1}.[1]

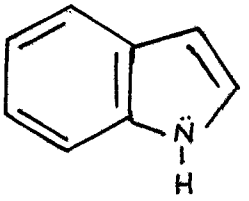

(I)

In aqueous solutions at pH 7, the ionization potential is 420 kJ mol^{-1}.[2] This aqueous phase ionization potential and the known singlet and triplet states of indole are shown in Figure 1.[3,4] The absorption spectrum of indole in aqueous solution at pH 7 is shown in Figure 2.[5] Thus, absorption of radiation with wavelengths in the range 304-260 nm (393-420 kJ mol^{-1}), by aqueous solutions of indole, produces S_1^v (vibrationally excited first singlet states) and S_1^0 (the vibrationless fluorescent state). Since charge-transfer-to-solvent (CTTS) states lie immediately below the aqueous phase ionization potential and are in near resonance with S_1^v, T_4^v and T_5^o, these CTTS states may also be produced, directly or indirectly, via S_1^v or S_1^0.

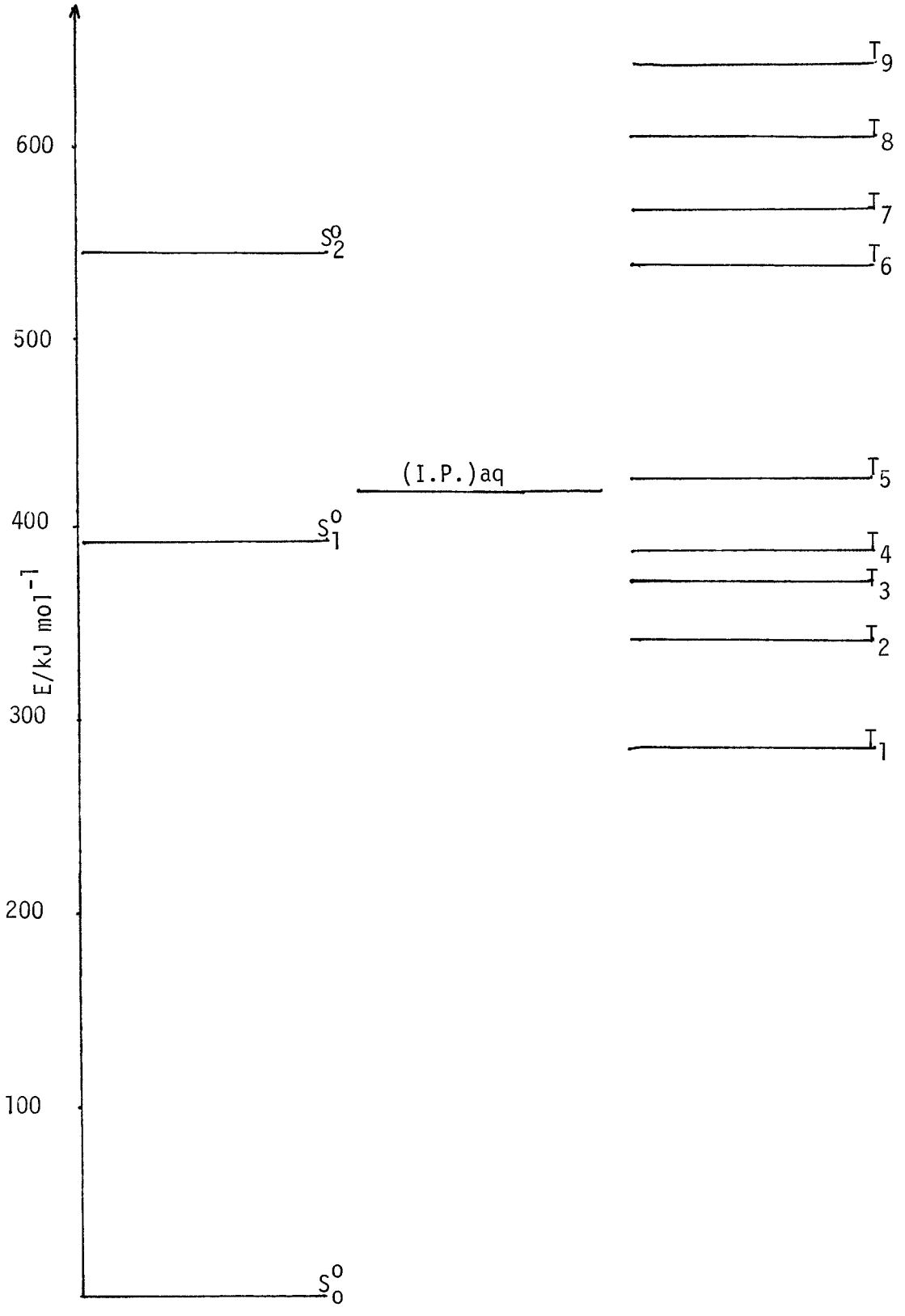

Figure (1): Aqueous Phase Ionization Potential, Singlet and Triplet Energy Levels of Indole.

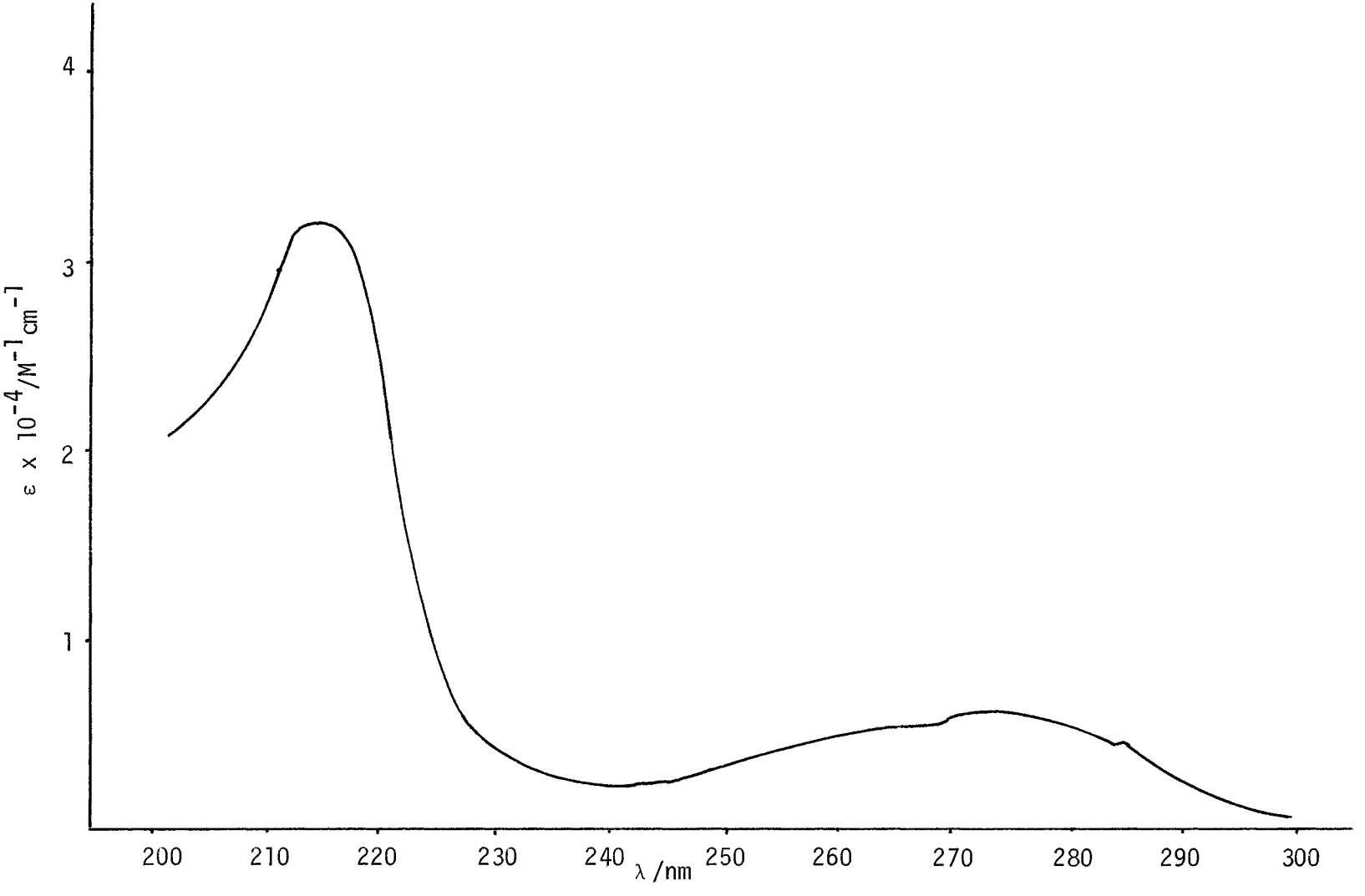

Figure (2): Absorption spectrum of indole in water.

Since intersystem crossing (ISC) from S_1 to T_4, followed by very fast internal conversion (IC) ($T_4 \rightsquigarrow T_1$), within the triplet manifold, is known to occur,[6,7] T_1 states will also be indirectly populated. It is, therefore, not surprising that fluorescence emission from S_1^0, photoionization, and triplet-triplet absorption (T_1-T_n) are observed following $S_0 \longrightarrow S_1$ excitation of indole in aqueous solutions.

The fluorescence emission spectra of indole in water and in other polar and non-polar solvents are shown in Figure 3.[8] While there is no effect of solvent on the absorption spectra of indole,[9] the fluorescence spectra exhibit red shifts, i.e., the wavelength corresponding to maximum fluorescence emission increases as the polarity of the solvent increases. As the dipole moment of S_1 is 5.65 D[33] (which is much greater than the dipole moment of S_0 indole (2.2 D)[10,11]), excited solute dipole-solvent dipole interaction,[9] exciplex formation[8] and reorientation of solvent molecules about S_1^v [11] have been suggested as mechanisms for the stabilization of the S_1 state. Since stabilization energies increase as the dipole moments of solvent molecules increase, red shifts are expected to occur and to increase as the polarity of the solvent increases.

For indole in water at 25°C and pH 7, ϕ_F (the quantum yield of fluorescence) is in the range 0.23 to 0.45[12-17] and k_F (the rate constant for fluorescence emission) is in the range 5×10^7 to 1.1×10^8 s^{-1}.[16,18-20]Studies on the effect of temperature on ϕ_F, in the presence and absence of various quenchers (Q) of the fluorescent state

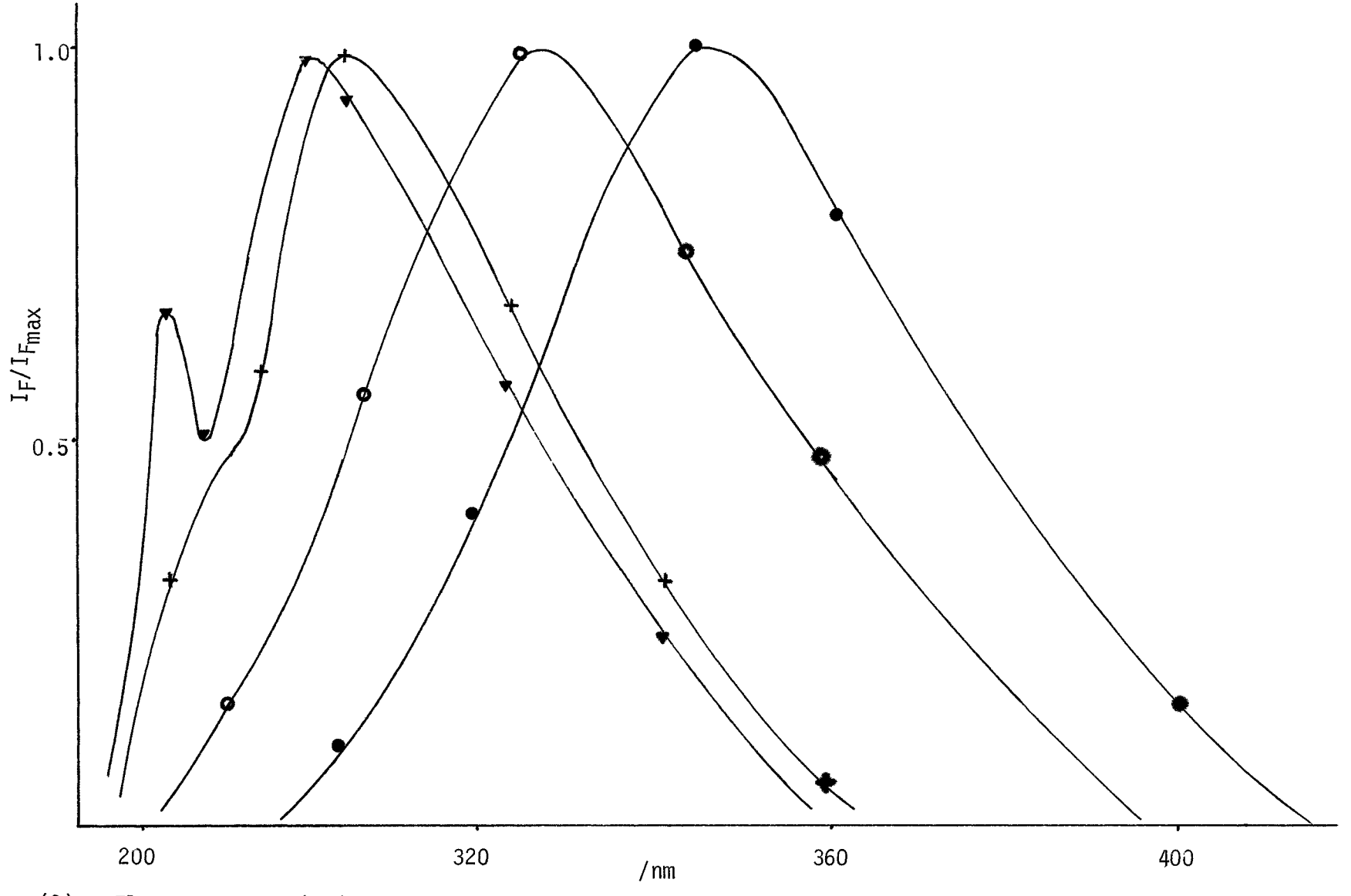

Figure (3): Fluorescence emission spectra of indole in water● ; n-butyl alcohol○ ; diethyl ether✤ ; and pentane▼ .

of indole in water, show that two radiationless deactivation processes, as well as collisional quenching, compete with fluorescence emission to the ground state.[15,18,21] The results of these studies are represented by (1)

$$k_F \left(\frac{1}{\phi_F} - 1 \right) = k_I + k_{II} + k_Q(Q) \qquad (1)$$

where k_I is the specific rate of the temperature independent radiationless deactivation process, $k_{II} = A_{II}e^{-E_{II}/RT}$ is the specific rate of the temperature-dependent radiationless deactivation process, and $k_Q = A_Qe^{-E_Q/RT}$ is the specific rate of the bimolecular quenching reaction involving the quencher at concentration (Q) M. Temperature independent radiationless deactivation, with $k_I \sim k_F \sim 10^8$ s^{-1}, has been considered to be an ISC to the triplet manifold.[15] A variety of interpretations of temperature dependent radiationless deactivation, with $A_{II} \sim 5 \times 10^{16}$ s^{-1}, $E_{II} \sim 48$ kJ mol^{-1} and $k_{II} \sim 2 \times 10^8$ s^{-1} at 25°C, have been made.[21]

Some workers have identified the temperature dependent radiationless deactivation with the photoionization of indole.

Bent and Hayon,[22] for example, observed an hydrated electron (e^-_{aq}) quantum yield, $\phi_{e^-_{aq}} = 0.26$, in 265 nm laser pulsed aqueous solutions of indole at 25°C, which was independent of pH in the range 3 to 11. These workers also found that $\phi_{e^-_{aq}}$ was temperature dependent in the range 10°C to 80°C. An Arrhenius plot of this data yielded

$E \sim 23$ kJ mol^{-1} in the range 10°C to 50°C and $E < 23$ kJ mol^{-1} at temperatures greater than 50°C.[23]

Feitelson[21] found H_2 production, (an indirect measure of photoionization), in UV irradiated (λ_{ex} = 254 nm) aqueous (pH = 3.1) solutions of indole containing 2-propanol to be temperature dependent with $A \sim 10^{18}$ s^{-1} and $E_{apparent} \sim 60$ kJ mol^{-1}.

The negligible temperature dependent quenching of the fluorescence of solutions of indole in cyclohexane,[18] accompanied by the absence of e^-_{aq} in these solutions,[24] has been taken as indirect evidence for identifying temperature dependent radiationless deactivation with photoionization.

Other interpretations of temperature dependent radiationless deactivation include: the formation of exciplexes, which possess charge-transfer-to-solvent character;[8] temperature dependent IC;[12] proton transfer from the excited state of indole to water to form a negatively charged excited species and an hydronium ion;[25] and temperature dependent ISC ($S_1 \rightsquigarrow T_5$) ($E \sim 35$ kJ mol^{-1}).

The effects of solutes on the quenching of indole fluorescence and on the specific rates k_I and k_{II} have been studied by Busel and coworkers[26] (see Table 1).

In general, the addition of these solutes caused ϕ_F to increase and k_{II}, the rate constant for temperature dependent radiationless deactivation, to decrease. Since $E_{II} = 47$ kJ mol^{-1} was unaffected by the solutes, the decrease in k_{II} was due to a decrease in A_{II}, the pre-

Table 1. Effect of Various Solutes (2N) on the Fluorescence of Indole at 25°C.

Solute	λ_{max}	ϕ_F	k_I/k_F	$\frac{k_{II}(\text{solute})}{k_{II}(\text{no solute})}$
pure H_2O	345	0.40 (assumed)	0.33	1.0
KF	346	0.46	0.34	0.70
$NaClO_4$	346	0.46	0.33	0.78
HCOOK	345	0.53	0.35	0.505
CH_3COONa	345	0.52	0.32	0.56
Na_2SO_4	346	0.46	0.34	0.75
LiCl	345	0.41	0.48	0.80
NaCl	345	0.42	0.48	0.80
KCl	345	0.43	0.43	0.75
$MgCl_2$	346	0.40	0.51	0.83
$CaCl_2$	347	0.41	0.49	0.81
NH_4Cl	345	0.34	0.75	0.79
$NH_3^+CH_2COO^-$	--	0.12	7.50	1.00

exponential factor for temperature dependent deactivation. The solute quencher effect on k_{II} was primarily an anionic quencher effect. Since no evidence was found for the formation of indole-ion complexes, it was concluded that the observed effects on k_{II} were due to solute induced changes in the properties of the solvent. The value of k_I, the rate constant for temperature independent deactivation, was increased by chloride-containing solutes and was unaffected by most other solutes. It was suggested that the value of k_I was increased by Cl^- ions by the heavy atom effect on ISC. Large increases in k_I, caused by additions of Br^- and I^- ions by the same heavy atom effect, have also been observed.[27] It has been shown in pH effect studies that ϕ_F is independent of pH in the range 2.5 to 10.5[22] and k_I and k_{II} are independent of pH in the range 3.1 to 7.

Photoionization of indole (IH) in water at pH 7 produces an hydrated electron (e^-_{aq}), the spectrum of which is shown in Figure 4,[28] and an indole radical cation ($IH^{+\cdot}$).[22] (2)

$$IH + h\nu \longrightarrow e^-_{aq} + IH^{+\cdot} \qquad (2)$$

While many studies have been performed on the decay kinetics of the hydrated electron, produced in the flash photolysis of indole derivatives,[22,29,30] no comparable studies have been performed on the decay kinetics of the hydrated electron, produced in the flash photolysis of indole.

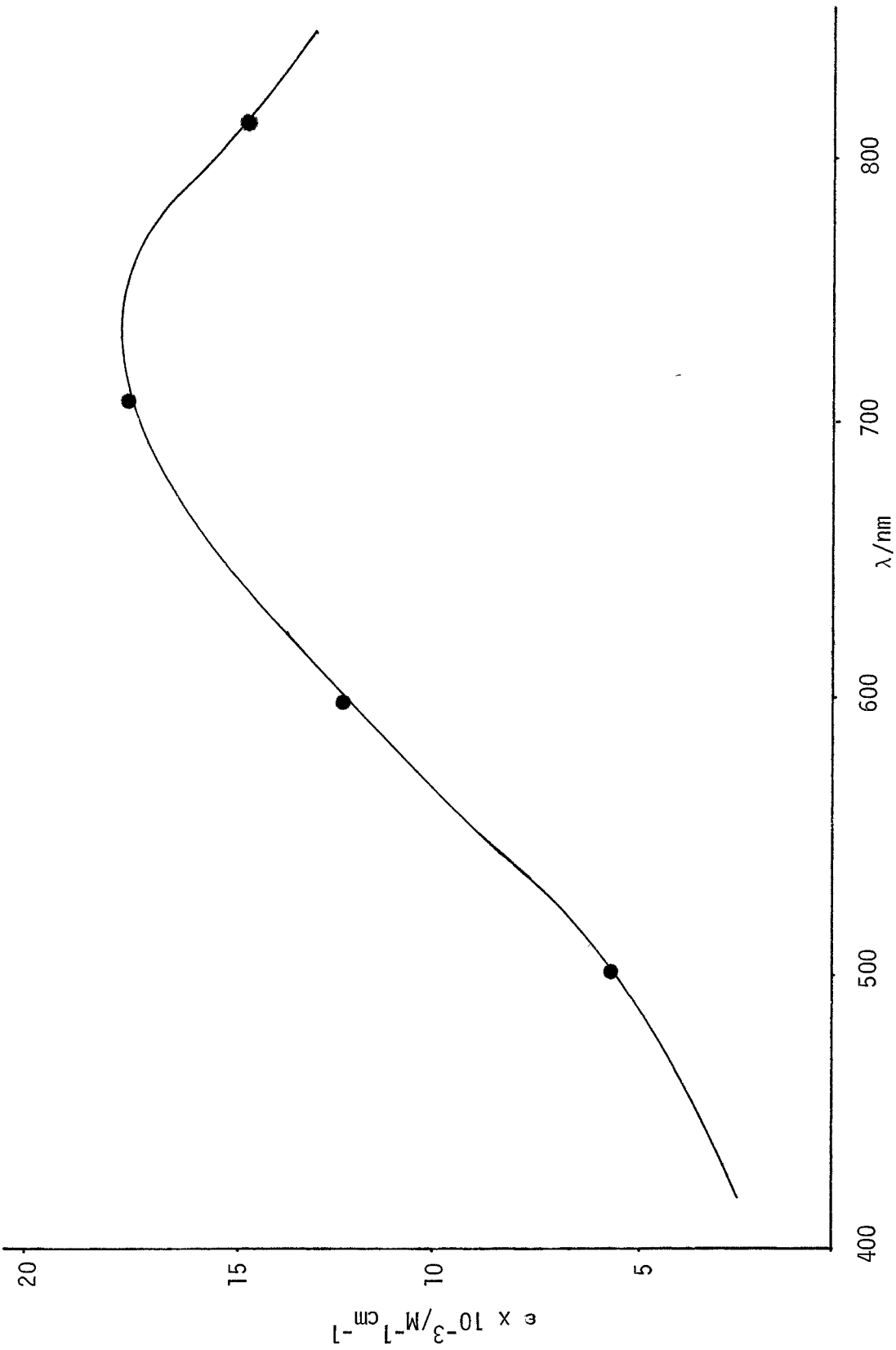

Figure (4):: Absorption spectrum of e^-_{aq} at 25°C.

Bryant et al.[29] studied the decay kinetics of e^-_{aq} produced in 265 nm laser pulsed aqueous solutions of tryptophan (TH) having pH values in the range 4.6 to 11.8. In solutions having (TH) = 1.5×10^{-3}M and pH = 7 , the hydrated electron was expected to decay by reactions (3) and (4) with specific rates 1.1×10^{10} M^{-1} s^{-1},[31] and 3.6×10^{8} M^{-1} s^{-1},[31] respectively.

$$e^-_{aq} + e^-_{aq} \longrightarrow H_2 + 2OH^- \qquad (3)$$

$$e^-_{aq} + TH \longrightarrow TH^{\bullet -} \qquad (4)$$

However, at very short times after the completion of the 17 ns laser pulse, it was found that electron decay was exponential with $t_{1/2} = 8 \times 10^{-7}$ s.

The disappearance of an hydrated electron-neutral radical complex (e^-_{aq}...T•) (reaction 5) was assumed to represent the decay. It was further assumed that within the primary tryptophan radical cation ($TH^{+\bullet}$)-hydrated electron pair, deprotonation took place very rapidly ($k = 1.5 \times 10^{6}$ s^{-1}) to form the (e^-_{aq}...T•) complex.

$$(T^{\bullet}...e^-_{aq}) \xrightarrow{H^+} TH \qquad (5)$$

Although a process analogous to (5) has not been identified in laser flash photolysis studies of indole in water, a process analogous to (4) is known to exist. This process is represented by (6), the specific rate of which is $k = 1.9 \times 10^{8}$ M^{-1} s^{-1}.[32]

$$e^-_{aq} + IH \longrightarrow IH^{-\bullet} \qquad (6)$$

According to Bent and Hayon,[22] the quantum yields for the hydrated electron ($\phi_{e^-_{aq}}$), indole radical cation ($\phi_{IH^{+\bullet}}$), indolyl neutral radical ($\phi_{I\bullet}$), and triplet state ($\phi_{^3IH^*}$), observed in the 265 nm laser flash photolysis of aqueous solutions of indole at 25°C, were found to be pH independent in the range 2.5 to 10.5 (Fig. 5). Above pH 10.5, the yields of all of the above species, as well as ϕ_F, decreased. Also, since temperature dependence studies showed that $\phi_{e^-_{aq}}$, $\phi_{IH^{+\bullet}}$ and $\phi_{I\bullet}$ increase and ϕ_F and $\phi_{^3IH^*}$ decrease with increasing temperature (Fig. 6) it was suggested that S_1^v was the hydrated electron precursor. However, Klein et al.[33] discovered that fluorescence lifetimes, as well as fluorescence quantum yields, of indole in aqueous solution decreased with increasing temperature. The observation of this effect on fluorescence lifetimes led to the suggestion that S_1^0, not S_1^v, was the hydrated electron procursor.

CTTS states may also be hydrated electron precursors since hydrated electron yields are known to increase with increasing bulk dielectric constant of the solvent.[5] The formation of CTTS states (solvated Rydberg states) has also been proposed by Busel et al.,[26] Feitelson,[21] Ottolenghi et al.[34] and Muto et al.[35] as photoionization intermediates in indole and other aromatic molecules.

As mentioned previously, photoionization of indole in water produces an hydrated electron and an indole radical cation, $IH^{+\bullet}$. The

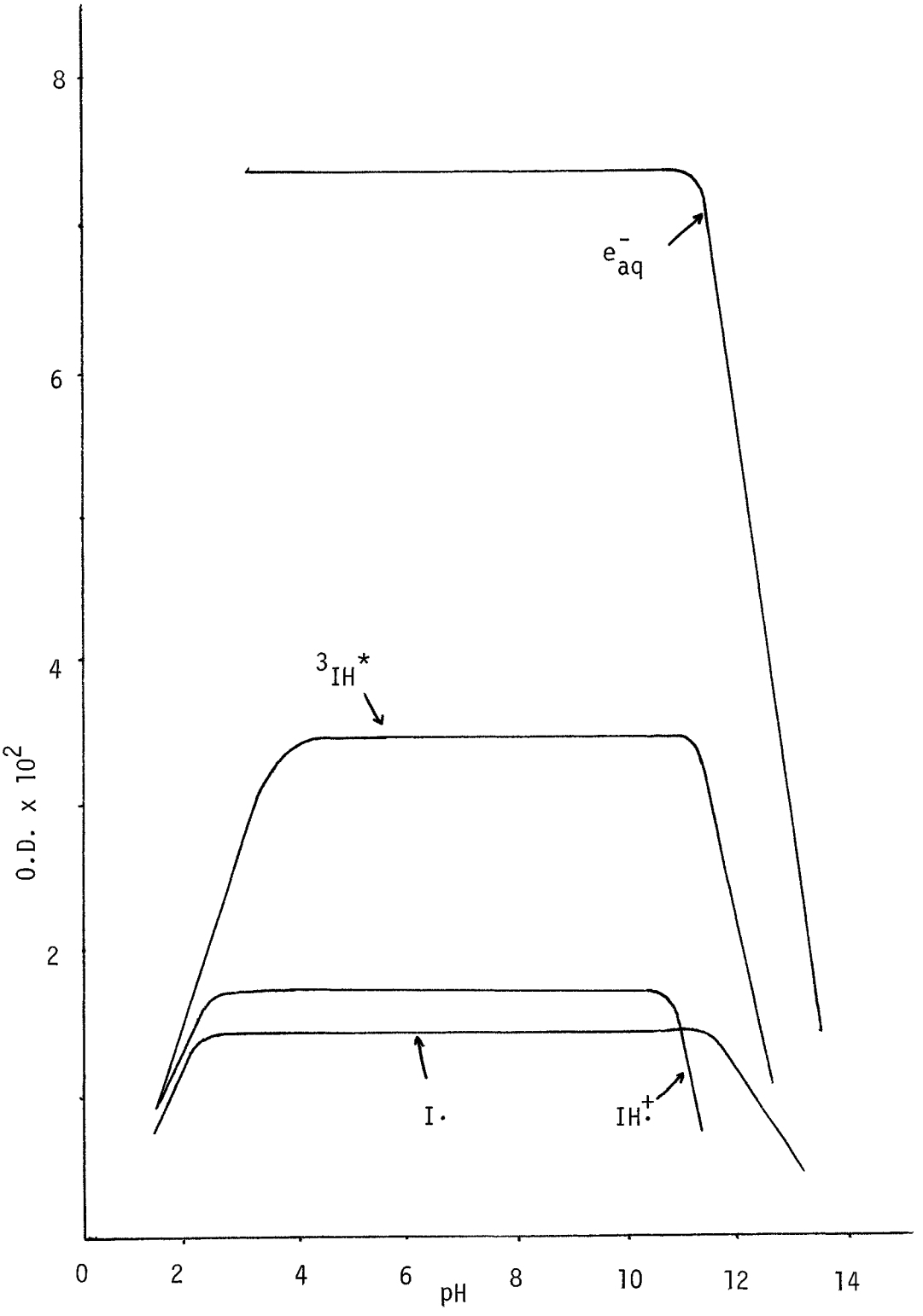

Figure (5): pH dependence of quantum yields of transient species produced in the laser photolysis of 1.5 x 10^{-4}M indole in O_2-free water at 25°C

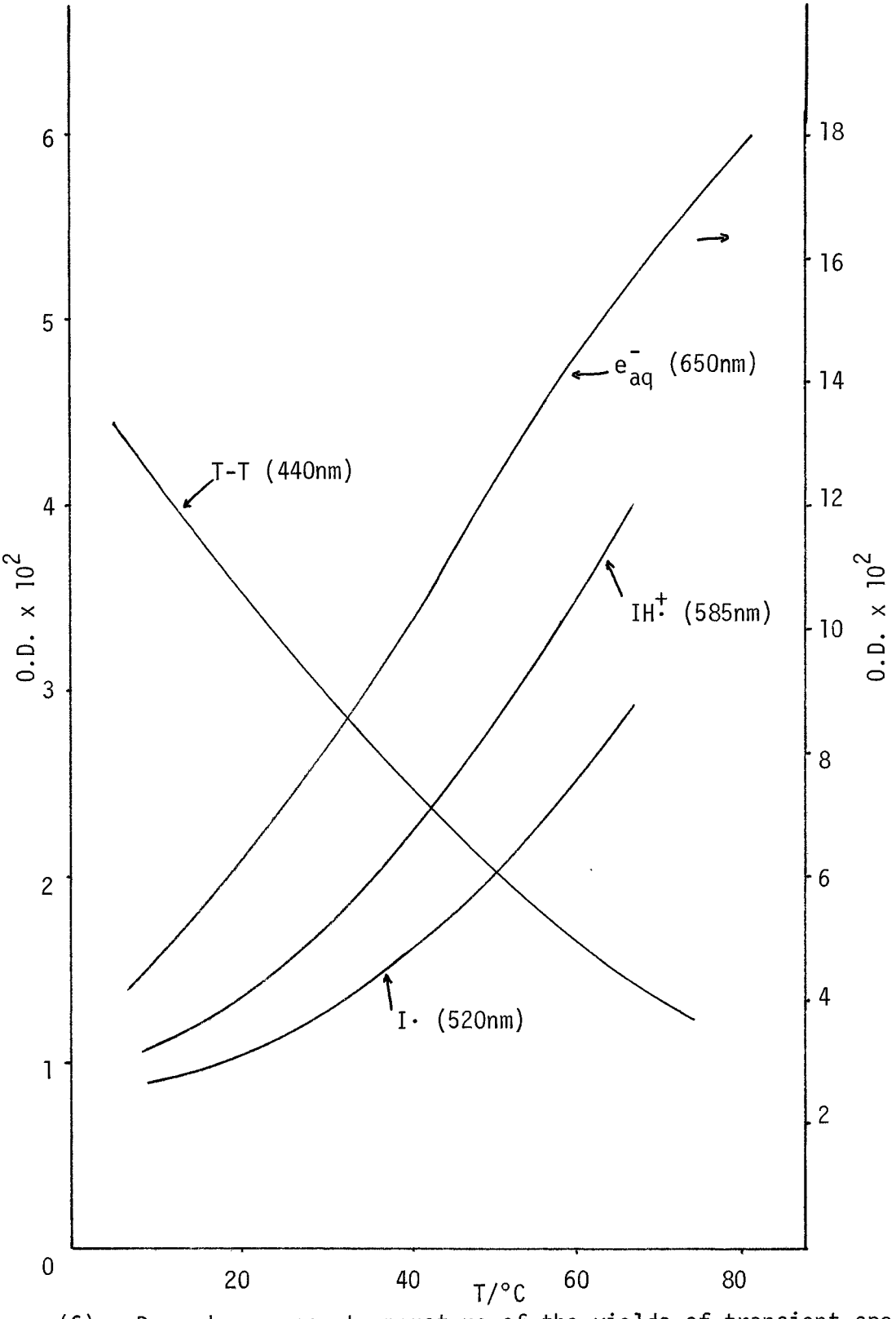

Figure (6): Dependence upon temperature of the yields of transient species produced from the laser photolysis of indole (1.5×10^{-4}M) at pH 7.5

absorption spectrum of $IH^{+}_{\bullet}$, as determined by Bent and Hayon, is shown in Figure 7.[22] The value of λ_{max} (λ_{max} = 585 nm) agrees well with the λ_{max} value found for the tryptophan radical cation formed in pulse radiolysis experiments performed by Posener et al.,[36] (λ_{max} = 570 nm). It has been suggested that $IH^{+}_{\bullet}$ also undergoes a very fast deprotonation (7) to form the indolyl neutral radical, I•.[22,29,37,38]

$$IH^{+}_{\bullet} \longrightarrow I\bullet + H^{+} \qquad (7)$$

The specific rate of (7) was found to be 10^4 to 10^5 s^{-1},[22] and 10^6 s^{-1},[22] at pH 3 to 4 and pH 7.5, respectively.

The absorption spectrum of the indolyl neutral radical (λ_{max} = 530 nm) is shown in Figure 8.[22] Second order radical-radical (8) and radical-electron (9) reactions have been suggested to account for the disappearance of the indolyl neutral radical.

$$I\bullet + I\bullet \longrightarrow \text{products} \qquad (8)$$

$$I\bullet + e^{-}_{aq} \xrightarrow{H^{+}} IH \qquad (9)$$

While the specific rate for recombination of neutral tryptophan radicals is known ($k = 2.4 \times 10^9$ M^{-1} s^{-1}),[39] the specific rate for recombination of indolyl neutral radicals has not been determined.

Although evidence has been found for the production of the indolyl neutral radical and H atoms, by N-H bond cleavage in irradiated solutions of indole in cyclohexane,[24] no H atoms have been detected in

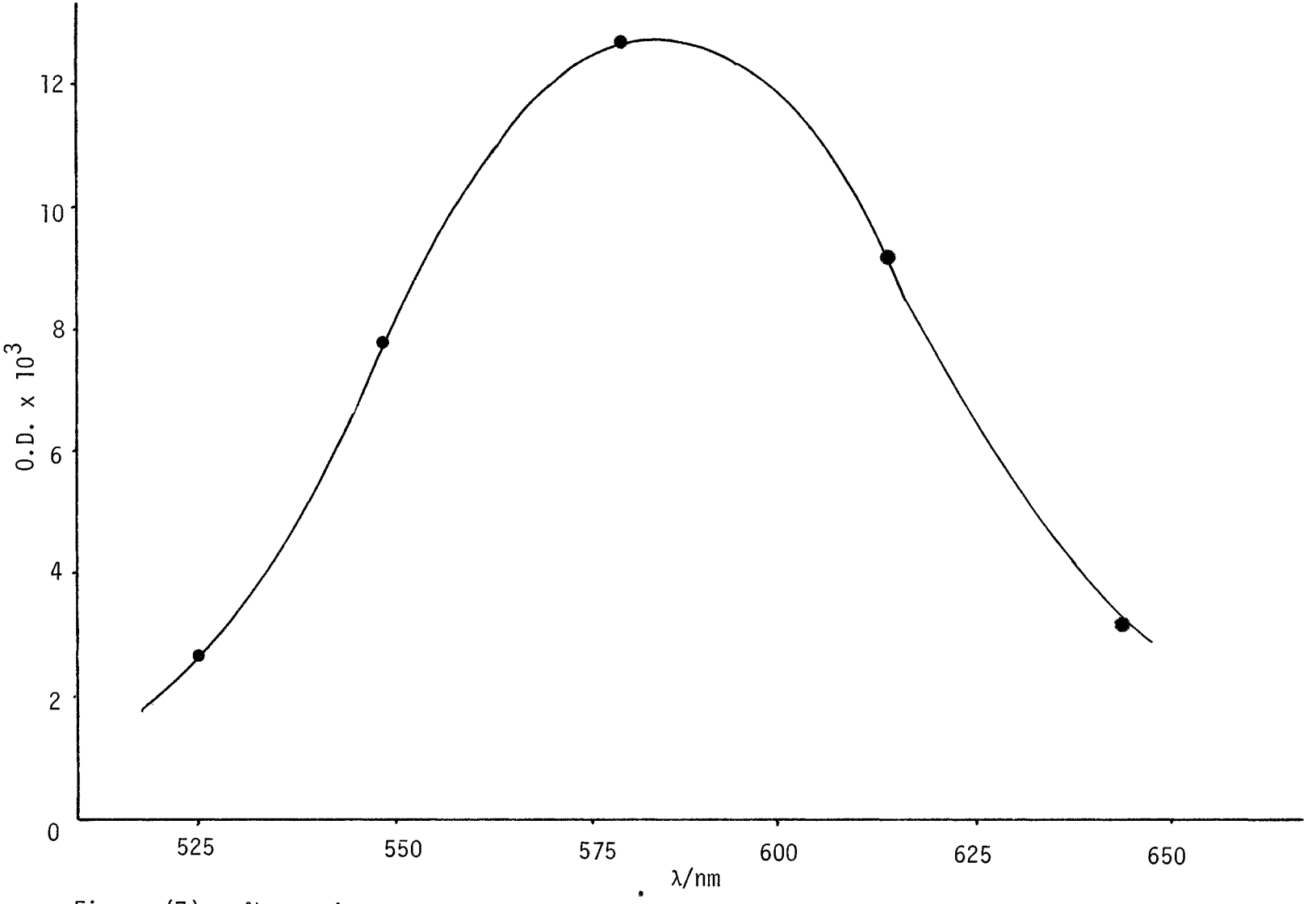

Figure (7): Absorption spectrum of the indole radical cation

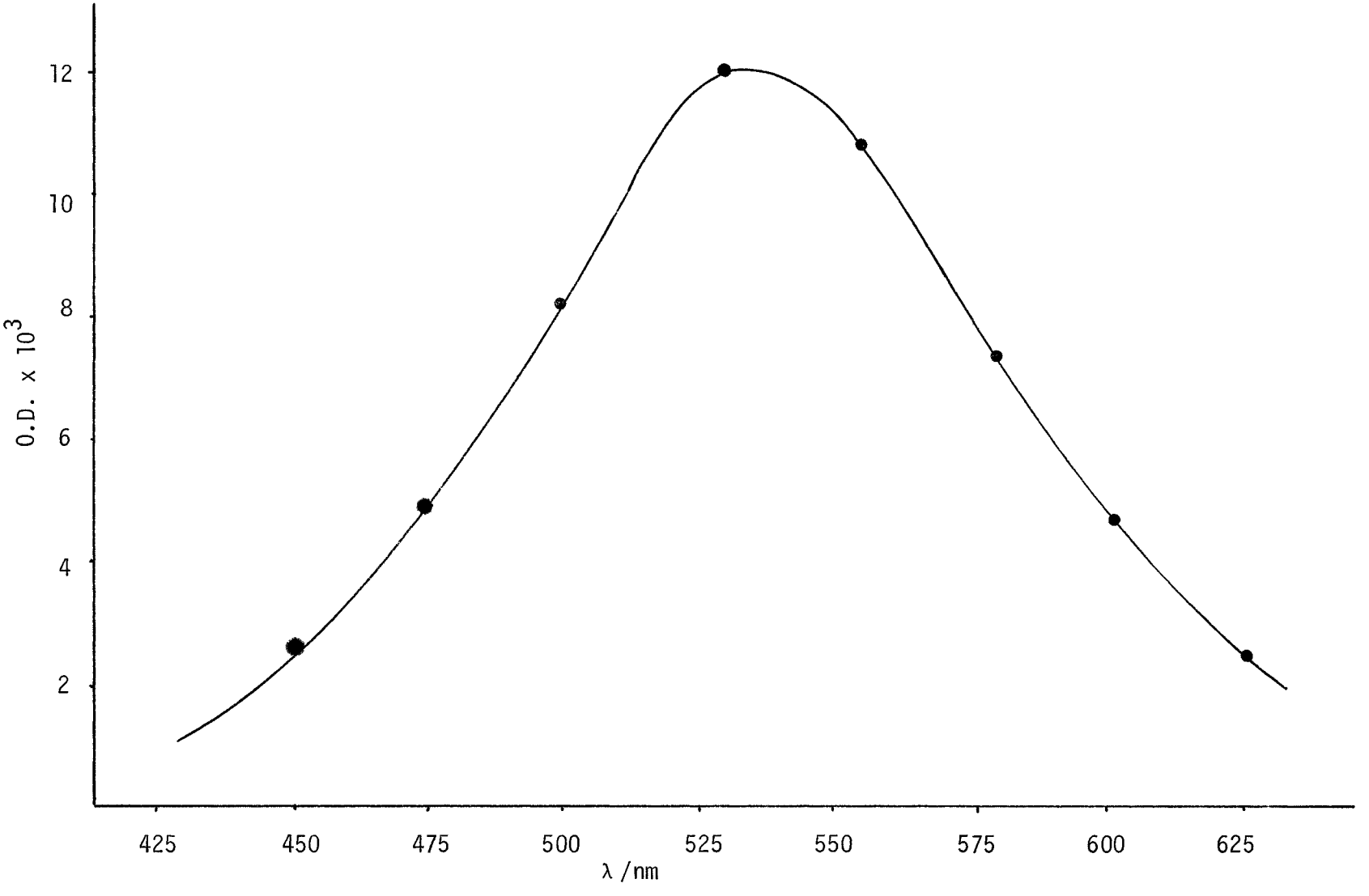

Figure (8): Absorption spectrum of the indolyl neutral radical

irradiated aqueous solutions of indole,[21] indicating N-H bond cleavage does not take place in water. This would suggest that radical cation deprotonation is the only source of indolyl neutral radicals in aqueous systems.

Triplet-triplet absorption is observed following $S_0 \longrightarrow S_1$ excitation of indole in water. A triplet-triplet absorption band (λ_{max} = 440 nm), corresponding to the transition $T_1 \longrightarrow T_6^V$, has been observed in laser and conventional flash photolysis studies of aqueous solutions of indole and indole derivatives.[22,29,37,39]

The triplet-triplet absorption spectrum of indole in water at pH 7.5 and 25°C is shown in Figure 9.[22] This absorption was found to decay by a first order process, independent of indole concentration up to 10^{-3} M, with rate constant $k = 8.6 \times 10^4\ s^{-1}$.[22] Diffusion controlled triplet quenching by oxygen occurs with rate constant $k = 5.3 \times 10^9\ M^{-1}\ s^{-1}$, which is comparable with oxygen quenching rate constants for the triplet states of other N-heterocyclic compounds.[40] It is generally believed that the formation of T_1 states occurs by ISC from S_1^0 to T_4 followed by fast internal conversion $T_4 \rightsquigarrow T_1$ within the triplet manifold.

In this study, fluorescence lifetimes and spectra, as well as production rates and decay kinetics of the hydrated electron, indole radical cation, indolyl neutral radical and triplet state, have been obtained in the presence and absence of various inorganic solutes. The solutes chosen were O_2 and $CdSO_4$, which are good electron scavengers[41,46]

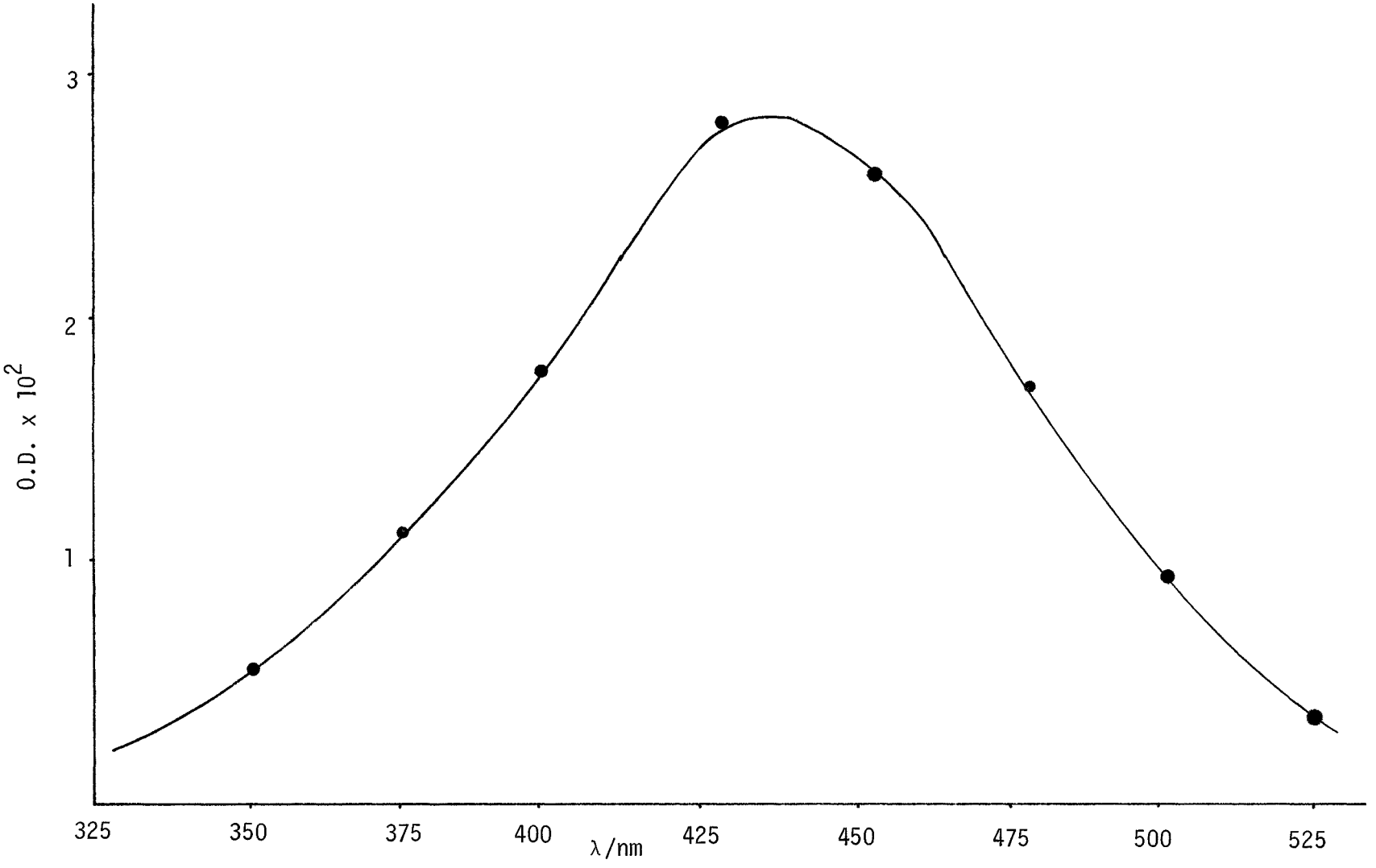

Figure (9): Indole triplet-triplet absorption sprectrum.

and promoters of ISC,[42] and $BaCl_2$ and NaBr which are good promoters of ISC[42] but which are relatively poor electron scavengers.[45]

It was anticipated that an improvement in our understanding of the primary photophysics and photochemistry of indole in aqueous solutions would be achieved thereby.

EXPERIMENTAL

I. Materials

Indole (C_8H_7N) (99.8%) and sodium bromide (NaBr (99%) were "reagent" grade from BDH Chemicals Ltd. Barium chloride dihydrate ($BaCl_2 \cdot 2H_2O$), sodium acetate trihydrate ($CH_3COONa \cdot 3H_2O$), 1,10 phenanthroline hydrate ($C_{12}H_8N_2 \cdot H_2O$), and sulphuric acid (H_2SO_4) were "analytical reagent" grade from BDH Chemicals Ltd. Cadmium sulphate ($CdSO_4$) was "reagent" grade from Fisher Scientific Company. Potassium ferrioxalate ($K_3[Fe_3(C_2O_4)_3] \cdot 3H_2O$) was "reagent" grade from Oxford Organic Chemicals. Glacial acetic acid (CH_3COOH) was "certified ACS reagent" grade from Allied Chemical and Caledon Laboratories Ltd. and "reagent" grade from BDH Chemicals Ltd. Xenon was "assayed" grade (99.995%) from Air Reduction Company, Inc. Helium was from Union Carbide Ltd.

Water was doubly distilled with a Corning AG-2 distilling apparatus.

II. Flash Photolysis Apparatus

Flash photolysis took place between a parallel pair of series-connected linear quartz flash lamps (Fig. 10) filled with 10 Torr xenon, as measured by a calibrated Alphatron 530 vacuum gauge. Flashes were produced by pulse-initiated discharge of 2,106 J stored in four, parallel-connected Sangamo laser energy storage capacitors ($C = 4.2115 \times 10^{-5}$ F) charged to 10 kV by a Hammond high voltage power supply. A block diagram of the pulsing system used, which had a variable time delay in the range 1 μs to 0.999 s, is shown in Appendix 1.

III. Kinetic Spectrophotometry

Figure 11 shows the optical train involved in the flash photolysis-kinetic spectrophotometric measurements. Kinetic spectrophotometry was performed at 632.8 nm, 585.0 nm, 530 nm and 457.9 nm with the monitoring sources indicated in Table 2. In addition, Jena Glaswerk Schott and Gen. transmission filters were used to ensure that only first order radiation was detected. The cutoffs (in nm) of these filters are also shown in Table 2. Monitoring source outputs passed through a collimating lens, the photolysis cell, a cylindrical focussing lens, and into a grating monochromator. Photomultiplier detection of monitoring source outputs was used.

The grating monochromator was a Jarrell Ash Czerny Turner model 78-446 with a 1 metre focal length and a range in air of 190 nm to

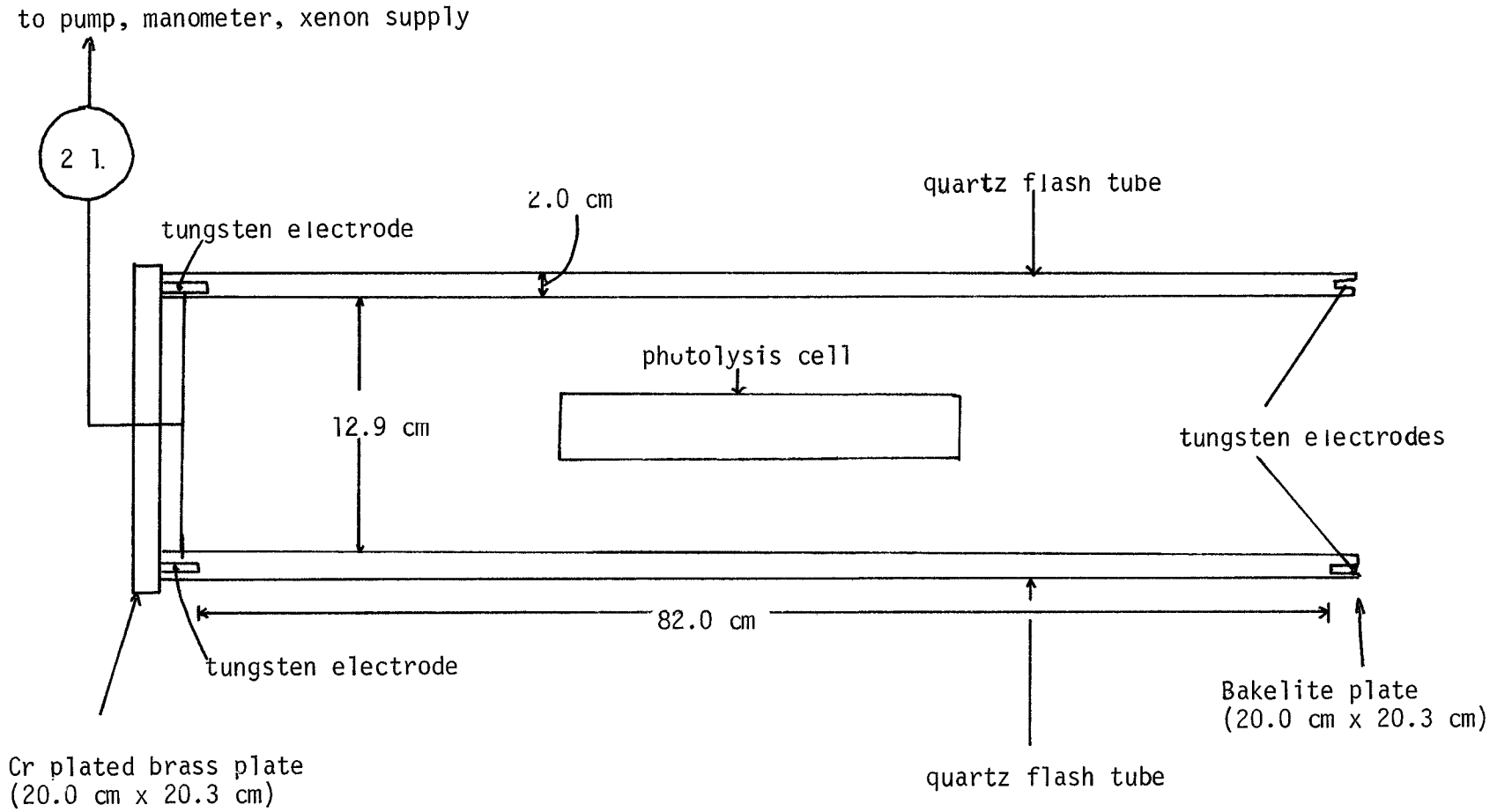

Figure (10): Flash Photolysis Apparatus.

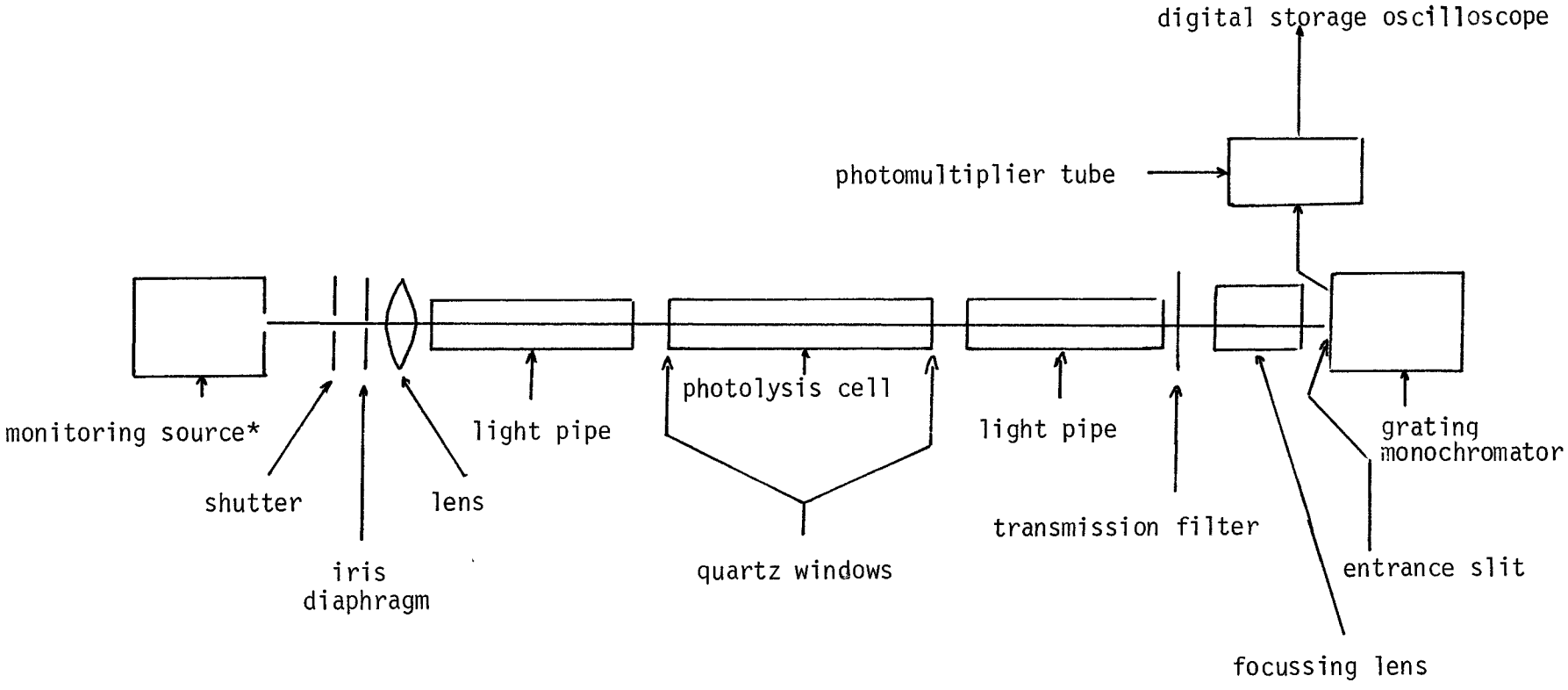

* see table ( )

Figure (11): Optical Train
(linearity of optical train verified by the use of neutral density filters).

Table 2. Monitoring Sources and Transmission Filters used in Kinetic Spectrophotometry.

Monitoring Wavelenth (nm)	Monitoring Source	Transmission Filter and Cutoff Wavelength (nm)
632.8	Electro Optics Associates LAS 2002 Helium-Neon Laser	OG 515, 490 nm
585.0	Philips 6550 15 Volt, 150 Watt Quartz-I_2 lamp or Sylvania 24 Volt, 150 Watt Quartz-I_2 lamp	GG 375, 340 nm
530.0	Philips 6550 15 Volt, 150 Watt Quartz-I_2 lamp or Sylvania 24 Volt, 150 Watt Quartz-I_2 lamp	GG 375, 340 nm
457.9	Coherent Radiation CR-3 Argon ion laser	WG 305, 260 nm

1600 nm. The grating was of the plane replica reflection type (102 mm by 102 mm) with 1180 grooves mm^{-1} and was blazed at 500 nm. The reciprocal linear dispersion at the exit slit was 8.2 Å mm^{-1}. This gave a band width of 0.041 nm when an entrance slit width of 50 μ was used.

The photomultiplier was an Hammamatsu model TV-R106. This nine stage photomultiplier had a fused silica window and an Sb-Cs photocathode. The photomultiplier power supply was either a Keithley 240A High Voltage Supply or a Harrison 6515A Hewlett Packard Power Supply. Figure 12 shows the spectral response of the photomultiplier.[49]

After preamplification, photomultiplier outputs were delivered to a Gould OS4000 "Advance" 10 MHz Digital Storage Oscilloscope equipped with a Gould 4001 digital-to-analog conversion output unit. The oscilloscope had a maximum sampling rate of 1.8 MHz equivalent to 0.55 μs per point. Hard copy data were recorded on a Coleman Hitachi 165 strip chart recorder.

Photolysis was carried out in a jacketted cylindrical quartz cell with path length = 39.5 cm and inner diameter 2.5 cm (Fig. 13). Before each run, the cell was rinsed several times with singly distilled and then doubly distilled water and dried on a vacuum line. Glacial acetic acid was placed in the cell jacket as an optical filter to ensure that only $S_0 \longrightarrow S_1$ excitation took place. The transmission spectrum of glacial acetic acid is shown in Figure 14 in relation to the absorption spectrum of indole.

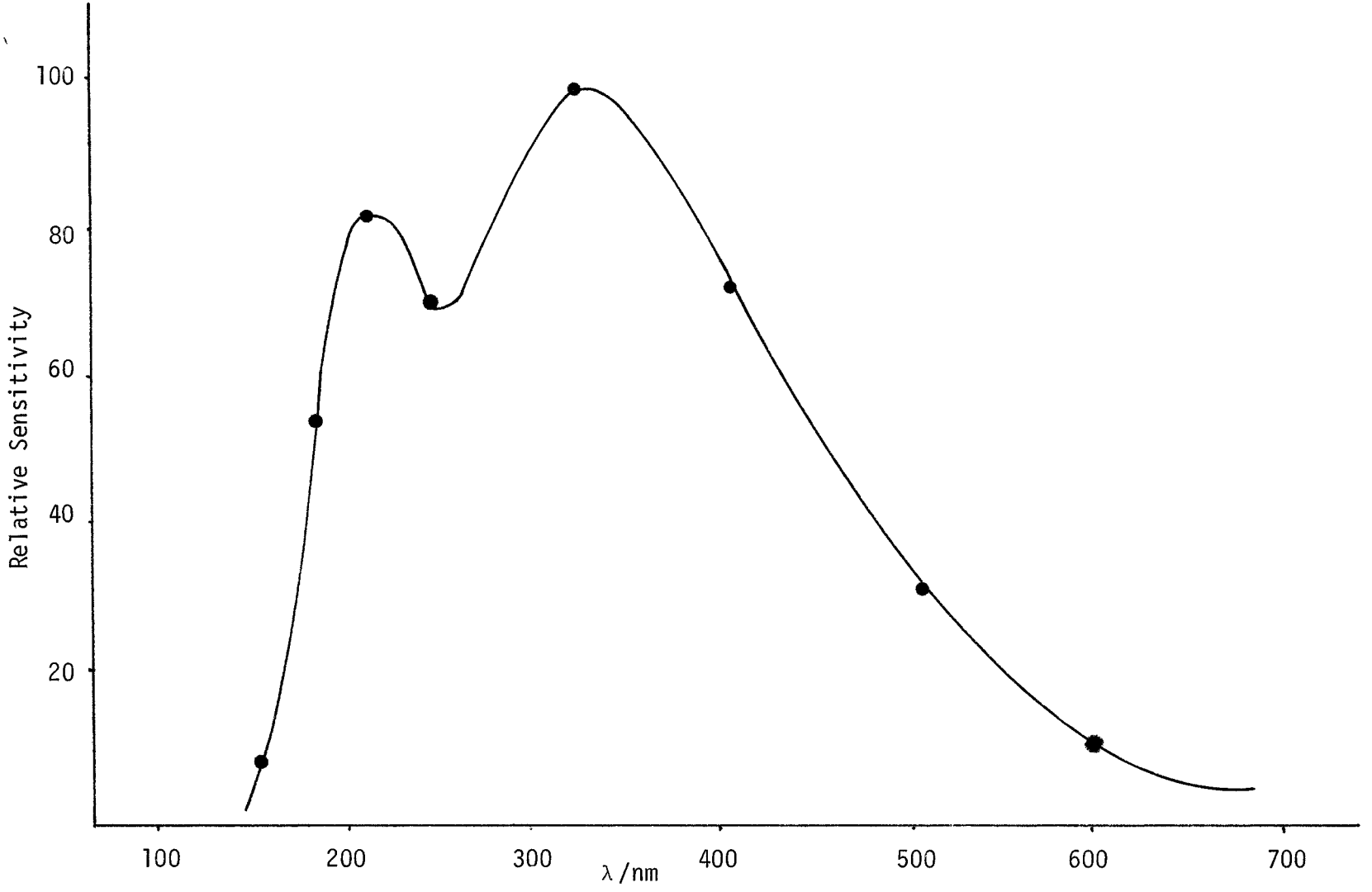

Figure (12): Spectral response of Hammamatsu R106 photomultiplier.

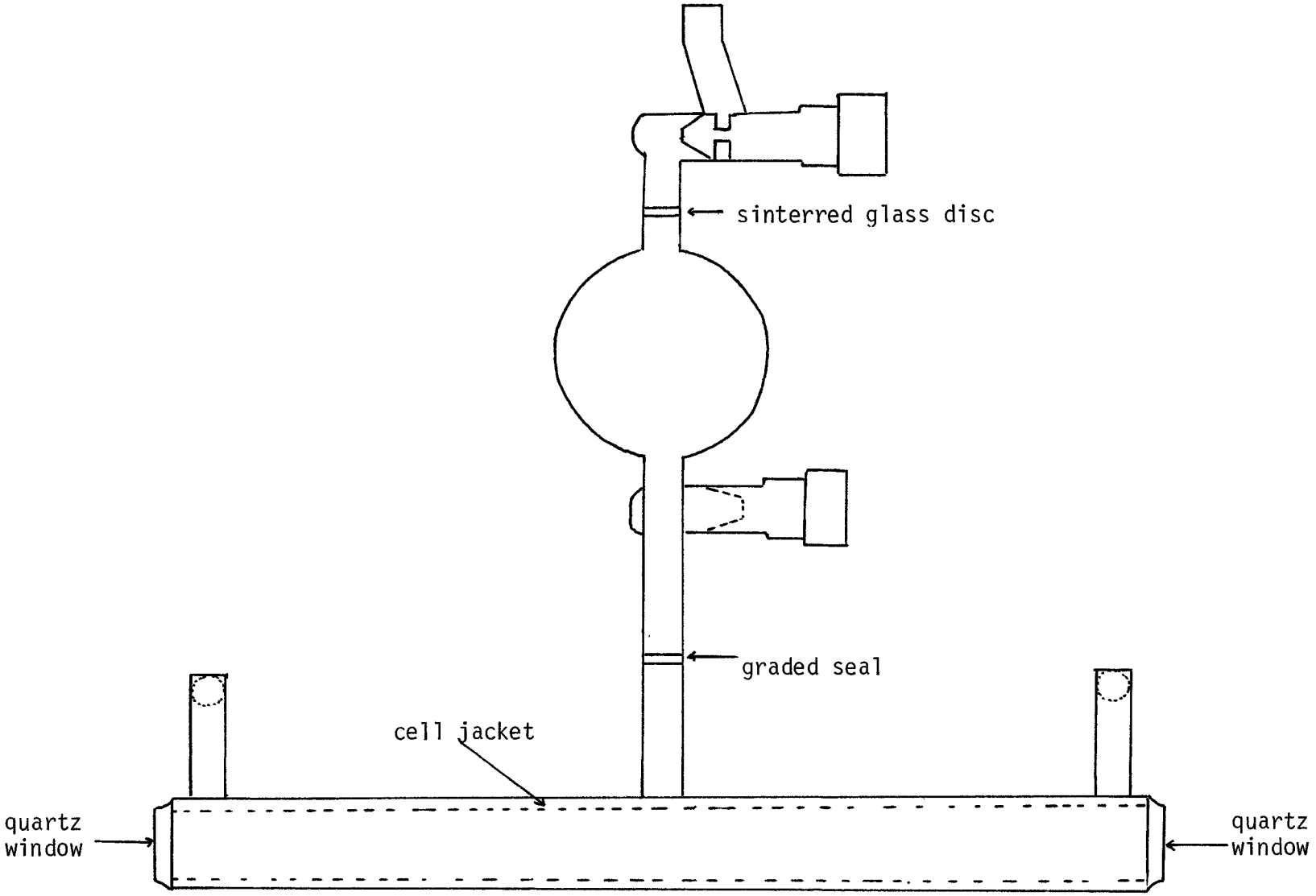

Figure (13): Flash Photolysis Cell

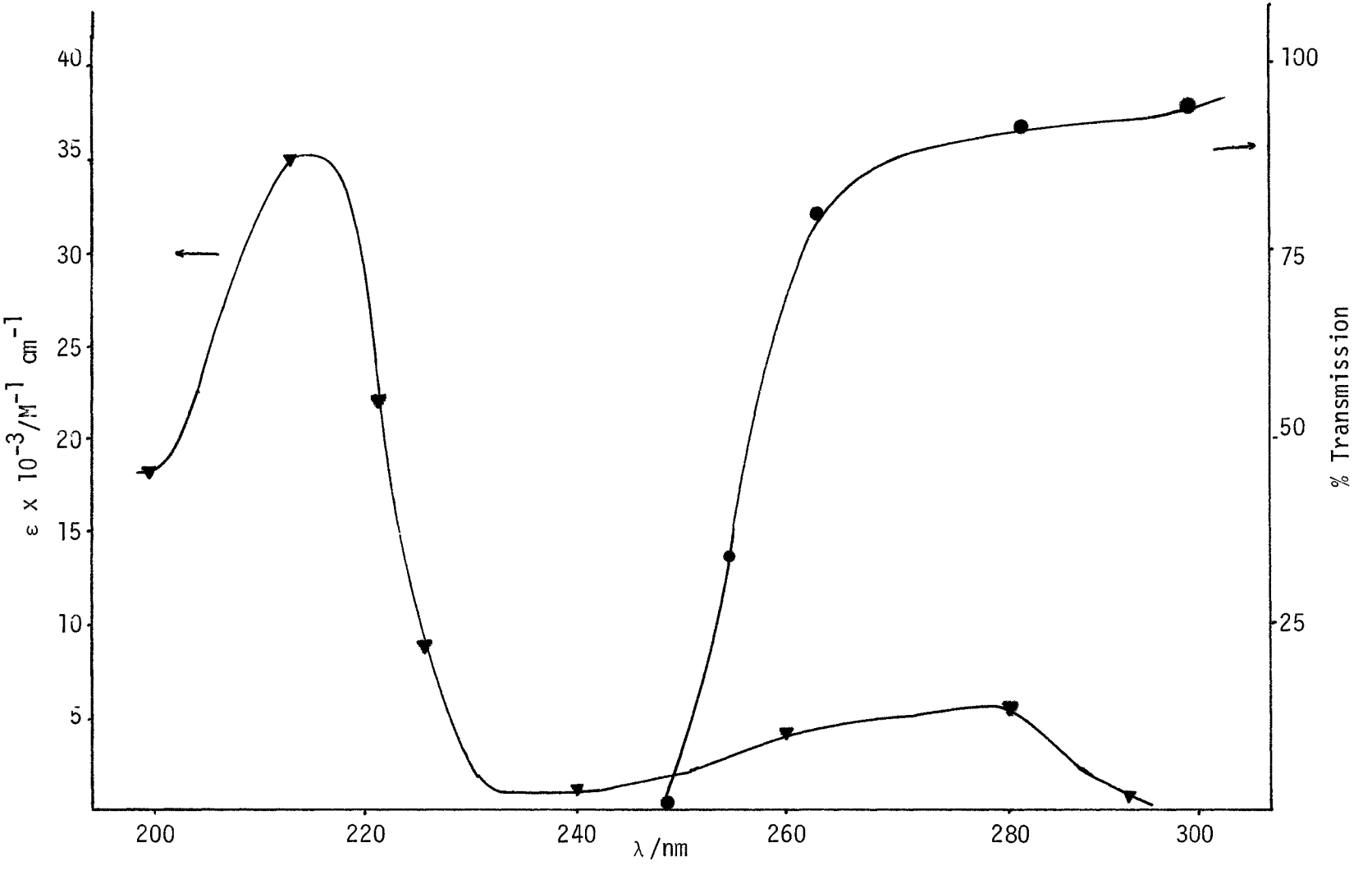

Figure (14): Transmission spectrum of glacial acetic acid (1.0 cm) in relation to the absorption spectrum of indole in water.

Solutions containing 5×10^{-4} M indole in water were prepared by adding 0.0586 grams of indole (M.W. = 117.15) to a one-litre volumetric flask containing ∿500 mL doubly distilled water with 20 minutes vigorous shaking. The flask was then filled to the mark with doubly distilled water. Solutions containing 5×10^{-4} M indole plus ∿5×10^{-6} M $CdSO_4$ were prepared by adding 0.0586 grams of indole and 0.0010 grams of $CdSO_4$ (M.W. = 208.4) to a one-litre volumetric flask containing ∿ 500 mL doubly distilled water with 20 minutes vigorous shaking. The flask was then filled to the mark with doubly distilled water. Solutions containing 5×10^{-4} M indole and 1×10^{-3} M $CdSO_4$ were prepared by adding 0.0586 grams of indole and 0.2084 grams of $CdSO_4$ to a one-litre volumetric flask containing ∿500 mL doubly distilled water with 20 minutes vigorous shaking. The flask was then filled to the mark with doubly distilled water. Solutions containing 5×10^{-4} M indole and 1.0 M NaBr were prepared by adding 25.73 grams of NaBr (M.W. = 102.9) to 250 mL of 5×10^{-4} M indole solution. Solutions containing 5×10^{-4} M indole and 0.25 M $BaCl_2 \cdot 2H_2O$ were prepared by adding 15.26 grams of $BaCl_2 \cdot 2H_2O$ (M.W. = 244.28) to 250 mL of 5×10^{-4} M indole solution. In some cases, it was necessary to filter the indole-$BaCl_2 \cdot 2H_2O$ solution before proceeding.

Absorption spectra and pH measurements were obtained for certain representative solutions prior to and after photolysis. Absorption spectra in the range 450 nm to 200 nm were obtained using a Cary 14 UV-visible spectrophotometer with 1 cm path length quartz cells. pH

measurements were made using a Fisher glass electrode, a Fisher calomel reference electrode and a Fisher Accumet model 210 pH meter.

Approximately 155 mL of the solution to be photolyzed was placed in the photolysis cell. With the cell in an inverted position (Fig. 15), helium was allowed to pass through the solution for 6.5 hours. The presence of a sinterred glass disc ensured uniform degassing of the solution by breaking up the flow of helium. Absorption spectra taken before and after degassing showed a negligible change in indole concentration.

The filled photolysis cell was then placed in the monitoring beam and the positions of the lenses of the optical train were adjusted to give a maximum photomultiplier output. The monochromator was adjusted to the monitoring wavelength and the monochromator entrance slit width and slit height, photomultiplier voltage, oscilloscope vertical sensitivity, oscilloscope sweep rate and pulsing unit time delay were selected according to Table 3. Also found in Table 3 are the monitoring sources used for each wavelength, the monochromator band width and the approximate photomultiplier output voltage observed.

The storage capacitors were charged to 10 kV and then discharged. Kinetic oscilloscope traces obtained at monitoring wavelengths of 530 nm, 585 nm and 632.8 nm showed considerable stray light. No stray light was observed at 457.9 nm. Observed kinetic traces obtained at 530 nm, 585 nm and 632.8 nm were corrected for the presence of the stray light pulses, as shown in Figure 16, yielding corrected transient

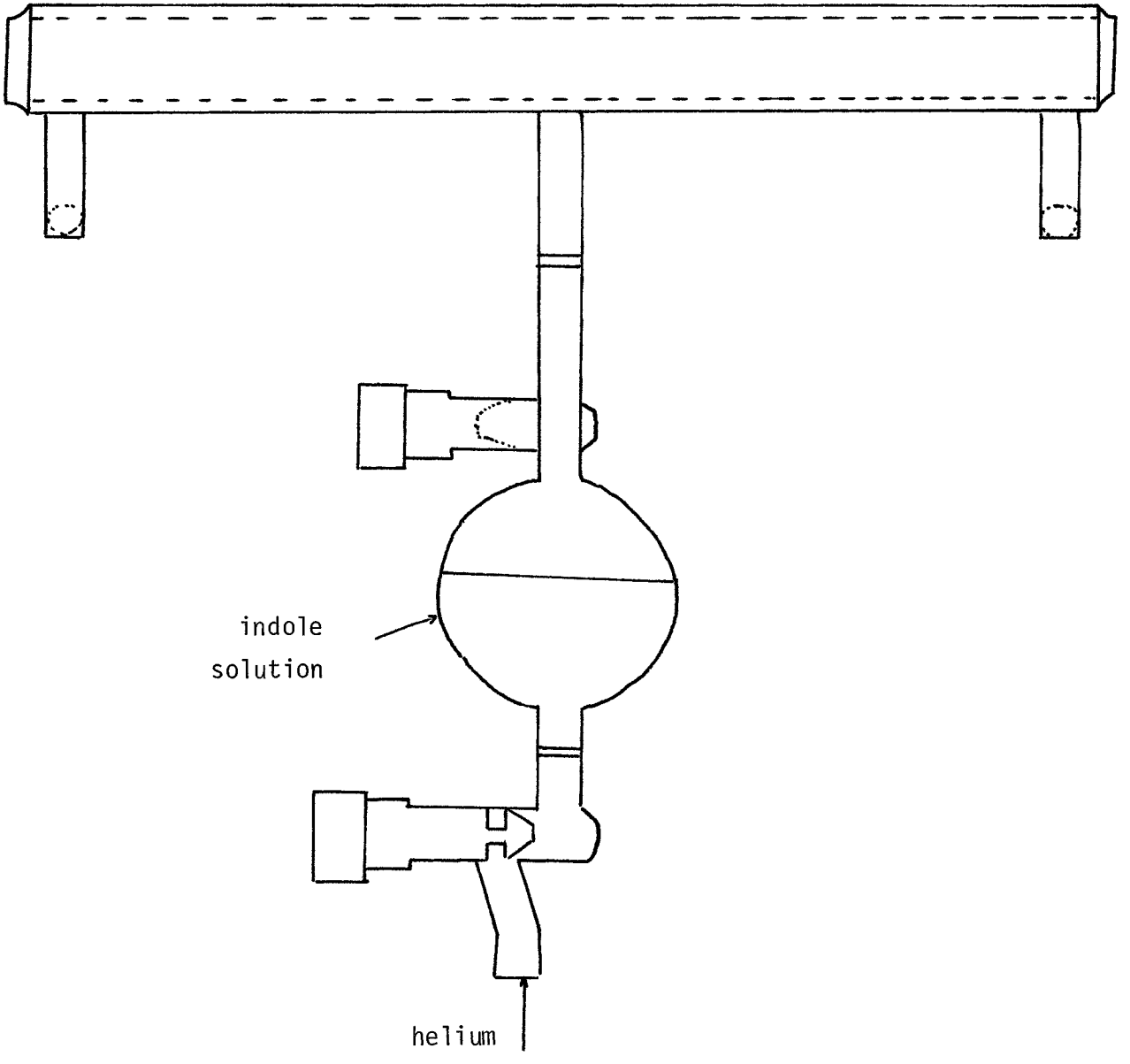

Figure (15) Inverted photolysis cell filled with indole solution

Table 3. Monochromator, Photomultiplier and Oscilloscope Parameters used in Kinetic Spectrophotometry.

Monitoring wavelength (nm)	Monitoring source	Comments	Monochromator band width (nm)	Monochromator slit height (mm)	Voltage applied to photo-multiplier (V)	PM output voltage (V)	Oscilloscope vertical sensitivity (V/cm)	Sweep rate (μs/cm)
632.8	He-Ne laser	--	0.041	4	∿350	∿2.54	0.5	50
585.0	Quartz-I_2 lamp	24 volt lamp was driven at 25 V, 15 V lamp was driven at 16.5 V	0.164	4	∿400	∿0.6	0.2	50
530.0	Quartz-I_2 lamp	"	0.164	4	∿400	∿0.7	0.2	200
457.9	Argon ion laser	--	0.033	4	∿270	∿2.5	0.5	50

Pulsing unit delay time = 50 μs.

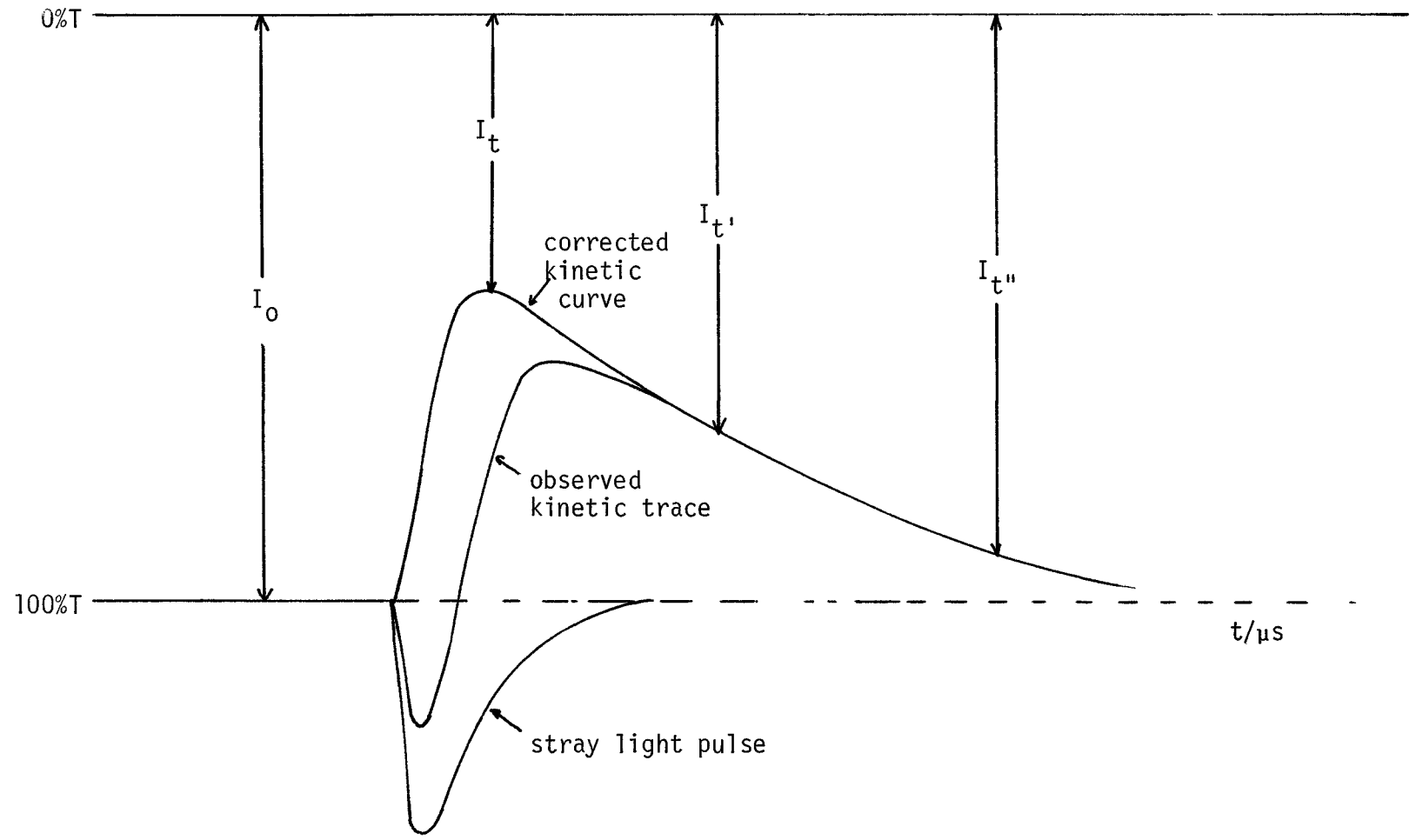

Figure (16): An example of the observed kinetic trace, stray light pulse, corrected kinetic curve, I_o and I_t.

kinetic curves. In order to obtain the 0% T line shown in Figure 16, the monitoring beam was shuttered, and with no energy stored in the capacitors, the pulsing unit was triggered. With the corrected kinetic curve and the 0% T line, it was possible to measure I_0 and I_t as shown in Figure 16. It was found (see Results) that it was necessary to process "first shot" data exclusively since repeated flash photolysis-kinetic spectrophotometry on the same solution resulted in a permanent change in the absorbance of that solution due to the accumulation of stable, absorbing photolysis products.

IV. Determination of Transient Concentration

Total absorbance at time t (A_t) is defined by (10)

$$A_t = \log_{10}(I_0/I_t) \tag{10}$$

If only one species is responsible for light absorption at a particular wavelength, the concentration of that species at time t (C_t) is given by (11)

$$C_t = \frac{A_t^{\lambda}}{\varepsilon^{\lambda}\ell} \tag{11}$$

where A_t^{λ} is the absorbance at time t and wavelength λ, ε^{λ} is the Beer-Lambert extinction coefficient of the species at λ, and ℓ is the path length of the cell.

If many species contribute to light absorption at a particular wavelength, the total absorbance, A_t^{λ}, at that wavelength, is the sum of absorbances due to each species. If these total absorbance values are monitored as a function of time at a number of different wavelengths (equal in number to the number of transient species present) and if the extinction coefficients of each species at each monitoring wavelength are known, concentration versus time curves can be obtained for each transient species.

Total absorbance values as a function of time were obtained at 632.8 nm, 585.0 nm, 530.0 nm and 457.8 nm for the flash photolysis of indole, in neutral pH, in the absence and presence of 1.0 M NaBr, 0.25 M $BaCl_2 \cdot 2H_2O$, 1 x 10^{-3} M $CdSO_4$ and $\sim$5 x 10^{-6} M $CdSO_4$ by the techniques outlined above.

Extinction coefficients were available for the hydrated electron,[28] indole radical cation,[4] indolyl neutral radical[29] and indole triplet state,[24] at the absorption maximum of each species. Extinction coefficients of these species at each monitoring wavelength used in this study were determined by direct proportion from published transient spectra.[22] These extinction coefficients are shown in Table 4. With total absorbance versus time and extinction coefficient data, the following set of four linear equations (12-15) was solved to give the concentration terms $C_{e^-_{aq}}$, $C_{IH^{\bullet}}^{+}$, $C_{I^{\bullet}}$ and C_{IH^*} at each time t, by the Gauss-Jordan elimination method with the aid of a Wang 2200 minicomputer.

Table 4. Extinction coefficients (M^{-1} cm^{-1}) for e^-_{aq}, $IH^{\cdot+}$, I· and $^3IH^*$.

λ	ε	$\varepsilon_{e^-_{aq}}$	$\varepsilon_{IH^{\cdot+}}$	$\varepsilon_{I\cdot}$	$\varepsilon_{^3IH^*}$
632.8		14.23×10^3	1.147×10^3	0.183×10^3	0
585.0		10.690×10^3	3.100×10^3	0.912×10^3	0
530.0		7.164×10^3	0.806×10^3	1.840×10^3	0.263×10^3
457.9		3.980×10^3	0	0.391×10^3	3.619×10^3

$$\frac{A_t^{632.8}}{\ell} = \varepsilon_{e^-_{aq}}^{632.8} C_{e^-_{aq},t} + \varepsilon_{IH^+_\bullet}^{632.8} C_{IH^+_\bullet,t} + \varepsilon_{I\bullet}^{632.8} C_{I\bullet,t} + \varepsilon_{^3IH^*}^{632.8} C_{^3IH^*,t} \tag{12}$$

$$\frac{A_t^{585}}{\ell} = \varepsilon_{e^-_{aq}}^{585} C_{e^-_{aq},t} + \varepsilon_{IH^+_\bullet}^{585} C_{IH^+_\bullet,t} + \varepsilon_{I\bullet}^{585} C_{I\bullet,t} + \varepsilon_{^3IH^*}^{585} C_{^3IH^*,t} \tag{13}$$

$$\frac{A_t^{530}}{\ell} = \varepsilon_{e^-_{aq}}^{530} C_{e^-_{aq},t} + \varepsilon_{IH^+_\bullet}^{530} C_{IH^+_\bullet,t} + \varepsilon_{I\bullet}^{530} C_{I\bullet,t} + \varepsilon_{^3IH^*}^{530} C_{^3IH^*,t} \tag{14}$$

$$\frac{A_t^{457.9}}{\ell} = \varepsilon_{e^-_{aq}}^{457.9} C_{e^-_{aq},t} + \varepsilon_{IH^+_\bullet}^{457.9} C_{IH^+_\bullet,t} + \varepsilon_{I\bullet}^{457.9} C_{I\bullet,t} + \varepsilon_{^3IH^*}^{457.9} C_{^3IH^*,t} \tag{15}$$

V. Fluorescence Spectra and Lifetimes

Air saturated solutions of 5×10^{-4} M indole, and 5×10^{-4} M indole in the presence of 1 M NaBr, 0.25 M $BaCl_2 \cdot 2H_2O$, 1×10^{-3} M $CdSO_4$ and $\sim 5 \times 10^{-6}$ $CdSO_4$ were prepared as described previously.

Fluorescence lifetimes of these solutions were determined on a Photochemical Research Associates Model 3000 Nanosecond Pulsed Single Photon Counting Fluorometer system interfaced to a MINC-II computer and graphics plotter located at the University of Western Ontario, London.

Fluorescence spectra of these solutions were obtained using an SLM Model 8000 Photon Counting Spectrofluorometer and a Hewlett-Packard X-Y recorder located at the State University of New York at Buffalo.

Fluorescence lifetimes and fluorescence spectra were both obtained using λ = 270 nm excitation.

VI. Actinometric Studies

Potassium Ferrioxalate actinometry was performed according to the procedure outlined by Calvert and Pitts.[50]

RESULTS

I. Absorption Spectra

Absorption spectra of 2 x 10^{-5} M indole in water, in the absence and in the presence of NaBr (0.04 M), $BaCl_2 \cdot 2H_2O$ (0.01 M), $CdSO_4$ (4 x 10^{-5} M) and $CdSO_4$ (2 x 10^{-7} M) and in the range 350 nm to 200 nm, are shown in Figure 17. Figure 18 shows the same spectra obtained after exposure to three photolysis pulses.

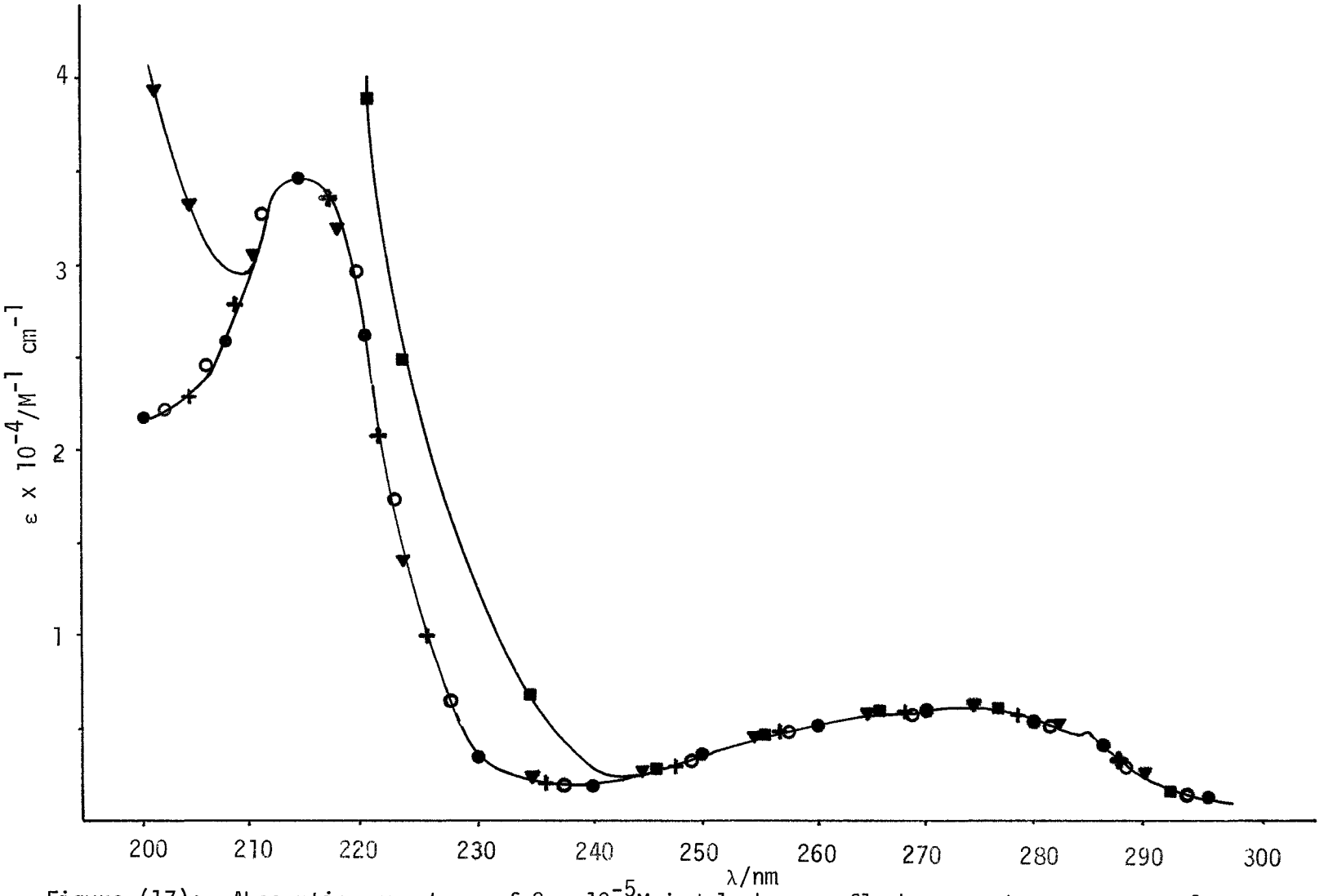

Figure (17): Absorption spectra of 2×10^{-5}M indole before flashing in the presence of: 0.04M NaBr■ ; 0.01M $BaCl_2 \cdot 2H_2O$▼; 4×10^{-5}M $CdSO_4$○ ; 2×10^{-7}M $CdSO_4$+ ; and in the absence of solute. ●

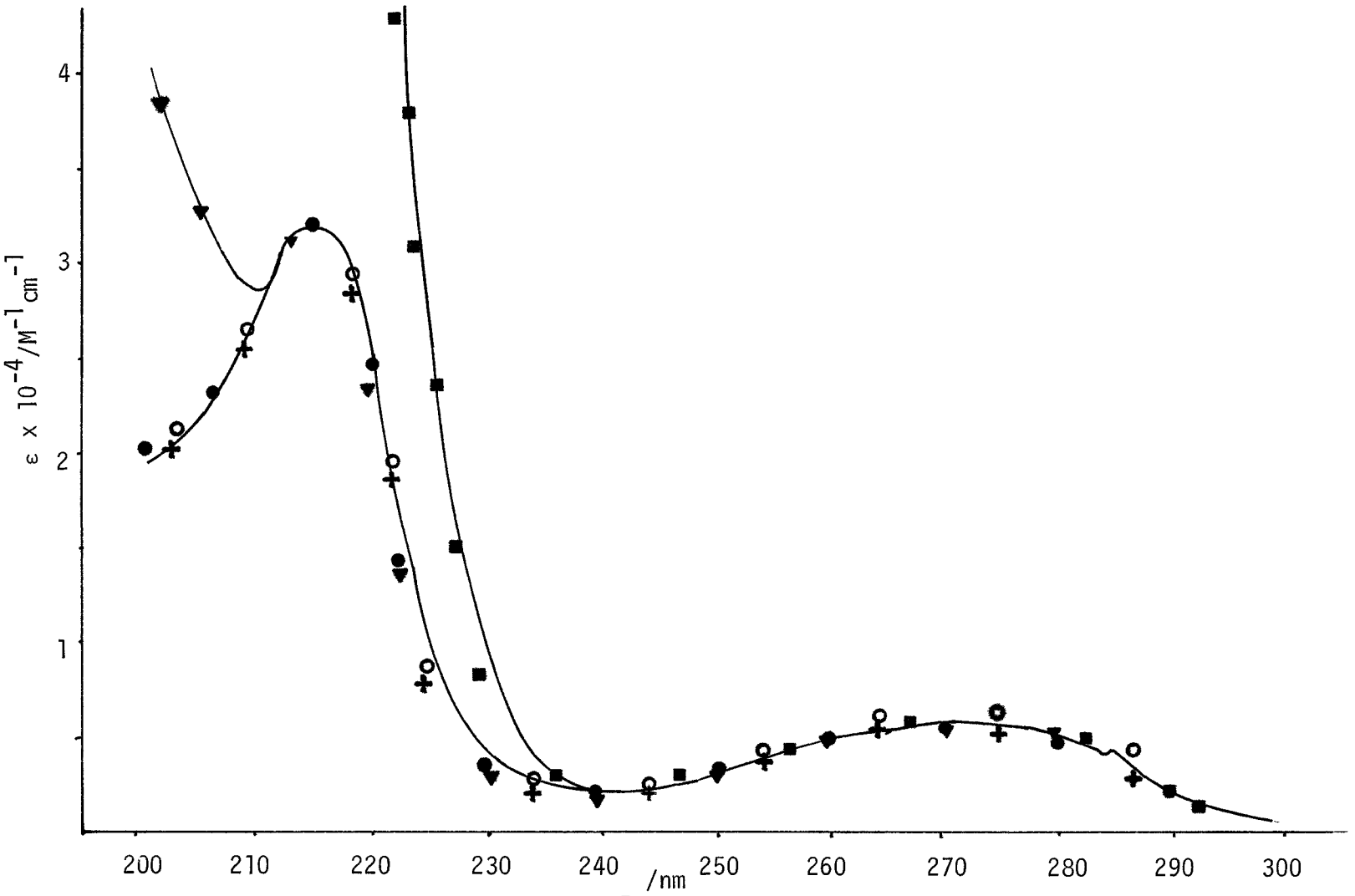

Figure (18): Absorption spectra of 2×10^{-5}M indole after flashing in the presence of: 0.04M NaBr■ ; 0.01M $BaCl_2 \cdot H_2O$▼ ; 4×10^{-5}M $CdSO_4$○ ; 2×10^{-7}M $CdSO_4$+ ; and in the absence of solute.●

II. Fluorescence Spectra

Fluorescence spectra of 2×10^{-5} M indole in water, in the absence and in the presence of NaBr (0.04 M), $BaCl_2 \cdot 2H_2O$ (0.01 M), $CdSO_4$ (4×10^{-5} M) and $CdSO_4$ (2×10^{-7} M) and in the range 400 nm to 290 nm, are shown in Figure 19. Integrated band intensity and λ_{max} values, for each spectrum, are given in Table 5.

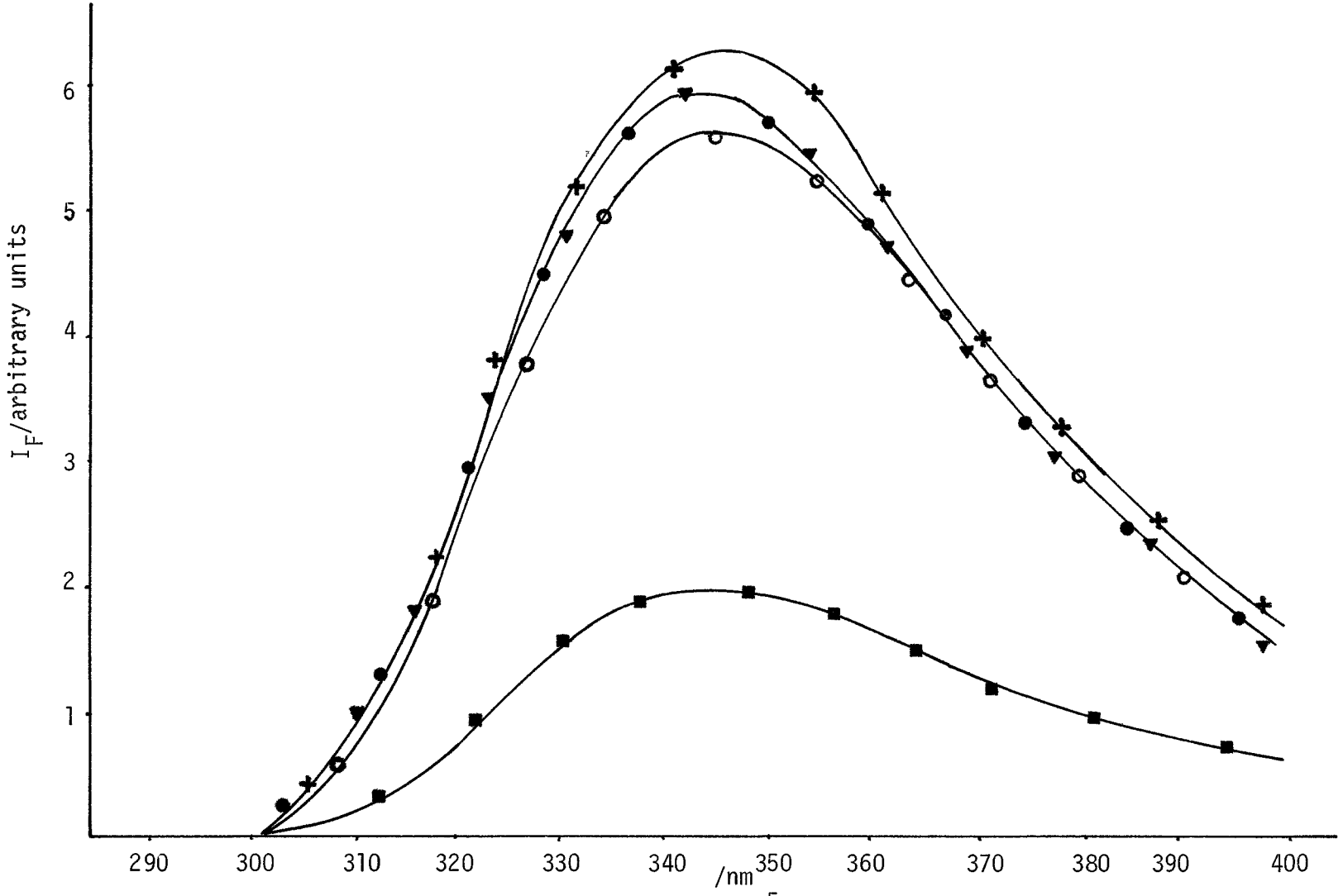

Figure (19): Fluorescence spectra of: indole (2×10^{-5}M) in water in the absence of solute ● ; and in the presence of NaBr (0.04M) ■ ; Ba $Cl_2 \cdot 2H_2O$ (0.01M) ▼ ; $ClSO_4$ (4×10^{-5}M) ◎ ; $CdSO_4$ (2×10^{-7}M) ✚.

Table 5. Fluorescence Spectra: λ_{max} and Integrated Band Intensities

Solute	Concentration (M)	λ_{max} (nm)	Integrated Band Intensity (arbitrary units)
none	--	345	816
NaBr	0.04	345	275
$BaCl_2 \cdot 2H_2O$	0.01	346	809
$CdSO_4$	4×10^{-5}	346	783
$CdSO_4$	2×10^{-7}	345	862

III. Fluorescence Lifetimes

Intensity of fluorescence emission (I_F) (λ = 350 nm), normalized at the maximum to 10^4 (arbitrary units), was obtained as a function of time for 2 x 10^{-5} M indole in water, which was partially saturated with helium, in the absence and in the presence of NaBr (0.04 M), $BaCl_2 \cdot 2H_2O$ (0.01 M), $CdSO_4$ (4 x 10^{-5} M) and $CdSO_4$ (2 x 10^{-7} M). These plots are shown in Figures 20-24.

The time dependence of the normalized fluorescence intensities is represented by Equation (16)

$$I_F/I_{F_{max}} = A_1 e^{-t/\tau_1} - A_2 e^{-t/\tau_2} \qquad (16)$$

where $I_{F_{max}} = 10^4$ (arbitrary units) and A_1 and A_2 are pre-exponential factors for processes with lifetimes τ_1 and τ_2

The A_1, A_2, τ_1 and τ_2 values obtained are shown in Table 6.

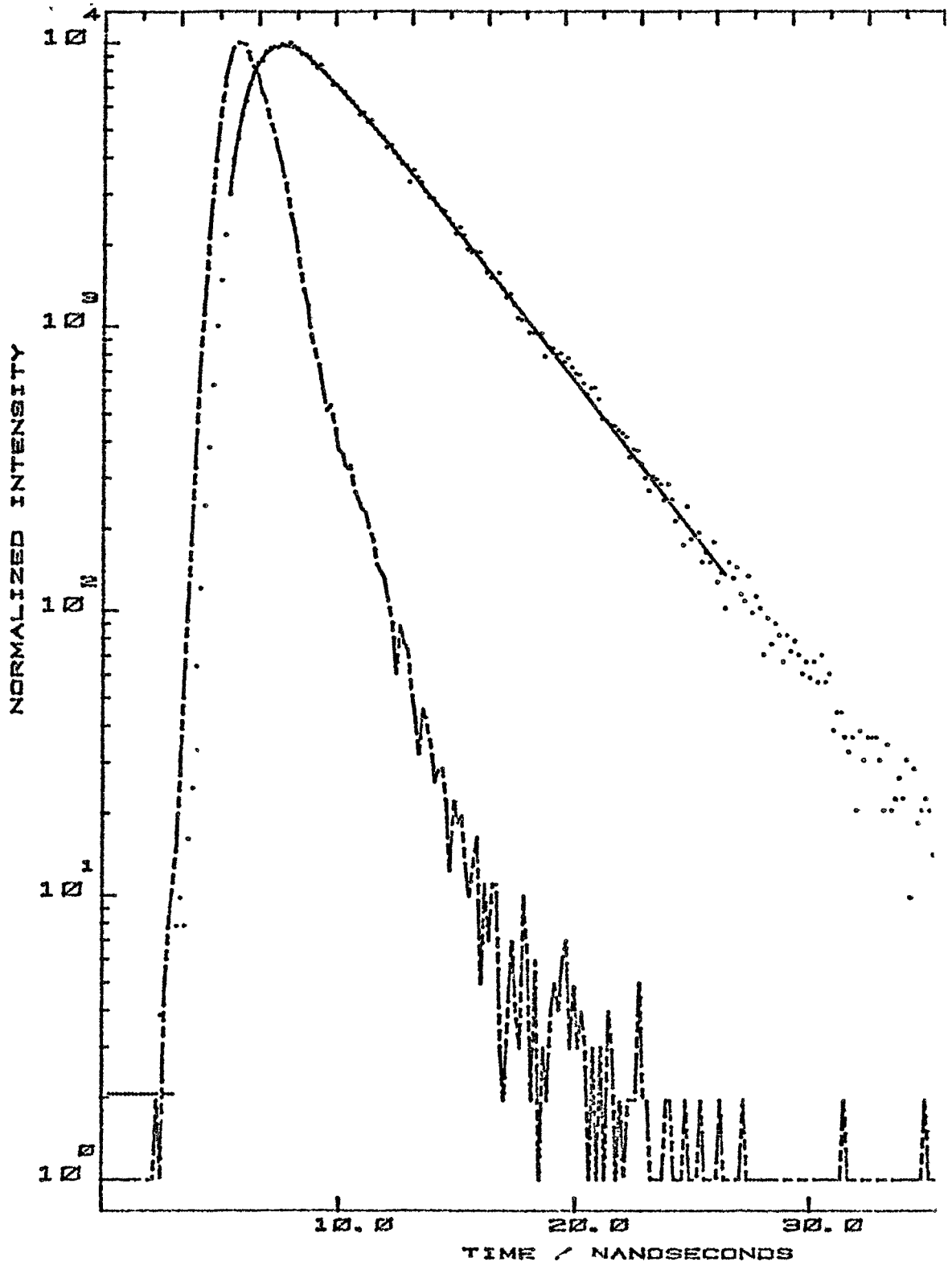

Figure (20): Normalized fluorescence intensity versus time plot for 2×10^{-5}M indole in water (air saturated) in the absence of solute.

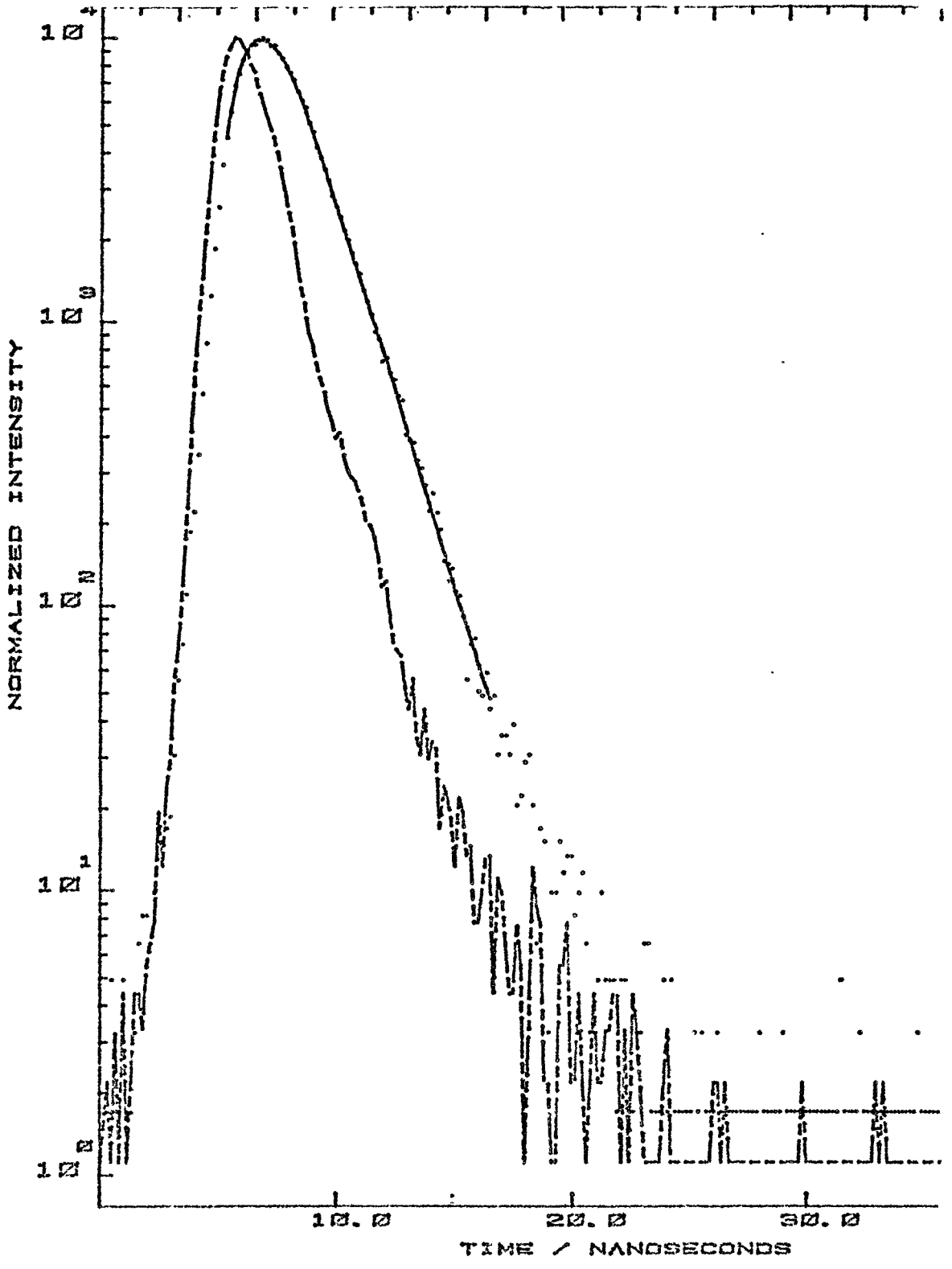

Figure (21): Normalized fluorescence intensity versus time plot for 2×10^{-5}M indole in water (air saturated) in the presence of 0.04M NaBr.

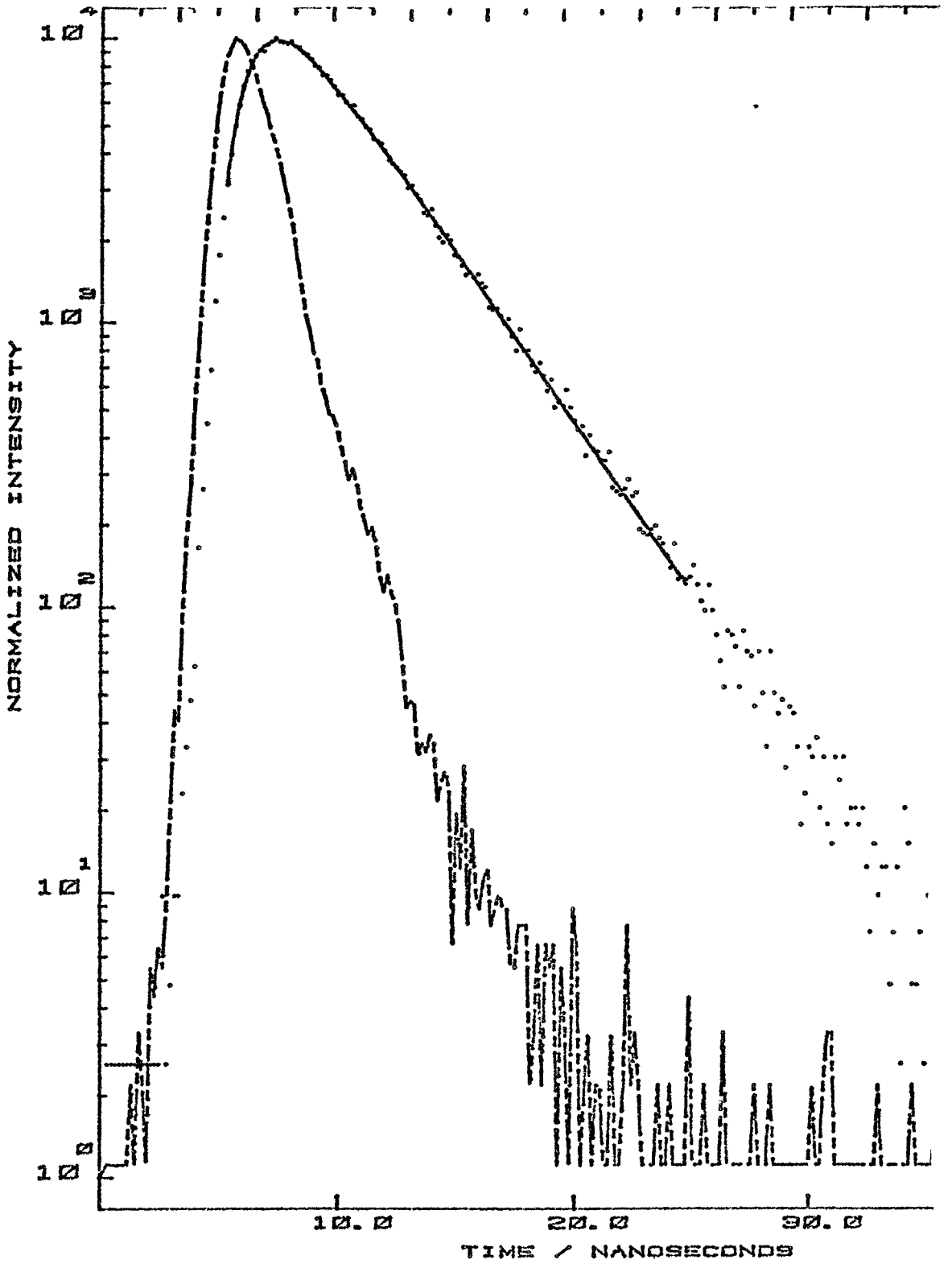

Figure (22): Normalized fluorescence intensity versus time plot for 2×10^{-5}M indole in water (air saturated) in the presence of 0.01M $BaCl_2 \cdot 2H_2O$.

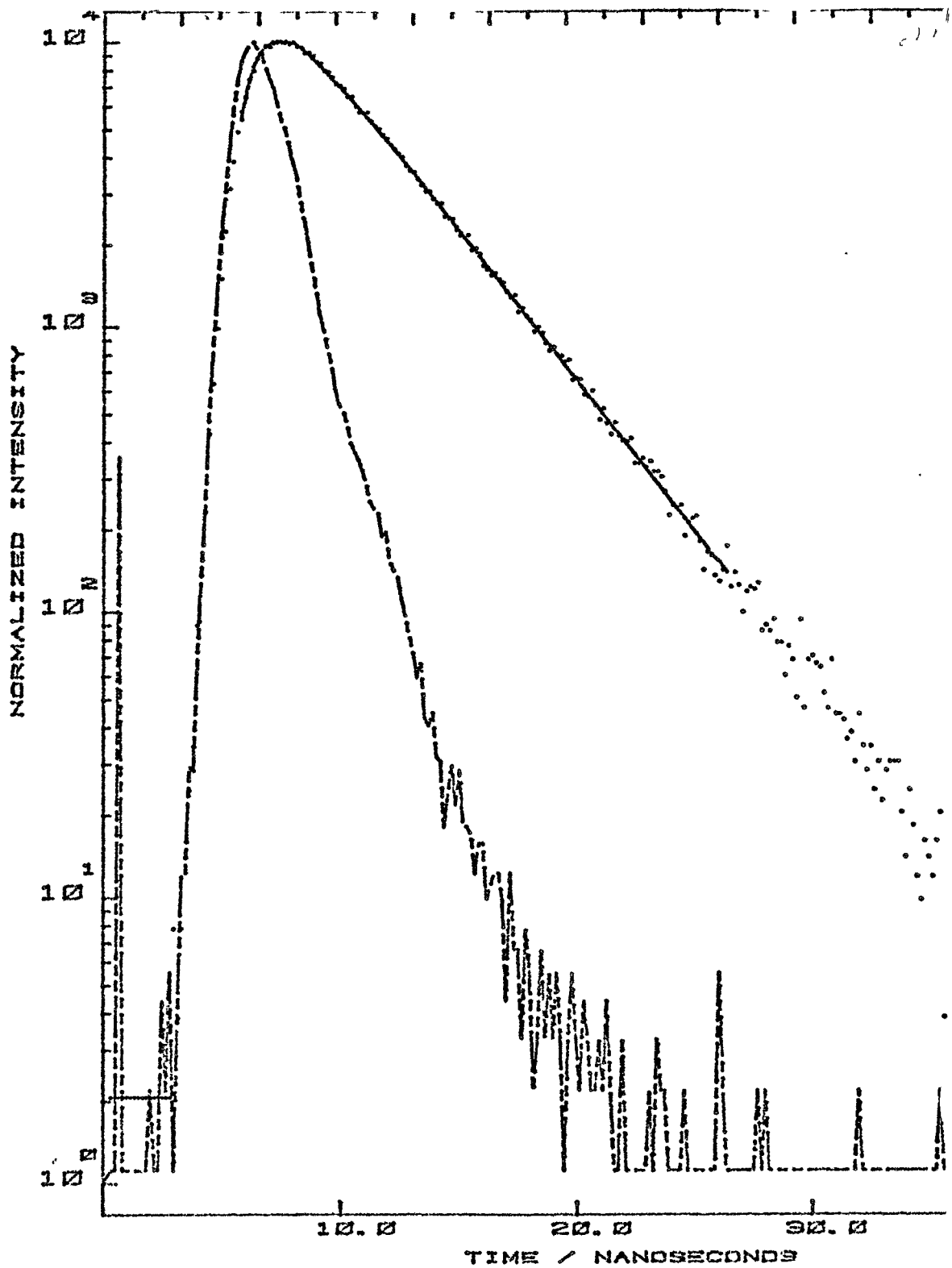

Figure (23): Normalized fluoresence intensity versus time plot for 2×10^{-5}M indole in water (air saturated) in the presence of 4×10^{-5}M $CdSO_4$.

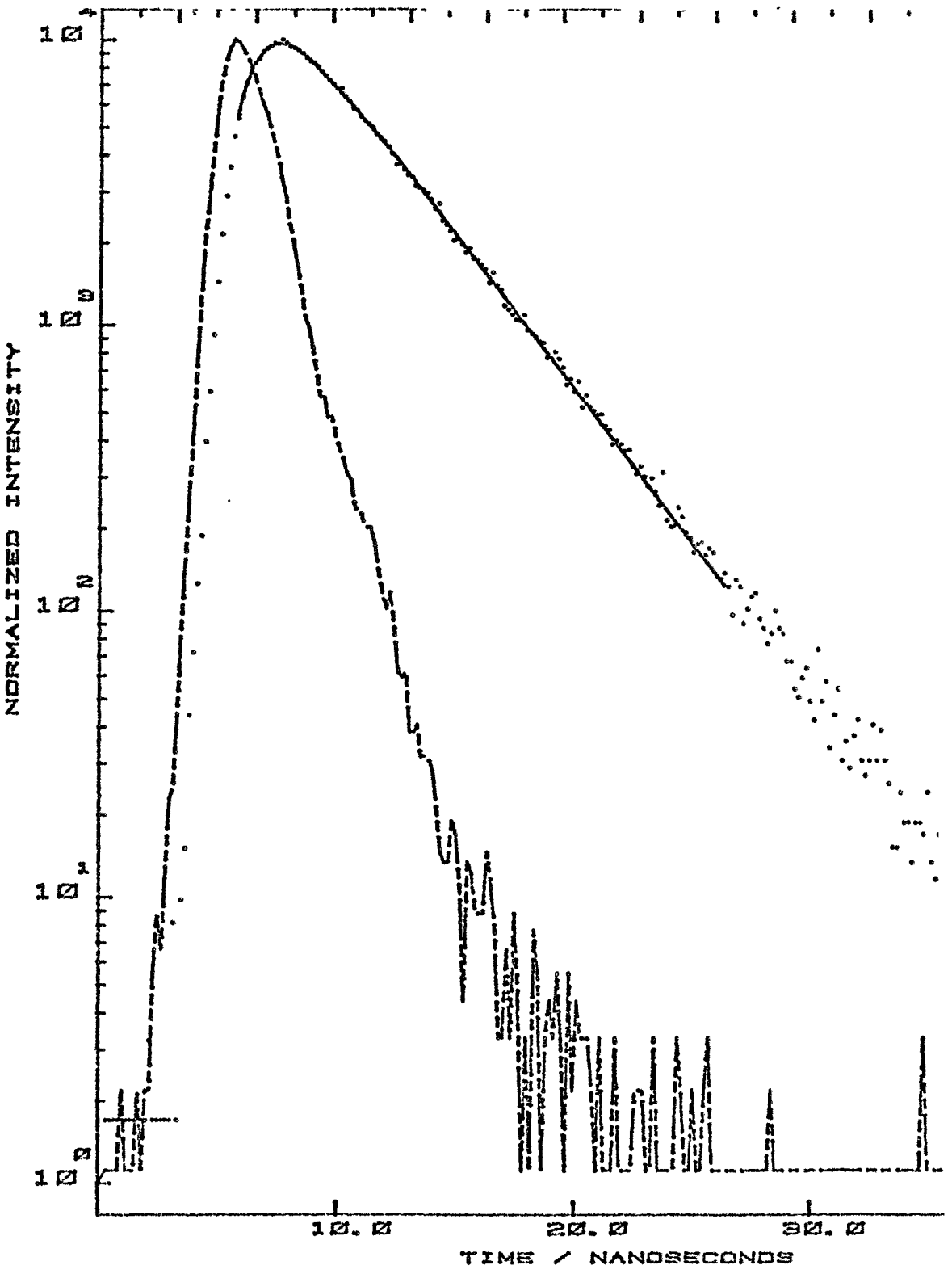

Figure (24): Normalized fluoresence intensity versus time plot for 2×10^{-5}M indole in water (air saturated) in the presence of 2×10^{-7}M $CdSO_4$.

Table 6. Fluorescence Lifetimes and Pre-exponential Factors

Solute	Concentration (M)	A_1	τ_1 (ns)	A_2	τ_2 (ns)
none	--	0.302 ± 0.002	4.477 ± 0.015	0.882	0.007 ± 0.003
NaBr	0.04	0.777 ± 0.069	1.378 ± 0.031	0.122 ± 0.051	0.587 ± 0.363
$BaCl_2 \cdot 2H_2O$	0.02	0.286 ± 0.002	3.964 ± 0.014	1.259 ± 0.509	0.005
$CdSO_4$	4×10^{-5}	0.299 ± 0.001	4.501 ± 0.014	20.629 ± 0.355	0.009
$CdSO_4$	2×10^{-7}	0.405 ± 0.002	4.393 ± 0.014	0.949	0.012 ± 0.005

IV. Flash Photolysis Studies

A. General Considerations

The determination of concentrations of the four transient species, e^-_{aq}, $IH^{+\bullet}$, I$\bullet$ and ^{3}IH*, by the simultaneous solution of four equations in four unknowns, outlined in the experimental section, yielded positive concentration values for e^-_{aq}, I$\bullet$ and ^{3}IH* but negative concentration values for $IH^{+\bullet}$. While these apparent negative concentration values do not exclude the existence of $IH^{+\bullet}$, they imply that the species is too short-lived to be detected by the apparatus used in this study. This conclusion is consistent with the results of Grossweiner et al.[29] who also failed to detect the presence of $IH^{+\bullet}$ within the 50 ns resolution of their instrumentation.

The determination of the concentrations of e^-_{aq}, I$\bullet$ and ^{3}IH* by the simultaneous solution of three equations in three unknowns was then performed by eliminating Equation 13 and the second terms of Equations 12, 14 and 15.

Concentration versus time data for the three species, in the absence and in the presence of NaBr (1 M), $BaCl_2 \cdot 2H_2O$ (0.25 M), $CdSO_4$ (1×10^{-3} M) and $CdSO_4$ (5×10^{-6} M), are shown in Figures 25-29. Also, concentration versus time data for each of e^-_{aq}, I$\bullet$ and ^{3}IH*, in the absence and presence of the above added solutes, are shown in Figures 30-32. First shot concentration versus time data were analyzed exclusively because the buildup of stable absorbing photo-products made analyses of subsequent shots impossible. An example of the effect

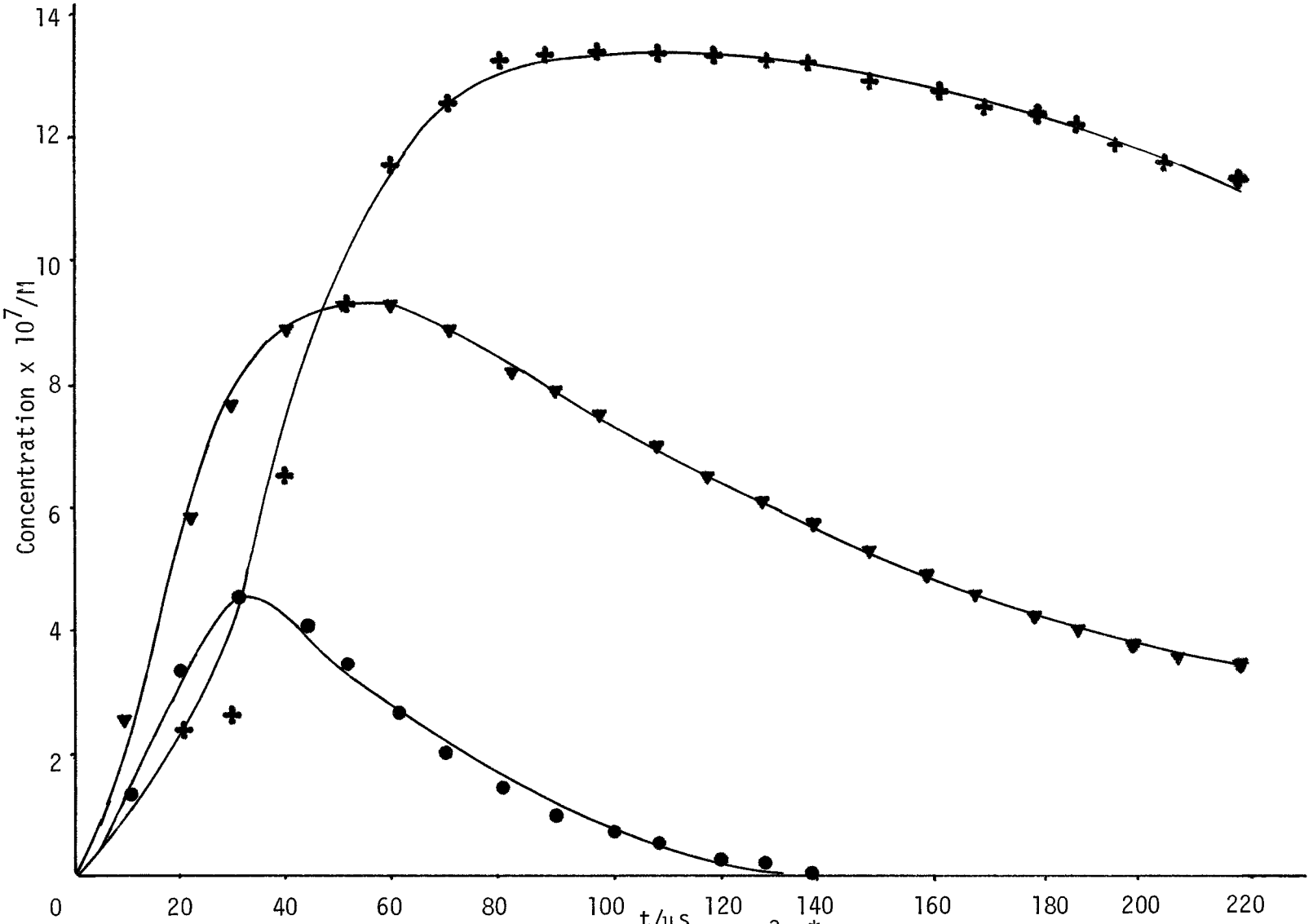

Figure (25): Concentration versus time plots for e^-_{aq} ● ; I· ✚ ; and $^3IH^*$ ▼ produced in the flash photolysis of aqueous solutions of indole (5×10^{-4}M) in the absence of solute.

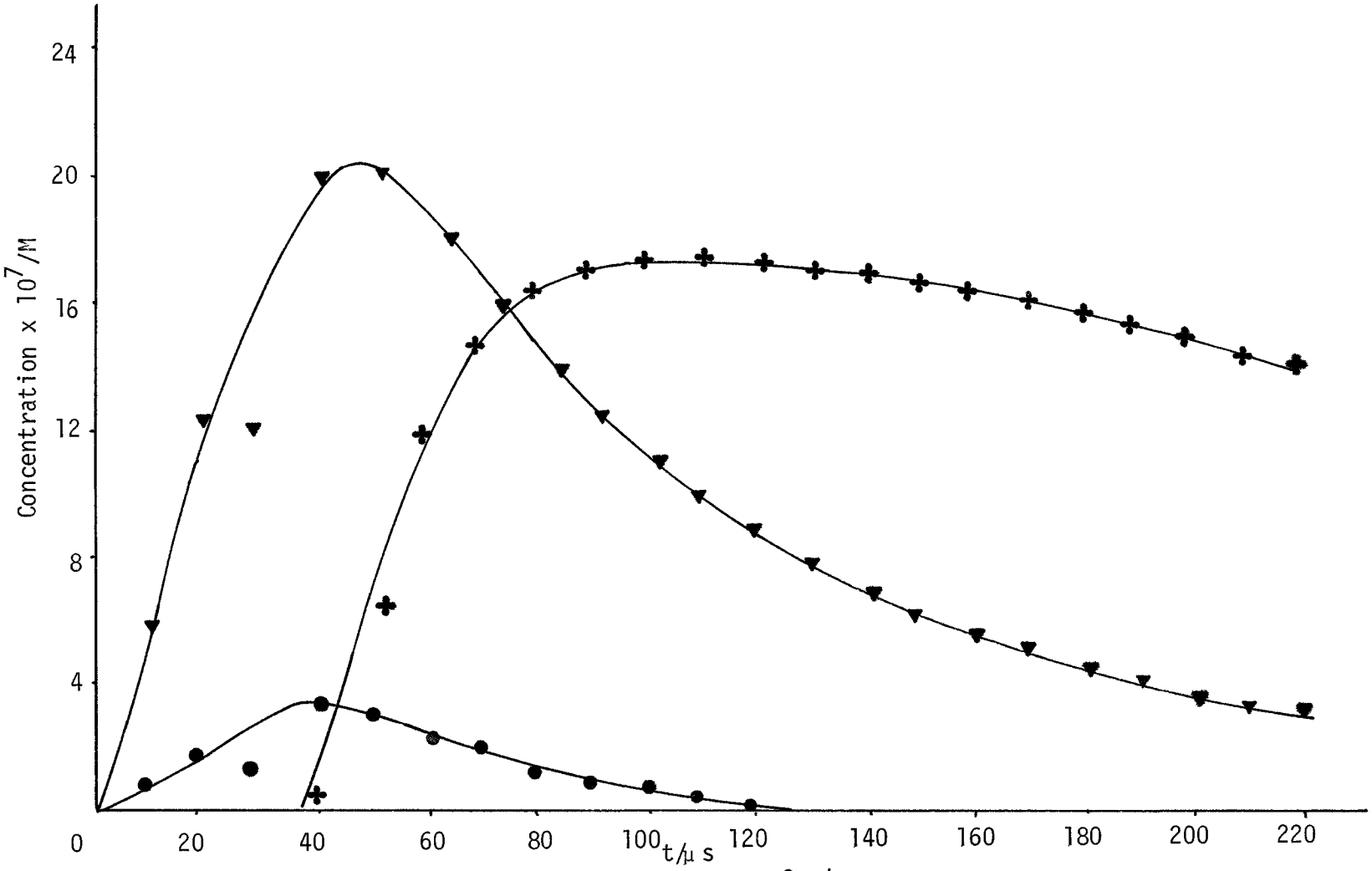

Figure (26): Concentration versus time plots for e^-_{aq} ●; I· ✚; and $^3IH^*$ ▼ produced in the flash photolysis of aqueous solutions of indole (5.0×10^{-4}M) in the presence of NaBr (1.0 M).

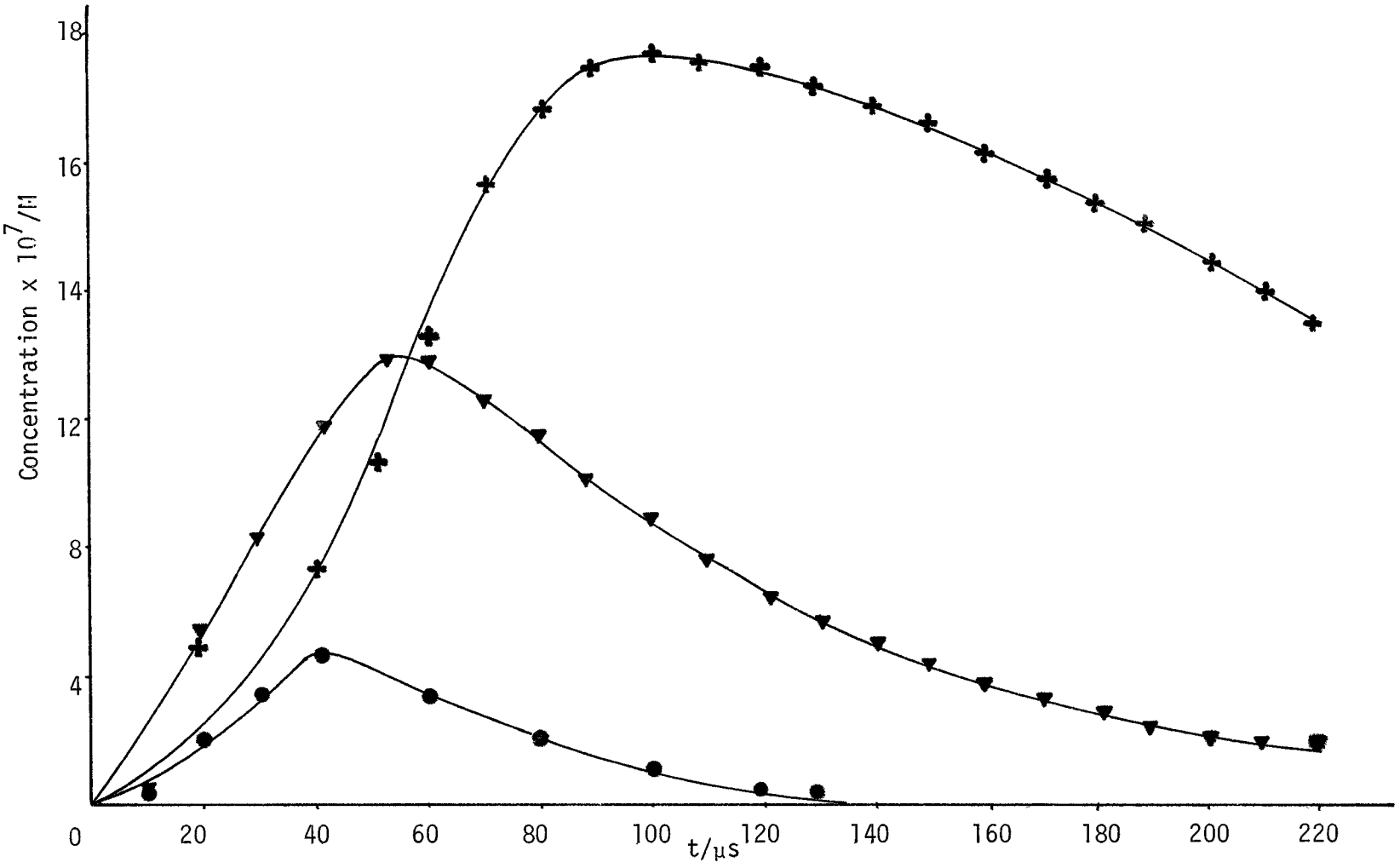

Figure (27): Concentration versus time for e^-_{aq} ● ; I· ✚ ; and $^3IH^*$ ▼ produced in the flash photolysis of aqueous solutions of indole (5.0×10^{-4} M) in the presence of $BaCl_2 \cdot 2H_2O$ (0.25 M).

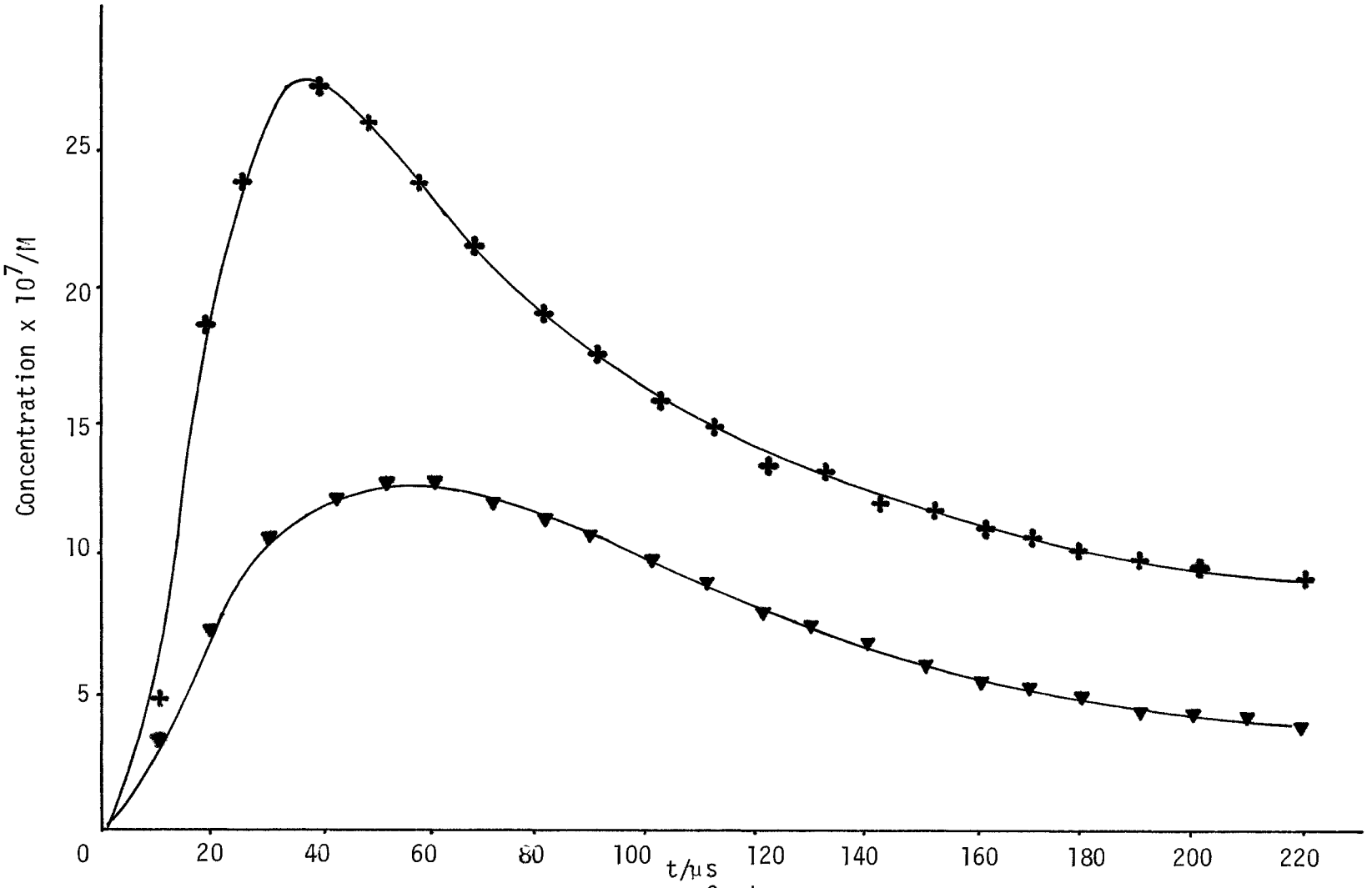

Figure (28): Concentration versus time plots for I·✚ ; and $^3IH^*$▼ produced in the flash photolysis of aqueous solutions of indole (5.0×10^{-4}M) in the presence of $CdSO_4$ (1.0×10^{-3}M).

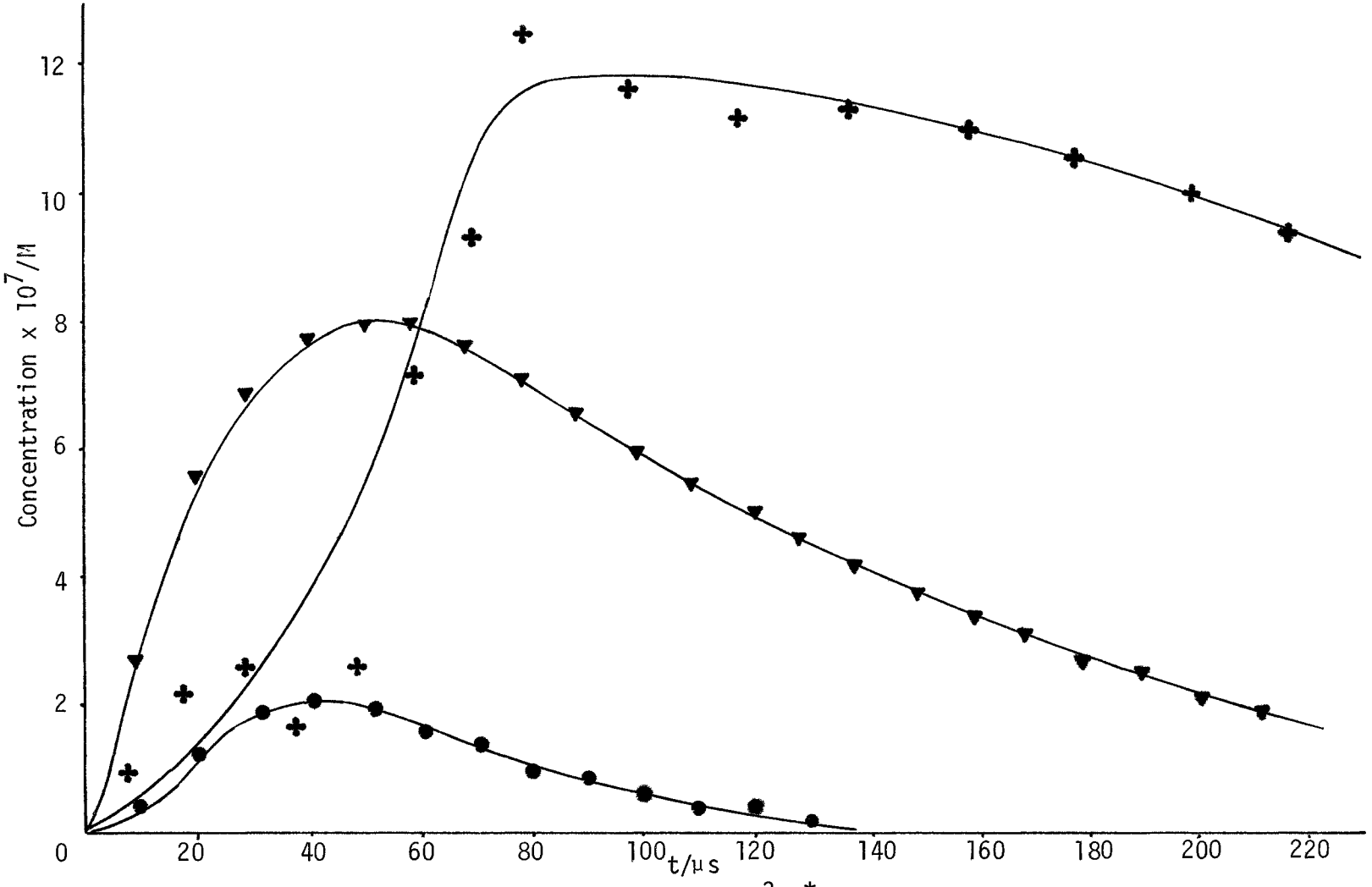

Figure (29): Concentration versus time plots for e^-_{aq} ● ; I· ✚; and $^3IH^*$ ▼ produced in the flash photolysis of aqueous solutions of indole (5.0×10^{-4}M) in the presence of $CdSO_4$ (5.0×10^{-6}M).

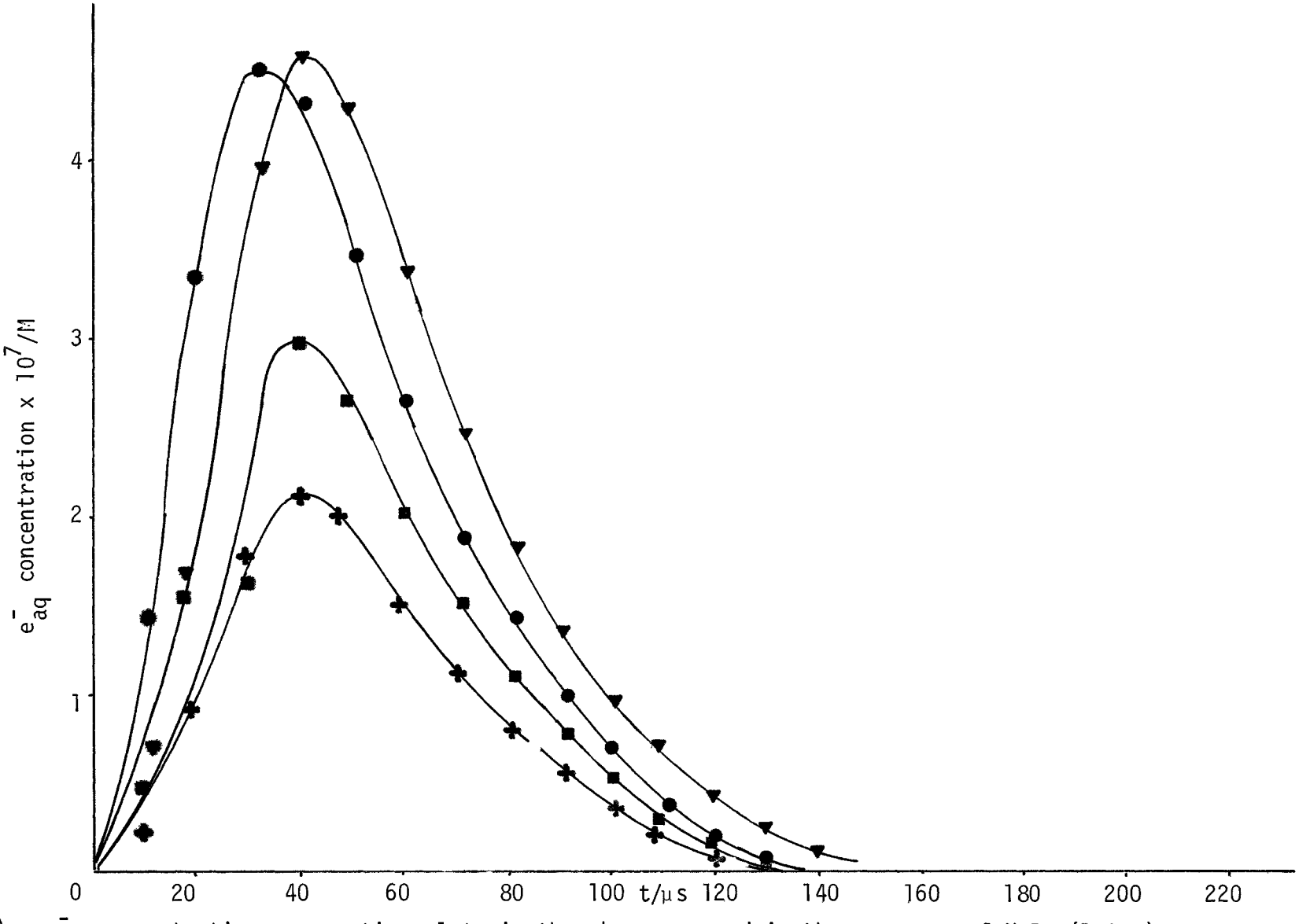

Figure (30): e^-_{aq} concentration versus time plots in the absence and in the presence of NaBr (1.0 M) ; $BaCl_2 \cdot 2H_2O$ (0.25 M)▼ ; and $CdSO_4$ (5.0×10^{-6}M)✤ .

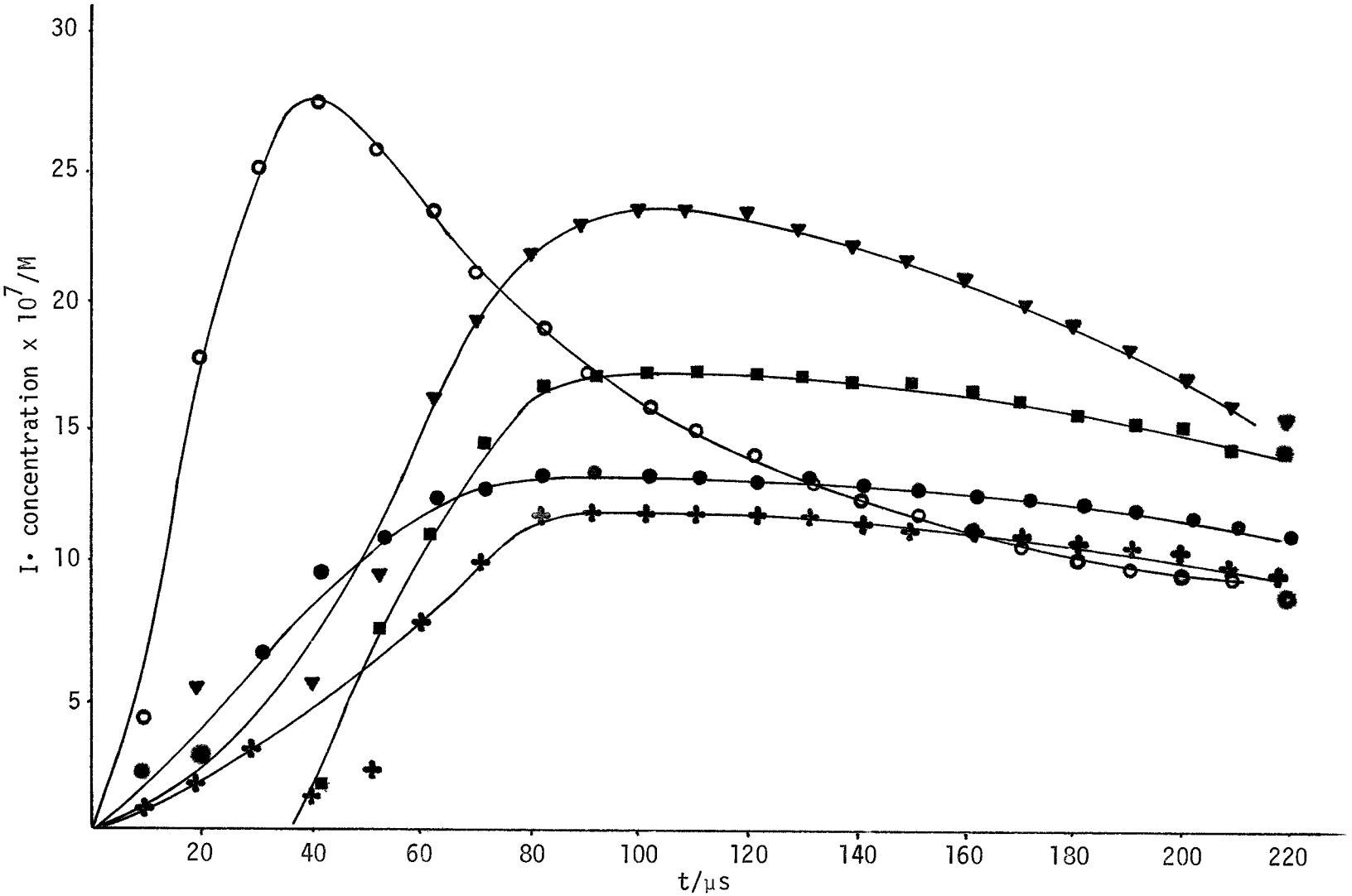

Figure (31) I· concentration versus time plot in the absence (●) and in the presence of NaBr (1.0 M)■; $BaCl_2 \cdot 2H_2O$ (0.25 M)▼; $CdSO_4$ (1×10^{-3} M)○; and $CdSO_4$ (5×10^{-6} M)✚.

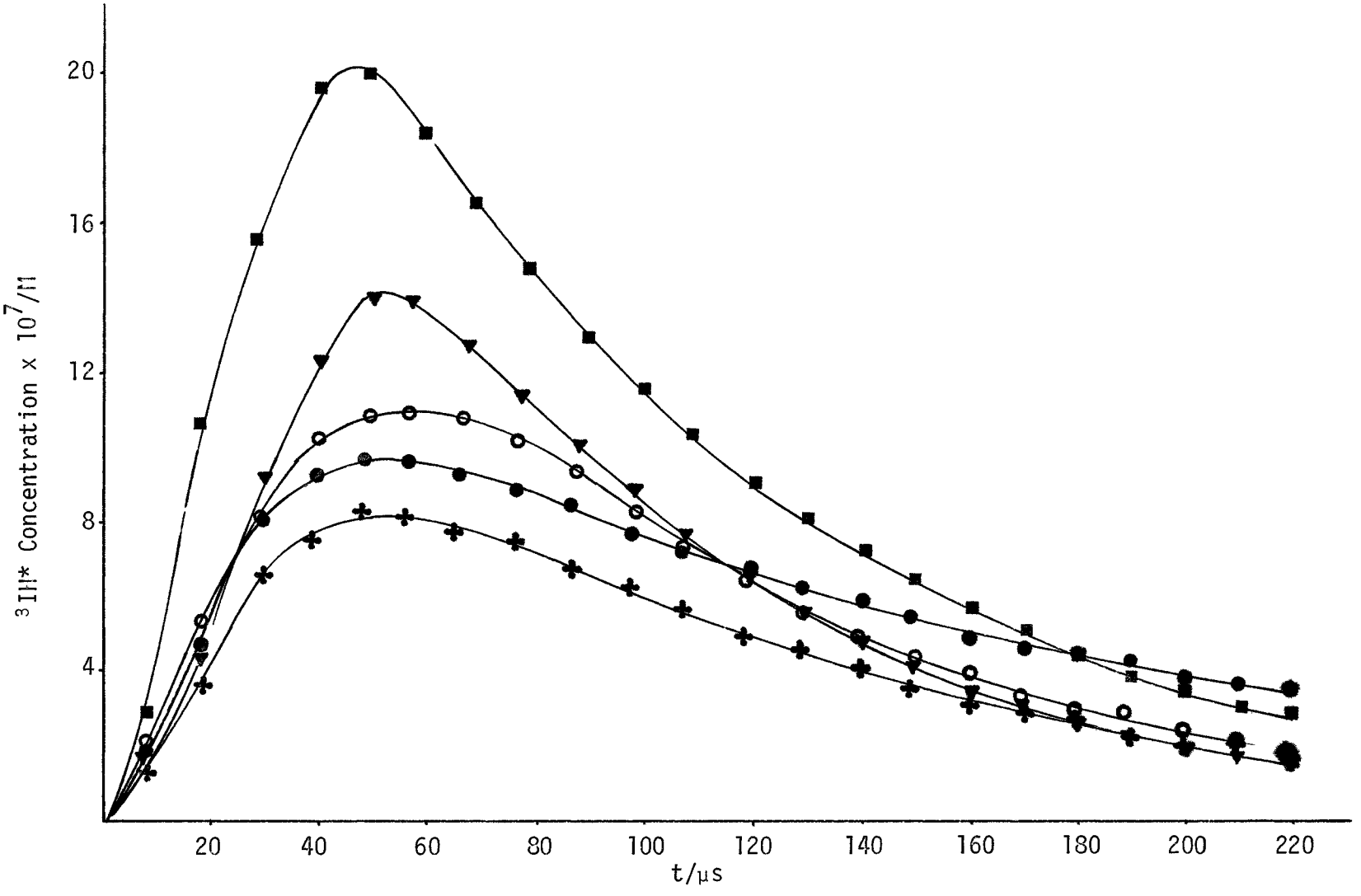

Figure (32) ^{3}IH* concentration versus time plot in the absence (●) and in the presence of: NaBr (1.0 M)■ ; $BaCl_2 \cdot 2H_2O$ (0.25 M)▼ ; $CdSO_4$ (1×10^{-3} M)○ ; and $CdSO_4$ (5×10^{-6} M)✚ .

of repeated flashing on total absorbance versus time curves is shown in Figure 33.

In general, $\frac{dC}{dt}$, the instantaneous rate of change of concentration, C (mol/L ≡ M), of any transient species, at time t, is represented by Equation 16.

$$\frac{dC}{dt} = \alpha[Gf(t)]^n - k_1C - k_2C^2 \qquad (16)$$

where G is a quantity, defined below, which is proportional to the quantum efficiency for the production of the transient species, f(t), also defined below, is the wavelength-independent, time-dependent, dimensionless photolysis pulse function, n is an index which is strictly equal to one, for monophotonic species generation, and strictly equal to two, for biphotonic species generation, and k_1 (s^{-1}) and k_2 ($M^{-1}s^{-1}$) are specific rate constants for the decay of the transient species which, in the general case, may be both first and second order.

For monophotonic (n = 1) (α = 1) species generation the quantity G is represented by Equation 17.

$$G = \bar{\phi} \cdot \bar{I}_M \qquad (17)$$

where $\bar{\phi}$ is the average quantum efficiency (mol $einstein^{-1}$) for the production of the transient species and $\bar{I}_M$, represented by 18, is the average maximum number of einsteins absorbed per litre per second by the system,

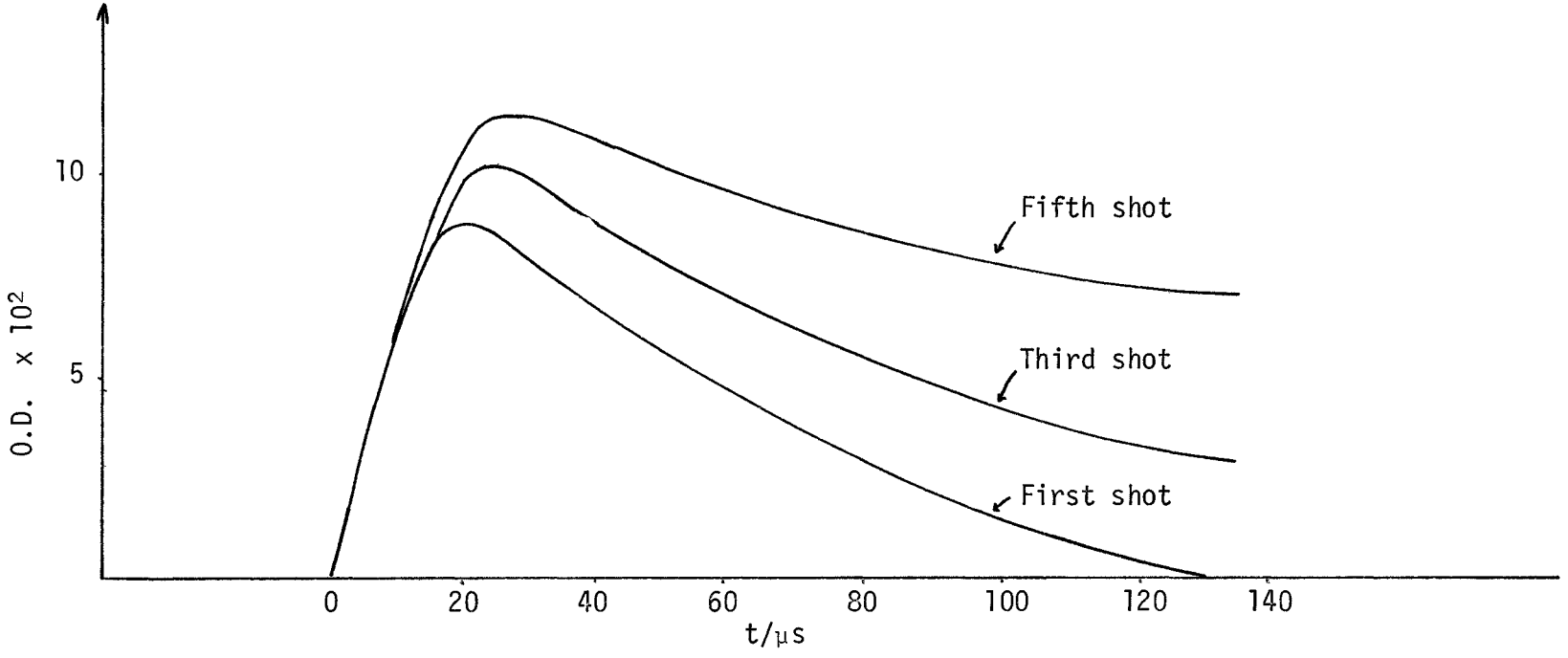

Figure (33) An example of the buildup of absorbance of photoproducts after repeated flashes.

$$\bar{I}_M = \frac{A}{V} \int F_M(\lambda)(1 - e^{-\beta})d\lambda \qquad (18)$$

where A and V are the irradiated area (cm^2) and volume (L), respectively; $F_M(\lambda)$ is the maximum number of einsteins incident on a square centimetre of solution surface per second at amy wavelength, λ; and β is represented by the Beer-Lambert term (19).

$$\beta = 2.303\varepsilon_\lambda (IH)_0 W \qquad (19)$$

where ε_λ is the extinction coefficient (M^{-1} cm^{-1}) for indole at wavelength λ (see Fig. 2), $(IH)_0$ is the initial indole concentration (M), and W is the average path traversed by the incident radiation through the cell (cm).[51]

The photolysis pulse function f(t) is represented by (20)

$$f(t) = I(t)/I_{max} \qquad (20)$$

where I(t) is the intensity, in arbitrary units, of the pulse at any time, t (as recorded by the digital storage oscilloscope), and I_{max} is the maximum intensity of the pulse.

An analytical expression for f(t) is given in Equation (21).

$$f(t) = \left(\frac{at}{2}\right)^2 \exp(2 - at) \qquad (21)$$

Where $a = \frac{2}{t_{max}}$ and t_{max} is the time taken for I(t) to become I_{max}.

The parameter, a, was measured with the photolysis cell empty, with distilled water in the cell and glacial acetic acid in the cell jacket and with no cell in position at various wavelengths in the range 280 nm to 600 nm. The results of this study, which are shown in Table 7, indicate that $a = (5.7872 \pm 0.1724) \times 10^4\ s^{-1}$ is independent of wavelength in the range 280 nm to 600 nm. Although Equation 21 reproduced experimental f(t) values for times up to 60 μs, calculated f(t) values after this time were significantly lower than those values determined experimentally. For this reason, a more accurate analytical expression for f(t) shown in Equation 22, was determined.

$$f(t) = \left(\frac{at}{2}\right)^m \exp(2 - at) \tag{22}$$

where m, obtained by n-th order regression analysis, is shown in (23) and t is in seconds.

$$m = 3.59 - 1.23 \times 10^5 t + 4.12 \times 10^9 t^2 - 6.21 \times 10^{13} t^3 + 3.48 \times 10^{17} t^4 \tag{23}$$

Figure 34 shows the inadequacy of the f(t) function (21) and the adequacy of the f(t) function (22) in representing the shape of the exciting photolysis pulse. Figure 34 also shows that the total pulse duration is 250 μs.

Table 7. Pulse Parameter "a" at various wavelengths

λ/nm	a ($\times 10^4$ s^{-1})			a ($\times 10^4$ s^{-1}) (average)	Standard Deviation
	1	2	3		
280	6.1853 6.4462	--	--	6.3158	±0.1845
300	5.5609	5.8004	5.9629	5.7627	±0.2028
350	5.3011	5.7733	5.7404	5.6409	±0.2673
400	5.8320	5.5413	6.0397	5.8013	±0.1845
450	5.6706	5.4637	5.9627	5.6656	±0.2540
500	5.9367	5.9817	5.8627	5.9270	±0.0600
550	5.9918	5.8259	6.0886	5.9864	±0.1346
600	5.8733	5.5129	5.7938	5.7266	±0.1037

1 without cell

2 empty cell in position

3 cell, containing distilled water and glacial acetic acid, in position

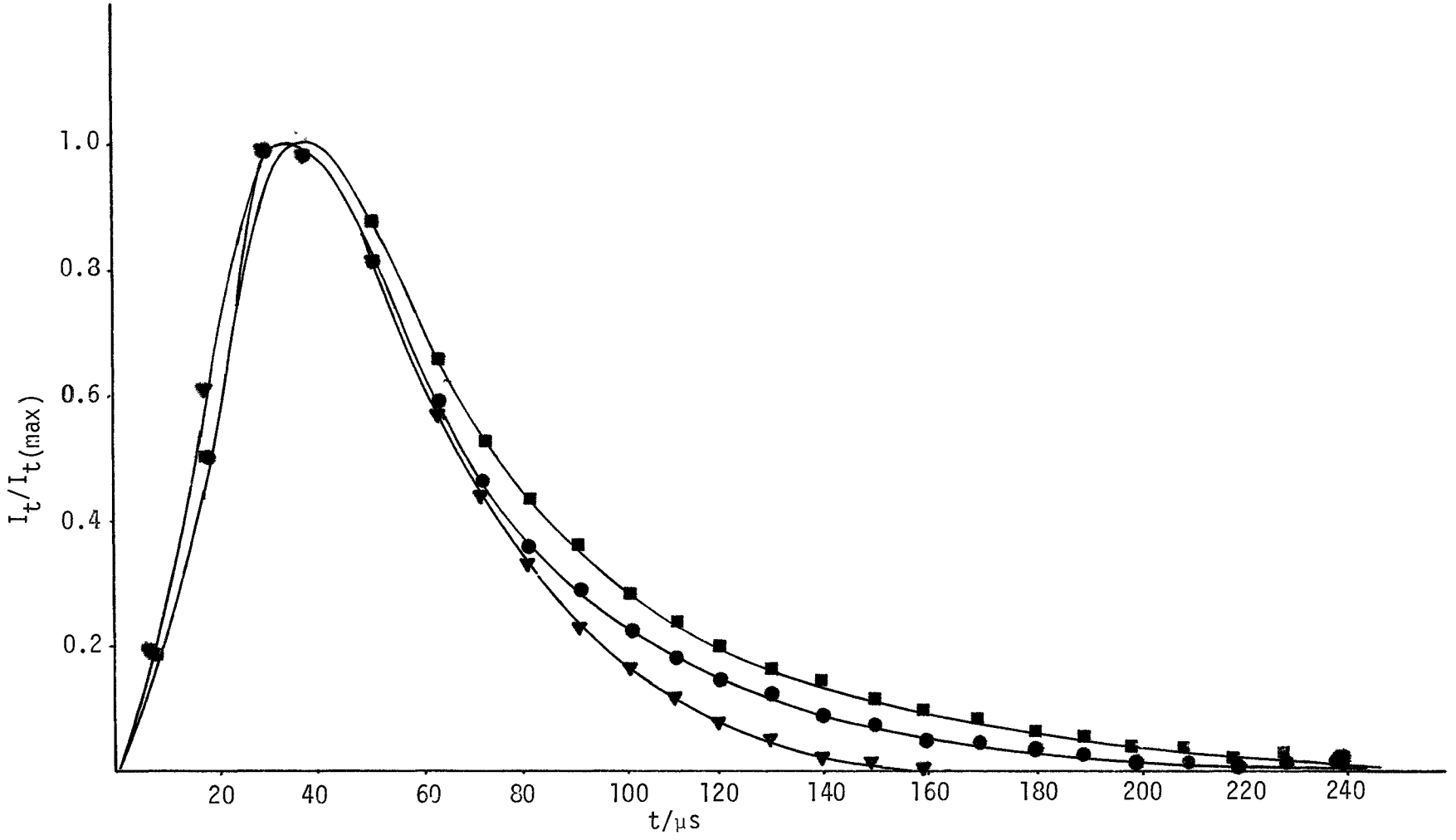

Figure (34) Photolysis pulse functions: f(t) function (21) ▼ ; f(t) function (22) ■ ; and experimental photolysis pulse ●

For multiphotonic ($n > 1$) species generation $\alpha[G(f(t))]^n$ or $\alpha[\bar{\bar{\phi}}\bar{\bar{I}}_M f(t)]^n$ must have the dimensions of M s^{-1}. The factor $\alpha(\neq 1)$ is introduced to provide the correct dimensions of the above term in the general equation.

B. Kinetic Analysis: e^-_{aq}

Several kinetic curves for the hydrated electron were obtained after single flashings of indole (5×10^{-4} M), in the absence and in the presence of NaBr (1.0 M), $BaCl_2 \cdot 2H_2O$ (0.25 M) and $CdSO_4$ (5×10^{-4} M). The e^-_{aq} concentration versus time data presented in this work represent the average e^-_{aq} concentrations, versus time, derived from the several kinetic curves obtained. The numerical values of these average (e^-_{aq}) concentrations are given in Appendix 2 for the various solutions studied. n-th order regression analysis was performed on the (e^-_{aq}) concentration versus time plots in the range 50 μs to 150 μs to obtain (e^-_{aq}) versus time equations of the form shown in Equation 24, where the B coefficients are given in Appendix 3 for each solution flashed.

$$(e^-_{aq}) = B_0 + B_1 t + B_2 t^2 + B_3 t^3 + B_4 t^4 \qquad (24)$$

Equation 24 was then differentiated to give Equation 25.

$$\frac{d(e^-_{aq})}{dt} = B_1 + 2B_2 t + 3B_3 t^2 + 4B_4 t^3 \qquad (25)$$

$\frac{d(e^-_{aq})}{dt}$ values were then calculated at 10 μs intervals from 50 μs to 150 μs.

Sets of $\frac{d(e^-_{aq})}{dt}$ and (e^-_{aq}) values were used to solve simultaneously for $\alpha(G_{e^-_{aq}})^n$, k_1 and k_2 in Equation 26.

$$\frac{d(e^-_{aq})}{dt} = \alpha(G_{e^-_{aq}} f(t))^n - k_1(e^-_{aq}) - k_2(e^-_{aq})^2 \qquad (26)$$

When values of n = 1, 1.5 and 2 were used in the above equation, at least one of $\alpha(G_{e^-_{aq}})^n$, k_1 or k_2 was always negative. On the assumption that e^-_{aq} was exhibiting either first or second order decay behaviour, the solution of Equations 27 and 28 was attempted in a manner similar to that described above.

$$\frac{d(e^-_{aq})}{dt} = \alpha(Gf(t))^n - k_1 e^-_{aq} \qquad (27)$$

$$\frac{d(e^-_{aq})}{dt} = \alpha(Gf(t))^n - k_2(e^-_{aq})^2 \qquad (28)$$

In these cases, when n = 1 and n = 2 were chosen for testing, positive values were not obtained for either $\alpha(G_{e^-_{aq}})^n$ and k_1 or $\alpha(G_{e^-_{aq}})^n$ and k_2 However, when n = 1.5 was chosen, positive values were obtained only for $\alpha(G_{e^-_{aq}})^n$ and k_1 with Equation 27. These values, together with standard deviations are listed in Table 8.

Table 8. Generation and Decay Parameters for the Hydrated Electron (n = 1.5)

Solute	Concentration (M)	$\alpha(G_{e^-_{aq}})^n$	$G^0_{e^-_{aq}}/G_{e^-_{aq}}$	k_1 (s^{-1})	k_1^0/k_1
none	--	$(2.89 \pm 1.31) \times 10^{-2}$	1	$(8.43 \pm 2.21) \times 10^4$	1
NaBr	1.0	$(1.19 \pm 0.26) \times 10^{-2}$	1.81 ± 1.26	$(5.71 \pm 0.57) \times 10^4$	1.48 ± 0.41
$BaCl_2 \cdot 2H_2O$	0.25	$(7.44 \pm 7.07) \times 10^{-2}$	0.532 ± 0.518	$(1.29 \pm 0.65) \times 10^5$	0.65 ± 0.37
$CdSO_4$*	1×10^{-3}	--	--	--	--
$CdSO_4$	5×10^{-6}	$(3.55 \pm 2.56) \times 10^{-3}$	4.06 ± 4.05	$(4.46 \pm 0.89) \times 10^4$	1.89 ± 0.62

$G^0_{e^-_{aq}}$ ≡ Generation parameter in the absence of solute.

k_1^0 ≡ k_1 parameter in the absence of solute.

* For indole (5×10^{-4} M) in the presence of $CdSO_4$ (1×10^{-3} M), zero e^-_{aq} concentration values were observed at all times up to and including 300 μs.

C. Kinetic Analysis: I•

Several kinetic curves for the indolyl neutral radical were obtained after single flashings of indole (5×10^{-4} M), in the absence and in the presence of NaBr (1.0 M), $BaCl_2 \cdot 2H_2O$ (0.25 M), $CdSO_4$ (1×10^{-3} M) and $CdSO_4$ (5×10^{-6} M). The I• concentration versus time data presented in this work represent the average I• concentrations, versus time, derived from the several kinetic curves obtained. The numerical values of these average I• concentrations are given in Appendix 2 for the various solutions studied. n-th order regression analysis was performed on the I• concentration versus time plots in the 350 μs to 1000 μs range to obtain I• versus time equations of the form shown in 29 where the B coefficients are given in Appendix 3 for each solution studied.

$$(I\cdot) = B_0 + B_1 t + B_2 t^2 + B_3 t^3 + B_4 t^4 \qquad (29)$$

Extrapolation of Equation 29 in the range ∿120 μs to 220 μs yielded (I•) values which were in relatively good agreement with experimentally determined values. Equation 29 was differentiated to give Equation 30.

$$\frac{d(I\cdot)}{dt} = B_1 + 2B_2 t + 3B_3 t^2 + 4B_4 t^3 \qquad (30)$$

For indole in water, in the absence and in the presence of all solutes, except 5×10^{-6} M $CdSO_4$, the following analytical treatment was used:

$\frac{d(I\cdot)}{dt}$ values were calculated at 50 μs intervals in the range 350 μs to 1000 μs. These $\frac{d(I\cdot)}{dt}$ values and $(I\cdot)$ values were substituted in Equation (31) to yield k_2 values which were then averaged.

$$\frac{d(I\cdot)}{dt} = -k_2(I\cdot)^2 \tag{31}$$

$\frac{d(I\cdot)}{dt}$ values were then calculated at 10 μs intervals in the range 120 μs to 220 μs. $\frac{d(I\cdot)}{dt}$ values, k_2 values, and $(I\cdot)$ values were substituted in Equation 32 to yield $\alpha(G_{I\cdot})^n$ values.

$$\frac{d(I\cdot)}{dt} = \alpha(Gf(t))^n - k_2(I\cdot)^2 \tag{32}$$

where n equal to 1.0 and 1.5 were tried. $\alpha(G_{I\cdot})^n$ and k_2 values calculated in this manner are shown in Table 9.

For indole in water with $CdSO_4$ (5×10^{-6} M) added the following analytical procedure was used:

$\frac{d(I\cdot)}{dt}$ values were calculated at 10 μs intervals in the range 140 μs to 220 μs. Sets of $\frac{d(I\cdot)}{dt}$ and $(I\cdot)$ values were used to solve (33) simultaneously for $\alpha(G_{I\cdot})^n$ and k_2.

$$\frac{d(I\cdot)}{dt} = \alpha(G_{I\cdot}f(t))^n - k_2(I\cdot)^2 \tag{33}$$

where n was set equal to 1.0 and 1.5. $\alpha(G_{I\cdot})^n$ and k_2 values calculated in this manner are shown in Table 10.

Table 9. Generation and Decay Parameters for the Indolyl Neutral Radical (n = 1).

Solute	Concentration (M)	$G_{I\cdot}$	$G^0_{I\cdot}/G_{I\cdot}$	k_2 (M^{-1} s^{-1})	k_2^0/k_2	k_2^* (M^{-1} s^{-1})
none	--	(2.27 ± 0.56) x 10^{-2}	1	(2.94 ± 0.12) x 10^9	1	2.72 x 10^9
NaBr	1.0	(8.52 ± 3.70) x 10^{-2}	0.27 ± 0.13	(2.88 ± 0.15) x 10^9	1.02 ± 0.02	2.68 x 10^9
$BaCl_2 \cdot 2H_2O$	0.25	(3.60 ± 0.20) x 10^{-2}	0.63 ± 0.18	(3.17 ± 0.10) x 10^9	0.93 ± 0.05	3.02 x 10^9
$CdSO_4$	1 x 10^{-3}	(5.64 ± 1.25) x 10^{-2}	0.40 ± 0.13	(4.57 ± 0.28) x 10^9	0.64 ± 0.05	4.42 x 10^9
$CdSO_4$	5 x 10^{-6}	(4.13 ± 3.05) x 10^{-2}	0.54 ± 0.43	(4.23 ± 0.58) x 10^9	0.70 ± 0.10	3.87 x 10^9

$G^0_{I\cdot}$ ≡ Generation parameter in the absence of solute.

k_2^0 ≡ k_2 parameter in the absence of solute.

k_2^* ≡ k_2 values from $\frac{1}{(I\cdot)}$ versus t analysis.

Table 10. Generation and Decay Parameters for the Indolyl Neutral Radical (n = 1.5).

Solute	Concentration (M)	$\alpha(G_{I\cdot})^n$	$G^0_{I\cdot}/G_{I\cdot}$	k_2 (M^{-1} s^{-1})	k^0_2/k_2
none	--	$(1.31 \pm 0.75) \times 10^{-1}$	1	$(2.94 \pm 0.12) \times 10^9$	1
NaBr	1.0	$(5.22 \pm 3.92) \times 10^{-1}$	0.39 ± 0.43	$(2.88 \pm 0.15) \times 10^9$	1.02 ± 0.07
$BaCl_2 \cdot 2H_2O$	0.25	$(2.63 \pm 0.45) \times 10^{-1}$	0.63 ± 0.48	$(3.17 \pm 0.10) \times 10^9$	0.93 ± 0.05
$CdSO_4$	1×10^{-3}	$(4.06 \pm 1.48) \times 10^{-1}$	0.47 ± 0.40	$(4.57 \pm 0.28) \times 10^9$	0.64 ± 0.05
$CdSO_4$	5×10^{-6}	$(7.40 \pm 1.48) \times 10^{-2}$	1.45 ± 1.12	$(4.23 \pm 0.58) \times 10^9$	0.70 ± 0.10

$G^0_{I\cdot} \equiv$ Generation parameter in the absence of solute.

$k^0_2 \equiv k_2$ parameter in the absence of solute.

For comparison, Table 9 also shows k_2 values obtained by plotting $\frac{1}{(I\bullet)}$ versus t, in the range 350 μs to 1000 μs. A typical $\frac{1}{(I\bullet)}$ versus t plot is shown in Figure 35.

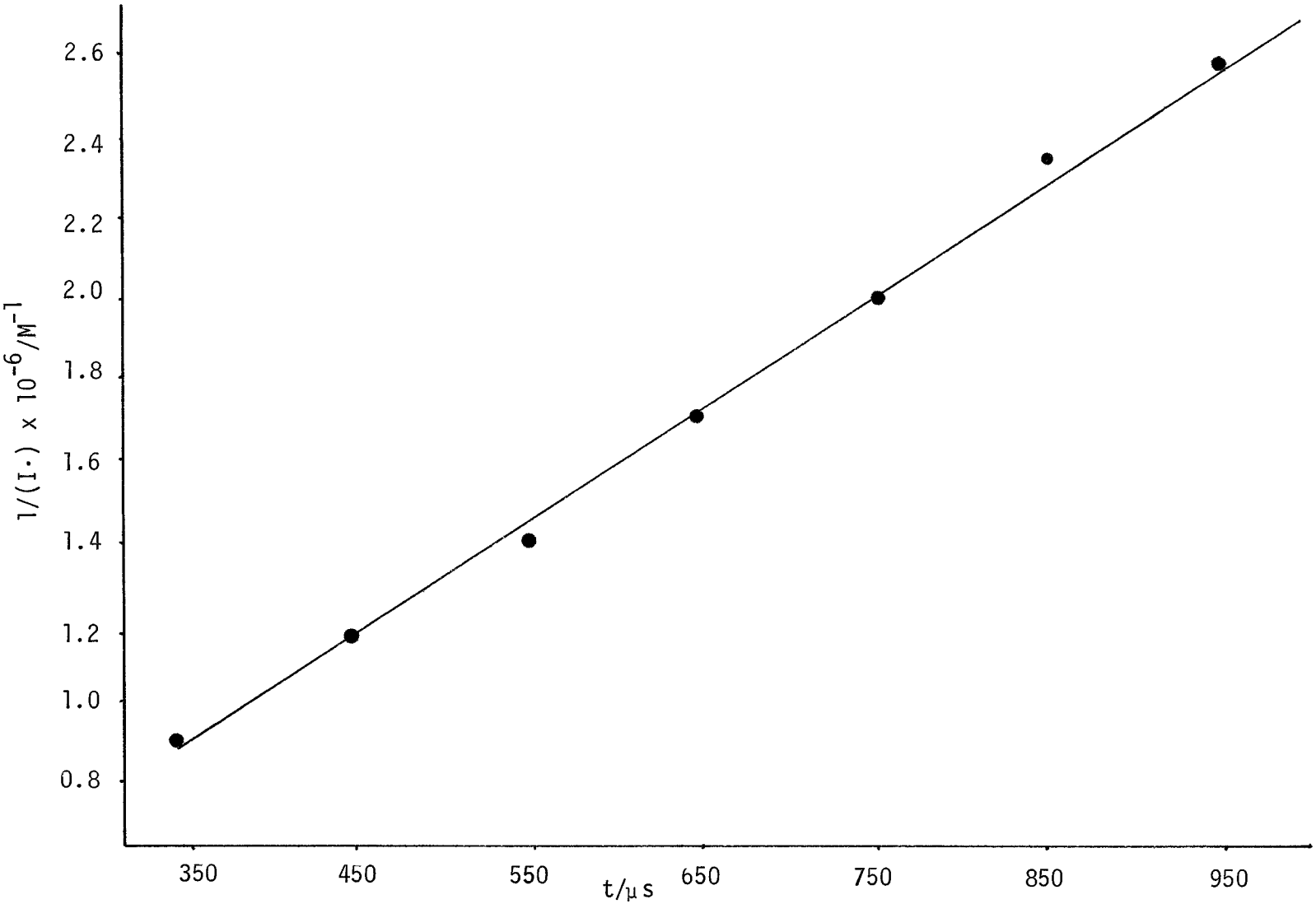

Figure (35): A typical 1/(I·) versus time plot.

D. Kinetic Analysis: $^3IH^*$

Several kinetic curves for the indole triplet state were obtained after single flashings of indole (5×10^{-4} M), in the absence and in the presence of NaBr (1.0 M), $BaCl_2 \cdot 2H_2O$ (0.25 M), $CdSO_4$ (1×10^{-3} M) and $CdSO_4$ (5×10^{-6} M). The $^3IH^*$ concentration versus time data presented in this work represent the average $^3IH^*$ concentrations versus time, derived from the several kinetic curves obtained. The numerical values of these average $^3IH^*$ concentrations are given in Appendix 2 for the various solutions studied. n-th order regression analysis was performed on the $^3IH^*$ concentration versus time plots in the range 60 μs to 220 μs to obtain $^3IH^*$ concentration versus time equations of the form shown in Equation 34 where B values are given in Appendix 3 for each solution studied.

$$(^3IH^*) = B_0 + B_1 t + B_2 t^2 + B_3 t^3 + B_4 t^4 \qquad (34)$$

Equation 34 was differentiated to give Equation 35 .

$$\frac{d(^3IH^*)}{dt} = B_1 + 2B_2 t + 3B_3 t^2 + 4B_4 t^3 \qquad (35)$$

$\frac{d(^3IH^*)}{dt}$ values were calculated at 10 μs intervals from 60 μs to 220 μs.

Sets of $\frac{d(^3IH^*)}{dt}$ and $(^3IH^*)$ values were used to solve simultaneously for $G_{3_{IH^*}}$, k_1 and k_2 in Equation 36 where n = 1.

$$\frac{d(^3IH^*)}{dt} = G_{3_{IH^*}} f(t) - k_1(^3IH^*) - k_2(^3IH^*)^2 \quad (36)$$

In the absence of added solutes, positive values of $G_{3_{IH^*}}$, k_1 and k_2 were obtained using Equation 36. In the presence of added solutes, negative values for at least one of $G_{3_{IH^*}}$, k_1 or k_2 were obtained in the majority of data sets with Equation 36. On the assumption that $^3IH^*$ was exhibiting either first or second order decay behaviour but not combined first and second order decay behaviour, the solution of Equations 37 and 38 was attempted in a manner similar to that described above.

$$\frac{d(^3IH^*)}{dt} = G_{3_{IH^*}} f(t) - k_1(^3IH^*) \quad (37)$$

$$\frac{d(^3IH^*)}{dt} = G_{3_{IH^*}} f(t) - k_2(^3IH^*)^2 \quad (38)$$

where n = 1. Again, negative values were obtained for $G_{3_{IH^*}}$ and k_1 and $G_{3_{IH^*}}$ and k_2 for the majority of data sets. All (n = 1.5) possibilities were explored and negative values for at least one of the generation or decay parameters were found. The positive values of $G_{3_{IH^*}}$, k_1 and k_2, obtained in the absence of added solutes, and $G_{3_{IH^*}}$, k_1 and k_2, $G_{3_{IH^*}}$ and k_1, and $G_{3_{IH^*}}$ and k_2 for indole in water in the presence of added solutes are given in Table 11.

The changes in pH which occurred upon single flashings of all solutions referred to above are collected together in Table 12.

Table 11. Generation and Decay Parameters for the Indole Triplet State (n = 1).

Solute	Concentration (M)	$G_{3_{IH^*}}$	$G^0_{3_{IH^*}}/G_{3_{IH^*}}$	k_1 (s^{-1})	k_1^0/k_1	k_2 (M^{-1} s^{-1})	k_2^0/k_2
none	--	$(9.45 \pm 2.33) \times 10^{-3}$	1	$(4.68 \pm 1.09) \times 10^{3}$	1	$(6.88 \pm 2.33) \times 10^{9}$	1
NaBr	1.0	$(2.35 \pm 1.09) \times 10^{-1}$	0.04 ± 0.02	$(9.75 \pm 2.79) \times 10^{3}$	0.48 ± 0.22	$(3.83 \pm 1.50) \times 10^{10}$	0.18 ± 0.09
$BaCl_2 \cdot 2H_2O$	0.25	$(6.80 \pm 0.08) \times 10^{-2}$	0.15 ± 0.03	$(2.45 \pm 0.21) \times 10^{4}$	0.20 ± 0.05	$(6.43 \pm 2.82) \times 10^{9}$	1.06 ± 0.59
$CdSO_4$	1×10^{-3}	$(5.47 \pm 2.22) \times 10^{-2}$	0.17 ± 0.08	$(1.03 \pm 0.33) \times 10^{4}$	0.45 ± 0.18	$(1.11 \pm 0.78) \times 10^{10}$	0.62 ± 0.48
		$(2.0 \pm 0.45) \times 10^{-2}$	--	$(1.31 \pm 0.10) \times 10^{4}$	--		--
		$(9.8 \pm 4.7) \times 10^{-2}$	--		--	$(3.09 \pm 1.07) \times 10^{10}$	--
$CdSO_4$	5×10^{-6}	5.60×10^{-3}	1.69 ± 0.42	1.05×10^{4}	0.45 ± 0.10	7.55×10^{8}	9.11 ± 3.08
		$(1.79 \pm 1.19) \times 10^{-2}$	--	1.31×10^{4}	--	--	--
		$(7.82 \pm 10.15) \times 10^{-2}$	--		--	$(2.09 \pm 1.07) \times 10^{10}$	--

$G^0 \equiv$ Generation parameter in the absence of solute

$k_1^0 \equiv k_1$ decay parameter in the absence of solute

$k_1^0 \equiv k_2$ decay parameter in the absence of solute

Table 12. pH values before and after flashing

Solute	Concentration (M)	pH before	pH after
none	--	6.5	6.2
NaBr	1.0	7.3	8.1
$BaCl_2 \cdot 2H_2O$	0.25	6.5	6.3
$CdSO_4$	1×10^{-3}	6.1	5.5
$CdSO_4$	5×10^{-6}	6.1	6.0

Actinometric Studies

Potassium ferrioxalate actinometry showed that 2×10^{19} Fe^{++} ions were produced in the actinometry solution per flash. Since the quantum yield for Fe^{++} production ($\phi_{Fe^{++}}$) is 1.20, in the range 253.7 nm to 436 nm, and decreases for $\lambda > 436$ nm,[50] and the spectral output of the flash lamp is not quantitatively known, it is only possible to give a lower limit (1.7×10^{19}) to the number of quanta absorbed per flash by the actinometry solution. The approximate lower limit to the number of einsteins absorbed $litre^{-1}$ s^{-1} by the actinometric solution = 0.74.

DISCUSSION

I. Effects of Solutes on Absorption and Fluorescence Spectra

The S_0-S_1 absorption band of indole did not exhibit red or blue shifts, new spectral features or band intensity changes upon the addition of NaBr (0.04 M), $BaCl_2 \cdot 2H_2O$ (0.01 M), $CdSO_4$ (4×10^{-5} M) and $CdSO_4$ (2×10^{-7} M) (Fig. 17), thus indicating that the added solutes do not interact with the ground state of indole.

The wavelength of maximum fluorescence emission was also unchanged upon addition of the above solutes (Table 5), indicating that the added solutes do not influence the energy of the S_1^0 state of indole. From integrated band intensity data (Table 5), it is clear that the number of fluorescing (S_1^0) molecules is unchanged for all solutes added except NaBr, which drastically reduces this number.

Similarly, τ_1, the fluorescence lifetime, defined in Equation 39, was unaffected by $CdSO_4$, slightly reduced by $BaCl_2 \cdot 2H_2O$ and significantly reduced by NaBr (Table 6).

$$\tau_1 = \frac{1}{k_F + k_I + k_{II} + k_Q(Q)} \tag{39}$$

Since k_F is known to be unaffected by solutes,[42] the effect of NaBr (and to a lesser extent $BaCl_2 \cdot 2H_2O$) must be to increase one or more of the remaining three rate constants. Although it is not possible to determine which specific rate is affected by NaBr, since the effects of

concentration and temperature on τ_1 were not examined in this study, Burshtein[27] has shown that Br^- increases the value of the specific rate of indole triplet production by ISC from the fluorescent state, S_1^0. The interpretation of τ_2, which for all solutes added was in the subnanosecond region, is not possible at this time, although τ_2 may be associated with the rotation of S_1^0 molecules during fluorescence emission.

II. Effects of Solutes on the Production and Decay of e^-_{aq} and I•

1. General Considerations

In the absence and in the presence of all solutes used in this work, the production of e^-_{aq} was found to exhibit a 1.5 power dependence on exciting light intensity. This power dependence suggests the existence of both monophotonic and biphotonic photoionization mechanisms. This result is not surprising, since monophotonic, biphotonic and mixed monophotonic-biphotonic photoionization have all been reported for indole and indole derivatives in aqueous solution. For example, Klein et al. found a monophotonic photoionization by laser flash photolysis of aqueous solution of indole at 60°C, biphotonic photoionization of the same solutions at 1.5°C and combined monophotonic and biphotonic photoionization of these solutions at 25°C.[33] Bent and Hayon have found that photoionization of aqueous solutions of tryptophan at 25°C, by laser flash photolysis, took place by a mixed monophotonic and biphotonic mechanism.[22] Hydrated electron concentrations (yields) exhibited a 1.5 power dependence on light intensity, for a laser pulse width of 4 ns, and 1.2 power dependence for laser pulse widths of 15 ns, which are comparable to the 20 ns widths of the laser pulses used by Klein et al. It seems that in the flash photolysis of aqueous solutions of indole and indole derivatives that monophotonic photoionization and biphotonic photoionization are both temperature dependent. Monophotonic photoionization is favoured at high temperatures and biphotonic photoionization is favoured at low temperatures. Also,

the relative importance of these two photoionization mechanisms is affected by excitation pulse widths.

The nature of the dependence of the production of the indolyl neutral radical on the exciting light intensity is not entirely clear. Values of the generation parameter, G_I, were calculated (see Results), assuming a strictly monophotonic production mechanism (n = 1) and mixed monophotonic-biphotonic mechanism (n = 1.5). Since standard deviations computed for G_I are comparable for both the n = 1 and n = 1.5 cases, it is not possible to conclude that one mechanism is favoured over the other.

In the absence and in the presence of all solutes, the disappearance of e^-_{aq} was found to involve a pseudo first order process or, very likely, the sum of pseudo first order processes (see below). Under the same conditions, the disappearance of I• was found to be a second order process involving the bimolecular recombination of I•. Although the identities of the products of this reaction have not been determined in this work, it is possible that indole dimers, which are known to exist[43] are formed.

$$I\bullet + I\bullet \longrightarrow \text{products}$$

B. The Effects of NaBr (1.0 M) on the Production and Decay of e^-_{aq} and I•

In the presence of NaBr, the generation parameter for e^-_{aq}, $G_{e^-_{aq}}$, was found to be less than the corresponding parameter found in the absence of added solutes (Table 8). By contrast, $G_{I\cdot}$ was found to be greater than the corresponding parameter found in the absence of NaBr (Table 10).

Table 13 shows $G_{I\cdot}/G_{e^-_{aq}}$ values in the absence and in the presence of added solutes.

Table 13. Effect of Solutes on $G_{I\cdot}/G_{e^-_{aq}}$

Solute	Concentration (M)	$G_{I\cdot}/G_{e^-_{aq}}$
none	--	2.71 ± 1.90
NaBr	1.0	12.43 ± 10.3
$BaCl_2 \cdot 2H_2O$	0.25	2.32 ± 2.23
$CdSO_4$	5×10^{-6}	7.50 ± 6.72

If e^-_{aq} and I• were generated in the same process one would expect the ratio $G_{I\cdot}/G_{e^-_{aq}}$ to be unity in all cases. However, it can be seen from the table that the ratios are very different from unity in all cases. It is possible that in addition to the measurable, slower pseudo first order decays of e^-_{aq}, which are explained below, that e^-_{aq} also decays by a very fast pseudo first order process which is not resolvable with

the equipment used in this work. The result of such a decay would be an apparent measured value of $G_{e^-_{aq}}$ which would be lower than both the primary $G_{e^-_{aq}}$ and $G_{I\cdot}$. This would then result in $G_{I\cdot}/G_{e^-_{aq}}$ values greater than unity.

The fact that $IH^{+}\cdot$, which decays by a very fast deprotonation ($k = 10^6\ s^{-1}$) ($t/_{\frac{1}{2}} = 0.7\ \mu s$), was not observed in this work suggests that e^-_{aq} decays, which are as fast or faster than $IH^{+}\cdot$ deprotonation, will also not be observed in this study. The existence of very fast e^-_{aq} decay has also been suggested by Grossweiner et al.[29] In the presence of NaBr, $G_{I\cdot}/G_{e^-_{aq}} = 12.4$ was greater by a factor of 4 than in the absence of solutes (Table 13). This is not surprising since Na^+, which at a concentration of 1.0 M acts as an efficient electron scavenger, would cause an apparent decrease in $G_{e^-_{aq}}$.

According to Grossweiner et al.,[29] the production of I· by the dissociation of an $(e^-_{aq}...IH^{+}\cdot)$ complex, is in competition with the reformation of indole within the complex. Efficient electron scavenging would increase the generation of I· by preventing the reformation of indole within the complex. It is not surprising therefore that Na^+, an electron scavenger, increases $G_{I\cdot}$.

The observed decay of e^-_{aq}, in the absence of oxygen, can be represented by the sum of pseudo first order processes shown in reactions 40-45.

$$e^-_{aq} + H^+ \xrightarrow{k_{H^+}} H \qquad k_{H^+} \simeq 2.0 \times 10^{10}\ M^{-1}\ s^{-1}\ ^{44} \qquad (40)$$

$$e^-_{aq} + H_2O \xrightarrow{k_{H_2O}} H + OH^- \qquad k_{H_2O} \simeq 2.0 \times 10^{1}\ M^{-1}\ s^{-1}\ ^{44} \qquad (41)$$

$$e^-_{aq} + IH \xrightarrow{k_{IH}} IH^{\bullet -} \qquad K_{IH} \simeq 2 \times 10^{8}\ M^{-1}\ s^{-1}\ ^{32} \qquad (42)$$

$$e^-_{aq} + Na^+ \longrightarrow Na \qquad k_{Na^+} \simeq 10^{5}\ M^{-1}\ s^{-1}\ ^{45} \qquad (43)$$

$$e^-_{aq} + Ba^{++} \longrightarrow Ba^+ \qquad k_{Ba^{++}} \text{ (unknown)} \qquad (44)$$

$$e^-_{aq} + Cd^{++} \longrightarrow Cd^+ \qquad k_{Cd^{++}} \simeq 5.5 \times 10^{10}\ M^{-1}\ s^{-1}\ ^{46} \qquad (45)$$

The total pseudo first order specific rate, k_1^T for the reaction of e^-_{aq} with water and the solutes H^+, IH, and S ≡ Na^+, Ba^{++} and Cd^{++} is given in Equation 46.

$$k_1^T = k_{H^+}(H^+) + k_{H_2O}(H_2O) + k_{IH}(IH) + k_S(S) \qquad (46)$$

The values for predicted and experimental pseudo first order rate constants for e^-_{aq} decay in the absence and in the presence of added solutes are given in Table 14.

Table 14. Pseudo First Order Rate Constants for Reactions of e^-_{aq} with Various Solutes.

Solute	Concentration (M)	$k_{H^+}(H^+)$ (s^{-1})	$k_{H_2O}(H_2O)$ (s^{-1})	$k_{IH}(IH)$ (s^{-1})	$k_S(S)$ (s^{-1})	$k_1^T{}_{pred}$ (s^{-1})	$k_1^T{}_{exp}$ (s^{-1})
none	--	$\sim 10^4$	$\sim 10^3$	$\sim 10^5$	--	$\sim 1.1 \times 10^5$	$(8.43 \pm 2.21) \times 10^4$
NaBr	1.01	$\sim 10^3$	$\sim 10^3$	$\sim 10^5$	$\sim 10^5$	2×10^5	$(5.71 \pm 0.57) \times 10^4$
$BaCl_2 \cdot 2H_2O$	0.25	$\sim 10^4$	$\sim 10^3$	$\sim 10^5$	--	1.1×10^5	$(1.29 \pm 0.65) \times 10^5$
$CdSO_4$	5×10^{-6}	$\sim 10^4$	$\sim 10^3$	$\sim 10^5$	$\sim 2.75 \times 10^5$	4×10^5	$(4.46 \pm 0.89) \times 10^4$

The predicted pseudo first order rate constant for e^-_{aq} decay in the presence of Na^+ was larger than that which was experimentally determined. In fact, the observed rate constant was comparable with that found for e^-_{aq} decay in the absence of added solute. The possibility that the reaction of e^-_{aq} with Na^+ is too fast to be resolved with the equipment used in this work may explain the experimental value of k_1^T. The larger predicted rate constant, however, does qualitatively support the explanations for both the increased $G_{I\cdot}/G_{e^-_{aq}}$ values and the increased $G_{I\cdot}$ value in the presence of NaBr.

The second order rate constant for decay of I· was found to be unaffected by NaBr. This observation supports the identification of I· as a neutral species since the presence of the ionic solute, Na^+Br^- would not affect the specific rates of bimolecular recombination of neutral species by the primary kinetic salt effect.

C. The Effect of $BaCl_2 \cdot 2H_2O$ on the Production and Decay of e^-_{aq} and I•

The generation parameter for e^-_{aq}, $G_{e^-_{aq}}$, was found to increase in the presence of $BaCl_2 \cdot 2H_2O$ compared with the value of $G_{e^-_{aq}}$ in the absence of added solute. The value of $G_{I\cdot}$ was increased in the presence of $BaCl_2 \cdot 2H_2O$ but not as greatly as in the presence of NaBr.

The ratio $G_{I\cdot}/G_{e^-_{aq}}$ in the presence of $BaCl_2 \cdot 2H_2O$ was similar to $G_{I\cdot}/G_{e^-_{aq}}$ in the absence of solutes. If Ba^{++} is a poor electron scavenger, it is not expected to participate in a fast, undetectable e^-_{aq} decay process and consequently $G_{I\cdot}/G_{e^-_{aq}}$ is not expected to be different from that observed in the absence of added solutes and the observed increase in $G_{I\cdot}$ is expected to be less than that observed in the presence of NaBr.

The measured pseudo first order rate constant for e^-_{aq} decay, k_1^T, in the presence of $BaCl_2 \cdot 2H_2O$ was comparable to both the predicted pseudo first order rate constant and k_1^T determined experimentally in the absence of solutes. This observation is also expected if Ba^{++} is a poor electron scavenger.

The second order rate constant for decay of I• was found to be unaffected by $BaCl_2 \cdot 2H_2O$. This observation also supports the identification of I• as a neutral species.

D. The Effects of $CdSO_4$ on the Production and Decay of e^-_{aq} and I•

The generation parameter for e^-_{aq}, $G_{e^-_{aq}}$, was found to decrease in the presence of $CdSO_4$ (5×10^{-6} M). As with NaBr, this decrease suggests the existence of a very fast e^-_{aq} scavenging by Cd^{++} (Table 14) which is not resolvable. The value of $G_{I\cdot}$ in the presence of $CdSO_4$ (5×10^{-6} M, 1×10^{-3} M) was found to increase as compared with $G_{I\cdot}$ in the absence of solutes. The scavenging of e^-_{aq} from an $(e^-_{aq}...IH^+_{\cdot})$ complex thus preventing reformation of IH would lead to an increased $G_{I\cdot}$ value.

In the presence of $CdSO_4$ (5×10^{-6} M) the ratio $G_{I\cdot}/G_{e^-_{aq}} \simeq 7.5$ was greater by a factor of three than in the absence of solutes. Again, efficient electron scavenging by Cd^{++} would cause an apparent increase in $G_{I\cdot}/G_{e^-_{aq}}$.

The predicted pseudo first order rate constant for e^-_{aq} decay, k_1^T, in the presence of Cd^{++}, was larger than that which was experimentally determined. In fact, the observed rate constant was smaller than that found for e^-_{aq} decay in the absence of added solutes. No explanation can be given for this difference at this time. The increased predicted rate constant, however, qualitatively supports the explanations for both the increased $G_{I\cdot}/G_{e^-_{aq}}$ and $G_{I\cdot}$ values in the presence of $CdSO_4$.

The second order rate constants for decay of I• were found to be increased in the presence of $CdSO_4$ (5×10^{-6} M, 1×10^{-3} M). This observation cannot be explained at this time.

III. The Effects of Solutes on the Production and Decay of $^3IH^*$

1. General Considerations

In the absence and in the presence of all solutes used in this study, the production of $^3IH^*$ was found to be monophotonic.

In the absence of solutes, and in the presence of NaBr and $BaCl_2 \cdot 2H_2O$, $^3IH^*$ decayed by combined first and second order processes. These processes may be represented by (47) and (48)

$$T_1 \overset{ISC}{\rightsquigarrow} S_0^v \tag{47}$$

$$T_1 + T_1 \longrightarrow S_0^v + S_0^v \tag{48}$$

with specific rates k_{T_1} and k_{T_2}, respectively. The enhancement of the specific rates of first and second order decay of $^3IH^*$ by the solutes used in this study, except for $CdSO_4$ (5×10^{-6} M) (see below), suggests that these decays may involve ISC to S_0^v since enhancement of k_{T_1} and k_{T_2} by heavy atoms and triplet states, respectively, is established.

B. Effect of NaBr on the Production and Decay of $^3IH^*$

The generation parameter, $G_{^3IH^*}$, was found to increase drastically in the presence of NaBr. This effect is expected since enhancement of ISC from S_1^0 by Br^- is well known. Busel *et al.*, for example, found that ISC enhancement for indole in water increased with the addition of halide ions.[26] The efficiency of ISC enhancement increased in the order $Cl^- < Br^- < I^-$. The increase in $G_{^3IH^*}$ is also consistent with the decrease in both the fluorescence lifetime, τ_1, and the integrated fluorescence band intensity.

The value of the first order rate constant, k_{T_1}, for triplet decay was found to be greater in the presence of NaBr than in the absence of added solutes. This is expected since heavy atom enhancement of ISC from T_2 to S_0^v is well known.[47] The value of the second order rate constant, k_{T_2}, was found to be greater in the presence of NaBr than in the absence of added solutes. The Br^- enhancement of S_0^v formation by triplet-triplet annihilation may explain the observed increase.

C. Effect of $BaCl_2 \cdot 2H_2O$ on the Production and Decay of $^3IH^*$

The generation parameter, $G_{^3IH^*}$, was found to increase in the presence of $BaCl_2 \cdot 2H_2O$ and this increase was less than that observed in the presence of NaBr. However, by contrast with NaBr, a very small decrease in fluorescence lifetime was observed and the integrated fluorescence band intensity was unchanged. It is expected that $^3IH^*$ production would increase in the presence of Ba^{++} and Cl^-, and that the increase would be less than that observed in the presence of Br^- since Busel *et al.*[26] and Burshtein[27] have shown that cation ISC enhancement is less efficient than anion ISC enhancement, and Cl^- ISC enhancement is less efficient than Br^- ISC enhancement. However, if ISC is $S_1^0 \longrightarrow T$, decreases in both fluorescence lifetime and integrated fluorescence band intensities are expected. While the former effect is observed, the latter is definitely not observed.

It appears that most $^3IH^*$ formation in the presence of $BaCl_2 \cdot 2H_2O$ does not occur by ISC from S_1^0. Nor can it be assumed that ISC from S_1^v occurs since this process, too, would decrease integrated fluorescence

band intensities. Another possibility for the production of $^3IH^*$ is ISC from CTTS states to the triplet manifold. These CTTS states may be produced independently of S_1 states and may be capable of forming both e^-_{aq} and $^3IH^*$.

The value of the first order rate constant, k_{T_1}, for triplet decay was found to be greater in the presence of $BaCl_2 \cdot 2H_2O$ than in the absence of added solutes. This is expected since heavy atom enhancement of ISC from T_1 to S_0^v is well known.[47] The value of the second order rate constant, k_{T_2}, was found to be greater in the presence of $BaCl_2 \cdot 2H_2O$ than in the absence of solutes. The Ba^{++} or Cl^- enhancement of S_0^v formation by triplet-triplet annihilation may explain the observed increase.

D. The Effect of $CdSO_4$ on the Production and Decay of $^3IH^*$

In the presence of $CdSO_4$ (5×10^{-6} M, 1×10^{-3} M), it was found that the production of $^3IH^*$ was by a monophotonic process. However, it was impossible to determine whether the decay of $^3IH^*$ was combined first and second order, strictly first order, or strictly second order.

At low concentrations (5×10^{-6} M), the generation parameter, $G_{^3IH^*}$ was comparable with $G_{^3IH^*}$ observed in the absence of $CdSO_4$. At higher concentrations (1×10^{-3} M), $G_{^3IH^*}$ was significantly greater than $G_{^3IH^*}$ observed in the absence of $CdSO_4$.

As with $BaCl_2 \cdot 2H_2O$, low and high concentrations of $CdSO_4$ have no influence upon integrated fluorescence band intensities. By contrast

with $BaCl_2 \cdot 2H_2O$, low and high concentrations of $CdSO_4$ have no effect upon the fluorescence lifetime. It is possible that for 1×10^{-3} $CdSO_4$, as for $BaCl_2 \cdot 2H_2O$, ISC occurs from CTTS states.

The value of the first order rate constant, k_{T_1}, for triplet decay, was greater in the presence of $CdSO_4$ (1×10^{-3} M) than in the absence of added solutes. This is expected since heavy atom enhancement of ISC from T_1 to S_0^v is well known.[47] The value of the second order rate constant, k_{T_2}, was greater in the presence of $CdSO_4$ (1×10^{-3} M) than in the absence of added solutes. The Cd^{++} enhancement of S_0^v formation by triplet-triplet annihilation may explain the observed increase.

The values of the first and second order rate constants increased and decreased respectively in the presence of $CdSO_4$ (5×10^{-6} M). These values cannot be regarded as accurate, however, since only one meaurement of the combined first and second order rate constants was made.

IV. Summary

A. Production of e^-_{aq}, I• and $^3IH^*$

It has been shown in this study that in the presence of Na^+ and Br^- ions, a marked reduction in emission from indole S_1^0 fluorescent states is accompanied by a marked increase in the production of indole triplet states. It has also been shown that in the presence of Ba^{++} and Cl^-, and Cd^{++} and $SO_4^=$ ions, increases in the production of indole triplet states are not accompanied by reductions in emission from indole fluorescent states.

It would seem, therefore, that $S_0 \longrightarrow S_1$ excitation of indole in aqueous solution to form triplet states occurs by intersystem crossing from fluorescent and non-fluorescent states. These non-fluorescent states may be CTTS states. Furthermore, it would appear that intersystem crossing from S_1^0 fluorescent states is the predominant mode of triplet production in the presence of Na^+ and Br^- ions, and that intersystem crossing from CTTS states is the predominant mode of triplet production in the presence of Ba^{++} and Cl^-, and Cd^{++} and $SO_4^=$ ions.

The ionization potential of indole in water, which in the absence of solutes corresponds to λ = 285 nm (E = 420 kJ mol^{-1}), lies within the S_0-S_1 absorption band.[2,5] It is suggested that the addition of 1.0 M Na^+ and Br^- ions decreases the aqueous phase ionization potential and hence lowers the energy of "closely spaced" CTTS states immediately below the ionization potential. Such reductions in aqueous phase ionization potentials of indole derivatives by added electrolytes are

known. Truong,[48] for example, found that the ionization potential of tryptophan in aqueous solutions decreased by as much as 180 kJ mol^{-1} in the presence of very large concentrations of ionic solutes. Even if the postulated decrease in the ionization potential of indole in the presence of Na^+ and Br^- ions was as small as 14 kJ mol^{-1}, it would no longer lie within the S_0-S_1 absorption band. This effect would make direct excitation to S_1^v states more probable than direct excitation to CTTS states. On the other hand, direct photoionization would also be enhanced. However, the fact that Na^+ and Br^- ions have no effect on the S_0-S_1 absorption band may indicate that direct photoionization of indole within this wavelength region is relatively unimportant. Production of S_1^0 fluorescent states and triplet states, by Br^- enhanced ISC from S_1^0 states, following the vibrational relaxation of S_1^v states, would account for both the increased triplet production and decreased fluorescence emission observed in the presence of NaBr (see Results)

It is also suggested that since Ba^{++}, Cl^-, Cd^{++} and $SO_4^=$ ions are present in smaller concentrations than Na^+ and Br^- ions, there would be a smaller effect upon the aqueous phase ionization potential of indole in the presence of these ions. If this effect were less than 14 kJ mol^{-1}, the ionization potential would lie within the S_0-S_1 absorption band and hence direct excitation to CTTS states would become as important as in the absence of solute. Production of triplet states by enhanced ISC from CTTS states would account for both the increased triplet production (relative to triplet production in the absence of

solutes), and unchanged fluorescence emission observed in the presence of $BaCl_2 \cdot 2H_2O$ and $CdSO_4$. What is tacitly assumed here is that in the presence of $BaCl_2 \cdot 2H_2O$ and $CdSO_4$, more triplet states are produced from CTTS states by ISC without affecting triplet state production and fluorescence emission from S_I^0 states.

It has been shown that in the absence and in the presence of all solutes used in this work, the hydrated electron is produced in aqueous solutions of indole by a monophotonic process and a biphotonic process. Although several suggestions can be made regarding the nature of these processes, in the presence of the different solutes, no definite conclusions can be arrived at because of the apparent nature of and uncertainty in $G_{e^-_{aq}}$ values measured in this work. Since very fast electron scavenging takes place in the presence of the solutes, particularly Cd^{++} and Na^+, $G_{e^-_{aq}}$ values obtained are apparent values. Neither is it possible to equate $G_{I\cdot}$ values with primary $G_{e^-_{aq}}$ values since the production of $I\cdot$ is dependent upon the electron scavenging abilities of the solute.

On taking into account the effects of NaBr on fluorescence emission and triplet production and the postulated effect upon the aqueous phase ionization potential of indole, it appears that monophotonic e^-_{aq} production may occur directly and by the dissociation of CTTS states. These CTTS states, which may be iso-energetic with S_I^0, would be formed by conversion of S_I^V states, and by direct excitation. Direct excitation of CTTS states may not be important in the presence of NaBr

because of the effect of the solute upon the aqueous phase ionization potential of indole and direct photoionization may also not be important since NaBr had no effect upon the S_0-S_1 band of indole.

On taking into account the effects of Ba^{++} and Cl^-, and Cd^{++} and $SO_4^=$ upon triplet state production, the absence of effects on fluorescence emission and the postulated absence of effects of these ions on the aqueous phase ionization potential of indole, it appears that monophotonic e^-_{aq} production may occur by the dissociation of CTTS states, formed directly, conversion of S_1^V states to CTTS states (which are no longer iso-energetic with S_1^0 states) and thermal excitation of S_1^0 states to CTTS states. Direct excitation to CTTS is probably more important in the absence of solutes and in the presence of Ba^{++} and Cl^-, and Cd^{++} and $SO_4^=$ ions because of the postulated absence of an effect of these ions upon the aqueous phase ionization potential. Since the S_0-S_1 absorption band of indole is unaffected by Ba^{++} and Cl^-, and Cd^{++} and $SO_4^=$, direct photoionization would occur to the same extent as in the absence of solutes.

Since $G_{e^-_{aq}}$ and $G_{I\cdot}$ values are apparent values and not primary values, it is impossible to conclude that I· is produced exclusively by deprotonation of $IH^{+}\cdot$, the primary ionization product.

Two biphotonic processes have been postulated for hydrated electron production in aqueous solutions of indole.[22] The processes 49 and 50 occur after primary absorption of quanta and involve absorption of the second photon by S_1^0 fluorescent states or by triplet states.

$$S_1^0 + h\nu'_E \longrightarrow e^-_{aq} + IH^{+\bullet} \quad (49)$$

$$T_1 + h\nu'_E \longrightarrow e^-_{aq} + IH^{+\bullet} \quad (50)$$

In order to discover whether the biphotonic mechanism involving (50) is important, it is necessary to compare primary $G_{3_{IH*}}$ values with primary $G_{e^-_{aq}}$ values. While the $G_{3_{IH*}}$ values obtained in this study are primary generation parameters, the $G_{e^-_{aq}}$ values are not. It is therefore impossible to determine the contribution made by triplet states to electron production in the flash photolysis of aqueous solutions of indole. The following monophotonic photophysical processes may occur in the absence of solutes and in the presence of Ba^{++}, Cl^-, Cd^{++}, $SO_4^=$ ions.

$$S_0^0 + h\nu_E \longrightarrow S_1^v \quad (51)$$

$$\longrightarrow \text{CTTS} \quad (52)$$

$$\longrightarrow e^-_{aq} + IH^{+\bullet} \quad (53)$$

$$S_1^v \rightsquigarrow \text{CTTS} \quad (54)$$

$$\rightsquigarrow S_1^0 \quad (55)$$

$$S_1^0 \longrightarrow \text{CTTS} \quad (56)$$

$$\longrightarrow S_0^0 + h\nu_F \quad (57)$$

$$CTTS \rightsquigarrow T_n \rightsquigarrow T_1 \tag{58}$$

$$\longrightarrow e^-_{aq} + IH\cdot \tag{59}$$

where (53) is relatively unimportant and (58) is heavy atom enhanced ISC to the triplet manifold.

The following monophotonic photophysical processes may occur in the presence of Na^+ and Br^- ions.

$$S_0^0 + h\nu_E \longrightarrow S_1^V \tag{60}$$

$$\longrightarrow CTTS \tag{61}$$

$$\longrightarrow e^-_{aq} + IH\cdot^+ \tag{62}$$

$$S_1^V \rightsquigarrow CTTS \tag{63}$$

$$\rightsquigarrow S_1^0 \tag{64}$$

$$S_1^0 \longrightarrow S_0^0 + h\nu_F \tag{65}$$

$$\rightsquigarrow T_n \rightsquigarrow T_1 \tag{66}$$

$$CTTS \longrightarrow e^-_{aq} + IH\cdot^+ \tag{67}$$

where (61) and (62) are relatively unimportant and (66) is Br^- enhanced ISC to the triplet manifold.

B. The Decay of e^-_{aq}, I· and ^{3}IH*

It has been shown in this study that the hydrated electron decays by several pseudo first order processes involving reactions with H^+, H_2O, IH and the added solutes. e^-_{aq} also undergoes very fast reactions with the solutes, especially the e^-_{aq} scavengers, Na^+ and Cd^{++}. These very fast processes, $\tau_{1/2} \sim 1$ μs, could not be observed with the apparatus used in this study. The indolyl neutral radical undergoes a second order recombination reaction, the specific rate of which is unaffected by NaBr and $BaCl_2 \cdot 2H_2O$ and is increased in the presence of $CdSO_4$. The product of this recombination reaction, although not identified in this study, may be an indole dimer.

The indole triplet state undergoes combined first and second order decay processes in the absence of solute and in the presence of NaBr and $BaCl_2 \cdot 2H_2O$. These processes, both of which are enhanced by the presence of heavy atoms have been identified as ISC from T_1 to S_0^v and triplet-triplet annihilation involving conversion of T_1 states to S_0^v states. The decay mechanism for ^{3}IH* in the presence of $CdSO_4$ is unclear.

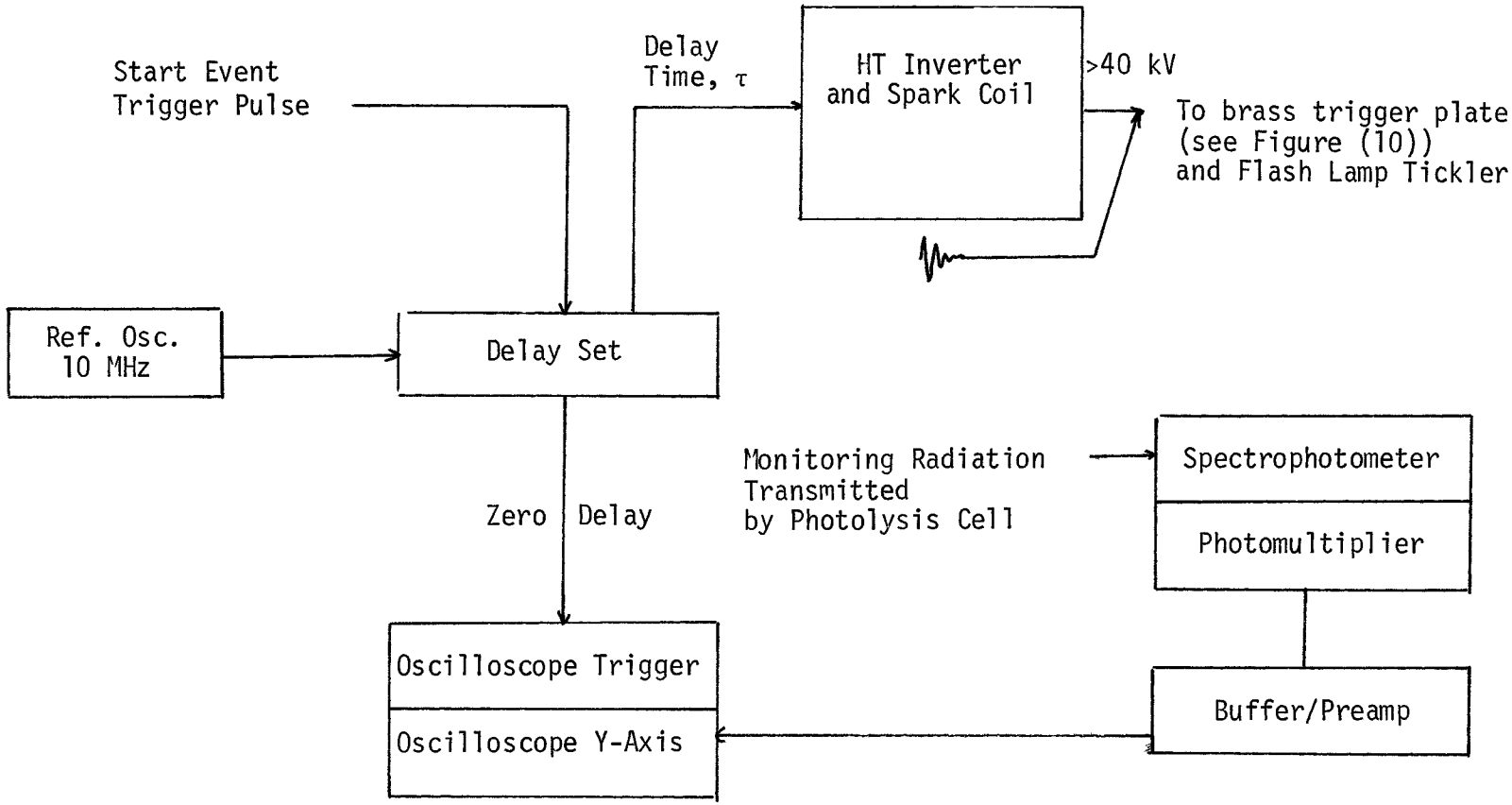

Appendix I. Schematic of Flash photolysis lamp pulsing system.

APPENDIX II

Concentration - Time Data

5×10^{-4} M indole (no solute added)

Time (μs)	Concentration of e^-_{aq} (M)	Concentration of I· (M)	Concentration of $^3IH^*$ (M)
0	0	0	0
10	1.479×10^{-7}	--	2.455×10^{-7}
20	3.411×10^{-7}	2.196×10^{-7}	5.693×10^{-7}
30	4.599×10^{-7}	2.596×10^{-7}	7.868×10^{-7}
40	4.366×10^{-7}	6.546×10^{-7}	8.839×10^{-7}
50	3.469×10^{-7}	9.373×10^{-7}	9.421×10^{-7}
60	$(2.634 \pm 0.13) \times 10^{-7}$	$(1.157 \pm 0.08) \times 10^{-6}$	$(9.367 \pm 0.22) \times 10^{-7}$
70	1.873×10^{-7}	1.252×10^{-6}	8.984×10^{-7}
80	1.313×10^{-7}	1.327×10^{-6}	8.392×10^{-7}
90	$(9.264 \pm 1.56) \times 10^{-8}$	$(1.345 \pm 0.09) \times 10^{-6}$	$7.783 \pm 0.12) \times 10^{-7}$
100	6.490×10^{-8}	1.345×10^{-6}	7.284×10^{-7}
110	4.332×10^{-8}	1.349×10^{-6}	6.755×10^{-7}
120	$(2.709 \pm 0.969) \times 10^{-8}$	$(1.338 \pm 0.04) \times 10^{-6}$	$(6.372 \pm 0.24) \times 10^{-7}$
130	1.566×10^{-8}	1.328×10^{-6}	5.920×10^{-7}
140	6.774×10^{-9}	1.327×10^{-6}	5.522×10^{-7}
150	1.256×10^{-9}	1.131×10^{-6}	5.094×10^{-7}
160	--	$(1.288 \pm 0.04) \times 10^{-6}$	$(4.729 \pm 0.05) \times 10^{-7}$
170	--	1.255×10^{-6}	4.422×10^{-7}
180	--	1.229×10^{-6}	4.150×10^{-7}
190	--	$(1.205 \pm 0.05) \times 10^{-6}$	$(3.846 \pm 0.13) \times 10^{-7}$
200	--	1.172×10^{-6}	3.644×10^{-7}
210	--	1.144×10^{-6}	3.416×10^{-7}
220	--	$(1.111 \pm 0.02) \times 10^{-6}$	$(3.221 \pm 0.23) \times 10^{-7}$

5×10^{-4} M Indole (1.0 M NaBr added)

Time (μs)	Concentration of e^-_{aq} (M)	Concentration of I• (M)	Concentration of ^{3}IH* (M)
0	0	0	0
10	4.289×10^{-8}	--	5.777×10^{-7}
20	1.700×10^{-7}	--	1.235×10^{-6}
30	1.641×10^{-7}	--	1.192×10^{-6}
40	2.995×10^{-7}	3.729×10^{-8}	2.006×10^{-6}
50	2.619×10^{-7}	6.434×10^{-7}	2.012×10^{-6}
60	$(1.982 \pm 0.10) \times 10^{-7}$	$(1.215 \pm 0.77) \times 10^{-6}$	$(1.865 \pm 0.07) \times 10^{-6}$
70	1.467×10^{-7}	1.504×10^{-6}	1.671×10^{-6}
80	1.041×10^{-7}	1.700×10^{-6}	1.460×10^{-6}
90	$(7.533 \pm 0.93) \times 10^{-8}$	$(1.779 \pm 0.1) \times 10^{-6}$	$(1.267 \pm 0.09) \times 10^{-6}$
100	5.197×10^{-8}	1.769×10^{-6}	1.096×10^{-6}
110	3.655×10^{-8}	1.764×10^{-6}	9.632×10^{-7}
120	$(2.467 \pm 0.44) \times 10^{-8}$	$(1.733 \pm 0.12) \times 10^{-6}$	$(8.489 \pm 1.13) \times 10^{-7}$
130	1.729×10^{-8}	1.699×10^{-6}	7.516×10^{-7}
140	1.191×10^{-8}	1.674×10^{-6}	6.678×10^{-7}
150	6.454×10^{-9}	1.642×10^{-6}	6.073×10^{-7}
160	2.709×10^{-9}	$(1.629 \pm 0.07) \times 10^{-6}$	$(5.415 \pm 0.835) \times 10^{-7}$
170	--	1.587×10^{-6}	4.861×10^{-7}
180	--	1.554×10^{-6}	4.336×10^{-7}
190	--	$(1.518 \pm 0.06) \times 10^{-6}$	$(3.864 \pm 0.714) \times 10^{-7}$
200	--	1.495×10^{-6}	3.414×10^{-7}
210	--	1.460×10^{-6}	3.068×10^{-7}
220	--	$(1.415 \pm 0.06) \times 10^{-6}$	$(2.781 \pm 0.52) \times 10^{-7}$
	--	1.377×10^{-6}	2.492×10^{-7}

5×10^{-4} M Indole (0.25 M $BaCl_2 \cdot 2H_2O$ added)

Time (μs)	Concentration of e^-_{aq} (M)	Concentration of I• (M)	Concentration of $^3IH^*$ (M)
0	0	0	0
10	3.07×10^{-8}	8.046×10^{-7}	6.447×10^{-8}
20	1.818×10^{-7}	$5.572 \pm 2.781 \times 10^{-7}$	5.639×10^{-7}
30	3.602×10^{-7}	1.292×10^{-6}	8.479×10^{-7}
40	4.647×10^{-7}	5.861×10^{-7}	1.282×10^{-6}
50	4.330×10^{-7}	9.909×10^{-7}	1.436×10^{-6}
60	3.463×10^{-7}	1.488×10^{-6}	1.393×10^{-6}
70	2.472×10^{-7}	2.099×10^{-6}	1.266×10^{-6}
80	1.771×10^{-7}	2.253×10^{-6}	1.132×10^{-6}
90	1.219×10^{-7}	2.317×10^{-6}	9.999×10^{-7}
100	8.098×10^{-8}	2.364×10^{-6}	8.651×10^{-7}
110	5.309×10^{-8}	2.263×10^{-6}	7.583×10^{-7}
120	3.142×10^{-8}	2.316×10^{-6}	6.228×10^{-7}
130	1.717×10^{-8}	2.261×10^{-6}	5.426×10^{-7}
140	6.439×10^{-9}	2.697×10^{-6}	4.537×10^{-7}
150	--	2.131×10^{-6}	3.778×10^{-7}
160	--	2.034×10^{-6}	3.224×10^{-7}
170	--	1.934×10^{-6}	2.743×10^{-7}
180	--	1.875×10^{-6}	2.401×10^{-7}
190	--	1.793×10^{-6}	2.231×10^{-7}
200	--	1.702×10^{-6}	1.910×10^{-7}
210	--	1.609×10^{-6}	1.766×10^{-7}
220	--	1.518×10^{-6}	1.613×10^{-7}

5×10^{-4} M Indole (1×10^{-3} M $CdSO_4$ added)

Time (μs)	Concentration of e^-_{aq} (M)	Concentration of I• (M)	Concentration of $^3IH^*$ (M)
0	0	0	0
10	0	4.366×10^{-7}	3.074×10^{-7}
20	0	1.929×10^{-6}	6.400×10^{-7}
30	0	2.636×10^{-6}	1.025×10^{-6}
40	2.761×10^{-9}	2.801×10^{-6}	1.107×10^{-6}
50	3.630×10^{-9}	2.540×10^{-6}	1.290×10^{-6}
60	3.87×10^{-9}	$(2.350 \pm 0.05) \times 10^{-6}$	$(1.270 \pm 0.01) \times 10^{-6}$
70	0	2.090×10^{-6}	1.230×10^{-6}
80	0	1.905×10^{-6}	1.104×10^{-6}
90	0	$(1.689 \pm 0.04) \times 10^{-6}$	$(1.093 \pm 0.03) \times 10^{-6}$
100	0	1.565×10^{-6}	9.861×10^{-6}
110	0	1.454×10^{-6}	8.890×10^{-6}
120	0	$(1.371 \pm 0.16) \times 10^{-6}$	$(7.976 \pm 0.95) \times 10^{-7}$
130	0	1.312×10^{-6}	7.018×10^{-7}
140	0	1.250×10^{-6}	6.300×10^{-7}
150	0	1.189×10^{-6}	5.711×10^{-7}
160	0	$(1.141 \pm 0.15) \times 10^{-6}$	$(5.301 \pm 0.4) \times 10^{-7}$
170	0	1.098×10^{-6}	4.892×10^{-7}
180	0	1.050×10^{-6}	4.504×10^{-7}
190	0	$(9.994 \pm 1.1) \times 10^{-7}$	$(4.195 \pm 0.5) \times 10^{-7}$
200	0	9.595×10^{-7}	3.909×10^{-7}
210	0	9.097×10^{-7}	3.739×10^{-7}
220	0	$(8.641 \pm 0.85) \times 10^{-7}$	$(3.557 \pm 0.4) \times 10^{-7}$

5×10^{-4} M Indole ($\sim 5 \times 10^{-6}$ M $CdSO_4$ added)

Time (μs)	Concentration of e^-_{aq} (M)	Concentration of I• (M)	Concentration of $^3IH^*$ (M)
0	0	0	0
10	1.468×10^{-8}	8.928×10^{-8}	2.652×10^{-7}
20	9.576×10^{-8}	2.044×10^{-7}	5.533×10^{-7}
30	1.848×10^{-7}	2.697×10^{-7}	7.034×10^{-7}
40	2.125×10^{-7}	1.579×10^{-7}	7.873×10^{-7}
50	2.020×10^{-7}	2.420×10^{-7}	8.219×10^{-7}
60	$(1.423 \pm 0.05) \times 10^{-7}$	$(7.219 \pm 4.2) \times 10^{-7}$	$(8.148 \pm 0.4) \times 10^{-7}$
70	1.062×10^{-7}	9.287×10^{-7}	7.748×10^{-7}
80	7.169×10^{-8}	1.245×10^{-6}	6.932×10^{-7}
90	$(5.239 \pm 0.489) \times 10^{-8}$	$(1.197 \pm 0.13) \times 10^{-6}$	$(6.350 \pm 0.6) \times 10^{-7}$
100	3.678×10^{-8}	1.152×10^{-6}	5.920×10^{-7}
110	2.516×10^{-8}	1.128×10^{-6}	5.457×10^{-7}
120	$(1.900 \pm 0.89) \times 10^{-8}$	$(1.137 \pm 0.05) \times 10^{-6}$	$(4.977 \pm 0.73) \times 10^{-7}$
130	1.255×10^{-8}	1.140×10^{-6}	4.491×10^{-7}
140	7.714×10^{-9}	1.129×10^{-6}	4.074×10^{-7}
150	3.062×10^{-9}	1.117×10^{-6}	3.662×10^{-7}
160	--	$(1.098 \pm 0.06) \times 10^{-6}$	$(3.303 \pm 0.663) \times 10^{-7}$
170	--	1.078×10^{-6}	2.940×10^{-7}
180	--	1.062×10^{-6}	2.609×10^{-7}
190	--	$(1.032 \pm 0.04) \times 10^{-6}$	$(2.313 \pm 0.57) \times 10^{-7}$
200	--	1.009×10^{-6}	2.057×10^{-7}
210	--	9.767×10^{-7}	1.840×10^{-7}
220	--	$(9.401 \pm 0.2) \times 10^{-7}$	$(1.608 \pm 0.43) \times 10^{-7}$

APPENDIX III

Concentration - Time Equations

1. No solute added

(a) e^-_{aq}

$$C = 8.505 \times 10^{-7} - 9.263 \times 10^{-3}t - 6.970 \times 10^{1}t^2 - 1.268 \times 10^{6}t^3 - 4.313 \times 10^{9}t^4$$

$$\frac{dC}{dt} = -9.263 \times 10^{-3} - 1.398 \times 10^{2}t + 3.804 \times 10^{6}t^2 - 1.725 \times 10^{10}t^3$$

(b) $I\cdot$

$$C = 2.082 \times 10^{-6} - 6.510 \times 10^{-3}t + 1.052 \times 10^{1}t^2 - 8.443 \times 10^{3}t^3 + 2.681 \times 10^{6}t^4$$

$$\frac{dC}{dt} = -6.510 \times 10^{-3} + 2.104 \times 10^{1}t - 2.533 \times 10^{4}t^2 + 1.072 \times 10^{7}t^3$$

(c) $^3IH^*$

$$C = 1.194 \times 10^{-6} - 2.389 \times 10^{-3}t - 9.432 \times 10^{1}t^2 + 2.608 \times 10^{5}t^3 - 4.139 \times 10^{8}t^4$$

$$\frac{dC}{dt} = -2.389 \times 10^{-3} - 8.864 \times 10^{1}t + 7.824 \times 10^{5}t^2 - 1.656 \times 10^{9}t^3$$

2. NaBr added (1.0 M)

(a) e^-_{aq}

$$C = 8.218 \times 10^{-7} - 1.584 \times 10^{-2}t + 1.038 \times 10^{2}t^{2}$$
$$-2.126 \times 10^{5}t^{3} - 1.139 \times 10^{8}t^{4}$$

$$\frac{dC}{dt} = -1.584 \times 10^{-2} + 2.076 \times 10^{2}t - 6.378 \times 10^{5}t^{2} - 4.556 \times 10^{8}t^{4}$$

(b) I·

$$C = 2.581 \times 10^{-6} - 7.047 \times 10^{-3}t + 9.067 \times 10^{0}t^{2}$$
$$-5.666 \times 10^{3}t^{3} + 1.440 \times 10^{6}t^{4}$$

$$\frac{dC}{dt} = -7.047 \times 10^{-3} + 1.813 \times 10^{1}t - 1.699 \times 10^{4}t^{2} + 5.760 \times 10^{6}t^{3}$$

(c) $^3IH^*$

$$C = 3.921 \times 10^{-6} - 4.451 \times 10^{-2}t + 1.919 \times 10^{2}t^{2}$$
$$- 2.669 \times 10^{5}t^{3} - 1.301 \times 10^{8}t^{4}$$

$$\frac{dC}{dt} = -4.451 \times 10^{-2} + 3.838 \times 10^{2}t - 8.007 \times 10^{5}t^{2} - 5.204 \times 10^{8}t^{3}$$

3. $BaCl_2 \cdot 2H_2O$ added (0.25 M)

(a) e^-_{aq}

$$C = 1.545 \times 10^{-6} - 3.808 \times 10^{-2}t + 4.430 \times 10^{2}t^2$$
$$-2.917 \times 10^{6}t^3 + 8.195 \times 10^{9}t^4$$

$$\frac{dC}{dt} = -3.080 \times 10^{-2} + 8.860 \times 10^{0}t - 8.751 \times 10^{6}t^2 + 3.278 \times 10^{10}t^3$$

(b) $I\cdot$

$$C = 1.731 \times 10^{-6} + 5.911 \times 10^{-3}t - 2.796 \times 10^{2}t^2$$
$$+ 1.630 \times 10^{6}t^3 - 2.857 \times 10^{9}t^4$$

$$\frac{dC}{dt} = 5.911 \times 10^{-3} - 4.492 \times 10^{2}t + 4.892 \times 10^{6}t^2 - 1.143 \times 10^{10}t^3$$

(c) $^3IH^*$

$$C = 2.160 \times 10^{-6} - 7.096 \times 10^{-3}t + 1.181 \times 10^{1}t^2$$
$$- 9.665 \times 10^{3}t^3 + 3.099 \times 10^{6}t^4$$

$$\frac{dC}{dt} = -7.096 \times 10^{-3} + 2.362 \times 10^{1}t - 2.899 \times 10^{4}t^2 + 3.240 \times 10^{7}t^3$$

4. $CdSO_4$ added (1×10^{-3} M)

(a) e^-_{aq}

$C =$

$\frac{dC}{dt} =$

no data available

(b) $I\cdot$

$$C = 1.406 \times 10^{-6} - 3.735 \times 10^{-3}t + 5.156 \times 10^{0}t^2 - 3.778 \times 10^{3}t^3 + 1.183 \times 10^{6}t^4$$

$$\frac{dC}{dt} = -3.735 \times 10^{-3} + 1.031 \times 10^{1}t - 1.133 \times 10^{4}t^2 + 4.732 \times 10^{6}t^3$$

(c) $^3IH^*$

$$C = 7.536 \times 10^{-7} + 3.136 \times 10^{-2}t - 4.850 \times 10^{2}t^2 + 2.484 \times 10^{6}t^3 - 4.173 \times 10^{9}t^4$$

$$\frac{dC}{dt} = 3.136 \times 10^{-2} - 9.900 \times 10^{2}t + 7.452 \times 10^{6}t^2 - 1.655 \times 10^{10}t^3$$

5. $CdSO_4$ added (5×10^{-6} M)

(a) e^-_{aq}

$$C = 8.479 \times 10^{-7} - 2.118 \times 10^{-2}t + 2.112 \times 10^{2}t^2 - 9.685 \times 10^{5}t^3 + 1.689 \times 10^{9}t^4$$

$$\frac{dC}{dt} = -2.118 \times 10^{-2} + 4.224 \times 10^{2}t - 2.906 \times 10^{6}t^2 + 6.756 \times 10^{9}t^3$$

(b) $I\cdot$

$$C = 2.332 \times 10^{-6} - 9.235 \times 10^{-3}t + 1.684 \times 10^{1}t^2 - 1.407 \times 10^{4}t^3 + 4.450 \times 10^{6}t^4$$

$$\frac{dC}{dt} = -9.235 \times 10^{-3} + 3.368 \times 10^{1}t - 4.222 \times 10^{4}t^2 + 1.780 \times 10^{7}t^3$$

(c) $^3IH^*$

$$C = 1.281 \times 10^{-6} - 9.222 \times 10^{-3}t + 2.056 \times 10^{1}t^2 - 8.926 \times 10^{4}t^3 + 1.627 \times 10^{8}t^4$$

$$\frac{dC}{dt} = -9.222 \times 10^{-3} + 6.162 \times 10^{1}t - 2.678 \times 10^{5}t^2 + 6.508 \times 10^{8}t^3$$

REFERENCES

1. J. H. D. Eland, Int. J. Mass Spec. Ion Phys. 2, 471 (1969).
2. D. Grand, A. Bernas and E. Amouyal, J. Chem. Phys. 44, 73 (1979).
3. M. Sun and P. Song, Photochem. Photobiol. 25, 3 (1977).
4. E. M. Evleth, D. Chalvet and P. Bamiere, J. Phys. Chem. 81, 1913 (1977).
5. L. Kevan and H. B. Steen, Chem. Phys. Lett. 34, 184 (1975).
6. J. B. Birks, Organic Molecular Photophysics, Vol. 1 (Wiley-Interscience, New York, 1973), p. 36.
7. J. B. Birks, Organic Molecular Photophysics, Vol. 1 (Wiley-Interscience, New York, 1973), p. 187.
8. M. S. Walker, T. W. Bednar and R. Lumry, J. Chem. Phys. 47, 1020 (1967).
9. M. Mataga, Y. Torihashi and K. Ezumi, Theoret. Chim. Acta, 2, 158 (1964).
10. D. L. Horrocks and C. T. Perg, eds., Organic Scintillators and Liquid Scintillation Counting (Academic Press, 1971).
11. J. Chrysochoos, Mol. Photochem. 5, 1 (1973).
12. J. Eisinger and G. Navon, J. Chem. Phys. 50, 2069 (1969).
13. R. W. Cowgill, Arch. Biochem. Biophys. 100, 36 (1963).
14. J. Feitelson, Isr. J. Chem. 8, 241 (1970).
15. E. P. Kirby and R. F. Steiner, J. Phys. Chem. 74, 4480 (1970).
16. R. W. Ricci, Photochem. Photobiol. 12, 67 (1970).
17. J. W. Bridges and R. T. Williams, Biochem. J. 107, 235 (1968).
18. R. Klein and I. Tatischeff, Chem. Phys. Lett. 51, 333 (1977).
19. M. S. Walker, T. W. Bednar, R. Lumry and F. Humphries, Photochem. Photobiol. 14, 147 (1971).

20. W. B. deLander and P. Wahl, Biochim. Biophys. Acta 243, 153 (1971).

21. J. Feitelson, Photochem. Photobiol. 13, 87 (1971).

22. D. V. Bent and E. Hayon, J. Amer. Chem. Soc. 97, 2612 (1975).

23. E. A. Cherniak, unpublished results.

24. C. Pernot and L. Lindqvist, J. Photochem. 6, 215 (1976).

25. L. Stryer, J. Amer. Chem. Soc. 88, 5708 (1966).

26. E. P. Busel, T. L. Busheva and E. A. Burshtein, Opt. Spectry. 32, 158 (1972).

27. E. A. Burshtein, Biofizika, 13, 433 (1968).

28. E. J. Hart and M. Anbar, The Hydrated Electron (Interscience, New York, 1970) p. 44.

29. F. D. Bryant, R. Santus and L. I. Grossweiner, J. Phys. Chem. 79, 2711 (1975).

30. L. I. Grossweiner and J. F. Baugher, J. Phys. Chem. 81, 93 (1977).

31. M. Anbar, M. Bambenek and A. B. Ross, Nat. Stand. Ref. Data. Ser. Natl. Bur. Stand., no. 43 (1973).

32. R. C. Armstrong and A. J. Swallow, Nat. Stand. Ref. Data. Ser., Natl. Bur. Stand., no. 43 (1973).

33. R. Klein, I. Tatischeff, M. Bazin and R. Santus, J. Phys. Chem. 85, 670 (1981).

34. M. Ottolenghi, Chem. Phys. Lett. 12, 339 (1971).

35. Y. Muto, Y. Nakato and H. Tsubomura, Bull. Chem. Soc. Japan 49, 428 (1976).

36. M. L. Posener, G. E. Adams, P. Wardman and R. B. Cundall, J. Chem. Soc. Faraday I, 72, 2231 (1976).

37. J. F. Baugher and L. I. Grossweiner, J. Phys. Chem. 81, 1349 (1977).

38. R. Arce, A. Grimson, J. Revvelta and G. A. Simpson, Photochem. Photobiol. 21, 397 (1975).

39. H. Templar and P. J. Thistlethwaite, Photochem. Photobiol. 23, 79 (1976).

40. D. V. Bent and E. Hayon, J. Amer. Chem. Soc. 97, 2612 (1975) and references contained therein.

41. S. Gordon, E. J. Hart, M. S. Matheson, J. Rabani and J. K. Thomas, Nat. Stand. Ref. Data Ser., Natl. Bur. Stand., no. 43 (1973).

42. J. B. Birks, Photophysics of Aromatic Molecules (Wiley-Interscience, New York, 1970) pp. 209-214, 447.

43. R. J. Sundberg, The Chemistry of Indole (Academic Press, New York, 1970) p. 7.

44. E. J. Hart and M. Anbar, The Hydrated Electron (Interscience, New York, 1970) p. 76.

45. M. Anbar and E. J. Hart, Nat. Stand. Ref. Data Ser., Natl. Bur. Stand., no. 43 (1973).

46. J. H. Baxendale, E. M. Fielden, J. P. Keene, Nat. Stand. Ref. Data Ser., Natl. Bur. Stand., no. 43 (1973).

47. J. Birks, Organic Molecular Photophysics, (Wiley-Interscience, New York, 1973), p. 499.

48. T. B. Truong, J. Phys. Chem. 84, 964 (1980).

49. R. C. A. Electron Tube Handbook HB-3.

50. J. G. Calvert and J. N. Pitts, Photochemistry (John Wiley and Sons, New York, 1966) pp. 783-786 and references contained therein.

51. A. R. Watkins, Zeits. fur Physik. Chemie N. F., B. D. 96, 123 (1975).

" Pip, dear old chap, life is made of ever so many partings welded together, as I may say, and one man's a goldsmith, and one's a coppersmith. Divisions among such must come, and must be met as they come. If there's been any fault at all to-day, it's mine. You and me is not two figures to be together in London; nor yet anywheres else but what is private, and beknown, and understood among friends. It ain't that I am proud, but that I want to be right, as you shall never see me no more in these clother. I'm wrong in these clother. I'm wrong out of the forge, the kitchen, or off th' meshes. You won't find half so much fault in me if you think of me in my forge dress, with my hammer in my hand, or even my pipe. You won't find half so much fault in me if, supposing as you should ever wish to see me, you come and put your head in at the forge window and see Joe the blacksmith there at the old anwil, in the old burnt apron, sticking to the old work. I'm awful dull, but I hope I've beat out something nigh the rights of this at last. And so God bless you, dear old Pip, old chap, God bless you ! "

Joe Gargery

a "blacksmith".